



**UNIVERSITÀ
DEGLI STUDI
DI PADOVA**

UNIVERSITÀ DEGLI STUDI DI PADOVA

DIPARTIMENTO DI INGEGNERIA INDUSTRIALE

SCUOLA DI DOTTORATO DI RICERCA IN INGEGNERIA INDUSTRIALE

INDIRIZZO: INGEGNERIA CHIMICA, DEI MATERIALI E MECCANICA

CICLO XXIX

**IMPLEMENTATION OF CONTROL AND ACQUISITION SYSTEM
FOR A TIRE MACHINE**

Coordinatore: Ch.mo Prof. Paolo Colombo

Supervisore: Ch.mo Prof. Roberto Lot

Co-Supervisore: Ch.mo Prof. Vittore Cossalter

Dottorando: Tarek Jomaa

Dedication

I would like to dedicate this Doctoral dissertation to my father, Dr. Hassan Jomaa. There is no doubt in my mind that without him I would not be the man I am today. I also dedicate it to my beloved mother Taghrid Jomaa and dear Sister Tamara Jomaa for their continued support and counsel that helped me a lot to complete this process.

Many thanks and appreciation to all my colleagues and coworkers in the department for the constant support and help during my thesis.

I am grateful to for my friends for their support and their experience sharing which made my journey easier.

Acknowledgements

I would like to acknowledge the inspirational instruction and guidance of Dr. Roberto Lot and Dr. Vittore Cossalter. Both have given me a deep appreciation and love for the beauty and detail of this subject.

I would also like to acknowledge the support and assistance given me by Dr. Matteo Massaro. He has been very generous in his support of my academic pursuits and has contributed ideas, feedbacks and advices. In particular he assisted the project at the managerial and bureaucratic level which helped saving a tremendous amount of time.

Finally, I would like to thank M. Gian-Franco and M. Stefano Girardi for the full disposability, expertise and support during the construction phase of the project. I could not have completed this effort without their assistance, tolerance, and enthusiasm.

Abstract

The motorcycle dynamics research group “MDRG” of the University of Padova is dedicated for researches in the field of motorcycles stability and handling. Such research require having a tire model for dynamic simulation since tires play a principal role in motorcycles dynamics. For this reason the “Mototiremeter” was built, it is a tire testing machine that reproduces the behavior of a tire on the road in order to study its characteristics and deduce the Pacejka coefficients that are later on implemented in a tire model. It allows simulations closer to reality in order to achieve a better stability and higher performance which helps increasing road safety.

The first part of my dissertation was dedicated to the “Mototiremeter” machine which was operational but suffered from a poor control and data acquisition system. This resulted in loss of time and accuracy. Both, hardware and software were updated in order to facilitate testing and increase efficiency.

The main work of the thesis revolves around the new tire machine. The project was still in the design phase therefore the proposed design solutions and construction methods are explained. This new design offers a lot of improvements over the previous one. The main advantage is the new implemented load cell that allows the measurement of all six components (Forces and moments) at the wheel with higher accuracy.

After tire testing, the data are collected and processed by mean of a Matlab code. The program allows to plot the raw data (after down sampling and cancelling the curvature effect of the rotating disk) and perform the Pacejka fitting. The development of such code was also a part of the thesis.

Sommario

Il gruppo di ricerca sulla dinamica del motociclo "MDRG" dell'università di Padova è dedicato per le ricerche nel campo della stabilità dei motocicli. Tale ricerche richiedono avere un modello del pneumatico per le simulazioni, poiché ha un ruolo principale nella dinamica dei motocicli. Per questo motivo la macchina "Mototiremeter" è stata costruita, è una macchina di prova che riproduce il comportamento dei pneumatici sulla strada per studiare le caratteristiche e dedurre i coefficienti di Pacejka che sono implementati nel modello per simulazione. Concede simulazioni più vicine alla realtà per ottenere una migliore stabilità e aumentare la sicurezza stradale.

La prima parte della mia dissertazione è stata dedicata alla macchina "Mototiremeter". Era operativa ma aveva tanto problemi nel sistema di controllo e dell'acquisizione dei dati. C'era una perdita di tempo nelle prove e anche una mancanza di precisione. Il hardware e software erano aggiornati per facilitare la procedura delle prove e aumentare l'efficienza.

Il lavoro principale della tesi era sulla nuova macchina dei pneumatici. Il progetto era ancora nella fase di progettazione quindi le soluzioni proposte e metodi della costruzione sono spiegati. Il nuovo design offre miglioramenti su quello precedente. Il vantaggio principale è la nuova cella di carico che misura i sei componenti (Forze e coppie) con alta precisione.

Dopo le prove, i dati sono salvati ed elaborati con un codice di Matlab. Il programma traccia i dati necessari (dopo cancellare l'effetto di curvatures del disco) e calcola i coefficienti di Pacejka. Lo sviluppo di tale codice fa parte della tesi.

Introduction

Improving vehicle dynamics models requires having a more realistic tire model which can only be provided by tire testing (Chapter 1). Such tests are characterized with a very high cost which can limit researches in such areas (handling, stability...) due to limited financial resources. This need opened the opportunity to develop low cost tire testing machine in order to expand researches without worrying about the high price of tire testing.

The first section of the thesis deals with the actual tire machine in our laboratory. The control and data acquisition systems were updated (Chapter 2) as well as the appropriate software. In addition, the several tire test performed in our laboratory are described (Chapter 3) with a brief analysis of some test results.

The second section is dedicated to the Matlab code developed for data elaboration (Chapter 3). The software allows the processing of the data from the test in order to plot the necessary graphs (Side slip force, camber force, self-aligning torque, twisting torque...) and perform the Pacejka fitting of the data to deduce the appropriate coefficient which are used for building tire models for simulations.

The third section is about the new tire testing machine which represents the main work of the thesis. The design solutions and construction of the machine are summarized (Chapter 4) as well as the implementation of the control and data acquisition system of the two tire machines (Chapter 4). Such prototype offers many advantages over the previous machine. It allows measuring all the 6 components (forces and moments) at the tire by mean of one load cell. This load cell offers higher precision and allows us to measure the longitudinal force (acceleration and braking) which was not possible before. All the adjustments for the vertical load, toroid and rolling radius are fully automatic therefore increasing the safety of the user and reducing the testing time. Figure 1 illustrates the several activities performed during the three years of the doctoral study.

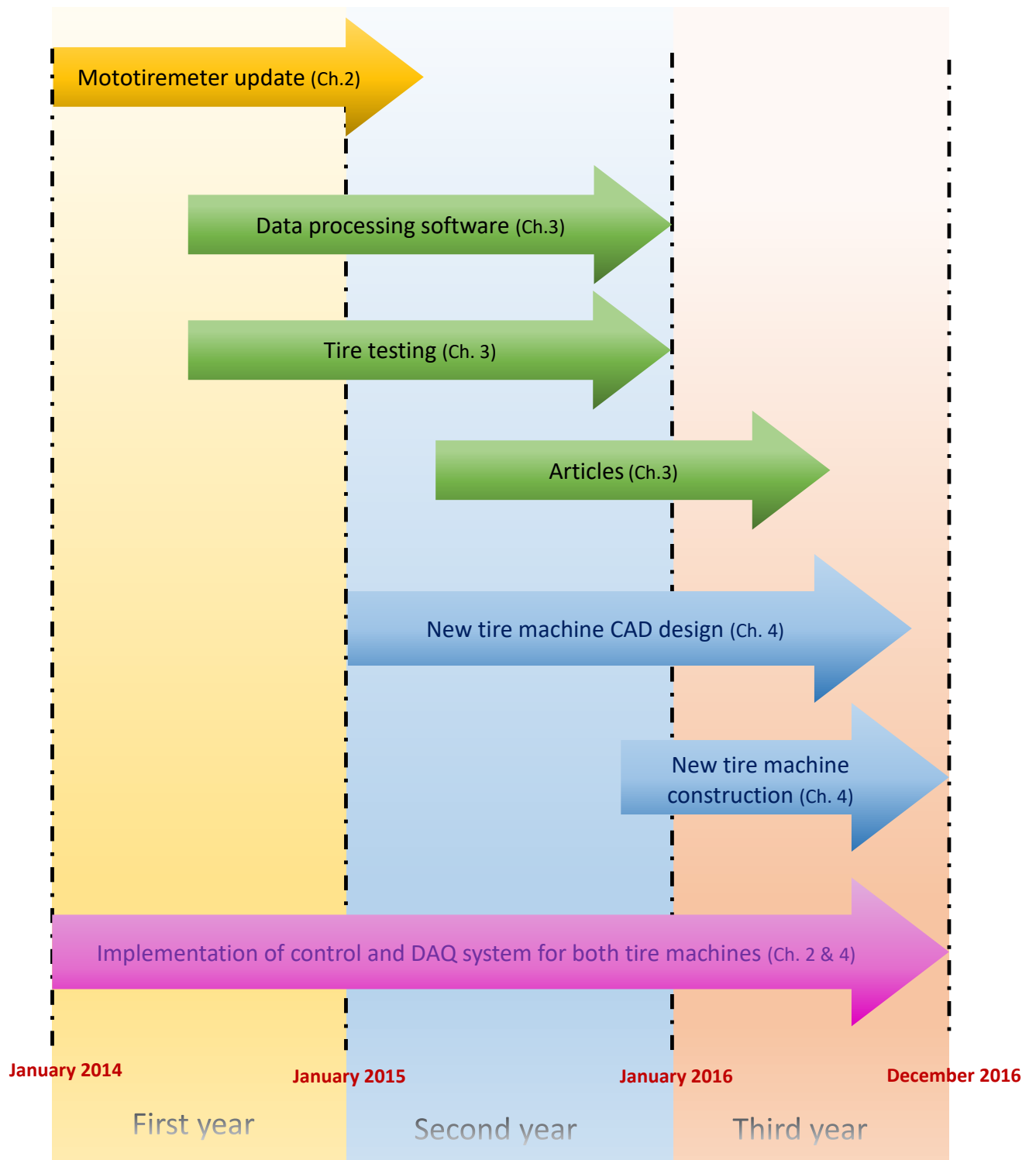


Figure 1: Grant chart illustrating the carried activities during the three doctoral years.

Chapter 1 – State of the art

Tires are the interface between the driver's input (steering, accelerating or braking) and the vehicle's response (turning, sliding...). A proper design [1] starts from choosing the right tire, then building the vehicle around it which is usually the case in racing since tires directly affect handling and stability [2], [3], [4]. The optimal conditions and limitations vary from one tire to another, this is why it is important to understand the subjected forces and moments at the contact patch. Motorcycle dynamics research, in the area of handling and stability, use tire data to build mathematical models [5], [6] for dynamics simulations.

Since the awareness of tire's importance, vehicle stability improved significantly therefore increasing road safety. Tires development [7] was not limited to safety, it also reduced fuel consumption [8] by minimizing rolling resistance [9] which helped increasing fuel efficiency [10] of vehicles and reducing pollution. In racing applications, understanding the tire is essential to achieve the desired yaw moment during cornering which makes the difference in lap-time [11]. Too much over-steer makes the vehicle slides from the rear which puts the driver in risk while too much under-steer increases the trajectory therefore increasing the lap-time [11].

The earliest tires were bands of leather, then iron, (later steel), placed on wooden wheels, used on carts and wagons. The first practical pneumatic tire was made in 1888. Keeping the vehicle stable and firm on the road depends on the amount of grip generated by the tire. The grip is generated by the rubber's deformation at the contact patch of the tire. The deformation shape depends on the vehicle maneuver resulting in lateral deformation during steering or longitudinal deformation during acceleration and braking. Lateral deformation creates a slip angle [12] which is simply the angle between the direction where the wheel is pointing and the direction where the wheel is going. The slip angle allows a certain amount of lateral force referred as the grip.

The lack of grip is caused when the lateral force from cornering is greater than the lateral force delivered by the tire which makes it slide. Oversteer occurs when the lack of grip is greater at the rear of the vehicle while understeer is the opposite. The same reasoning is valid for longitudinal forces where an excess in acceleration makes the wheel spinning while an excessive braking makes it sliding longitudinally.

One of the tire tests is the side slip test where the slip angle is varied under certain conditions (road surface, vertical load, inflation pressure, temperature...). The result is a graph of the lateral force against the slip angle. The amount of lateral force at a given slip angle varies with the conditions, mentioned earlier, therefore tire testing helps defining the grip as well as the optimal conditions for best tire performance.

The coefficient of friction varies with the road surface [12] , [13]. A dry asphalt surface has a higher coefficient of friction than a snow surface which requires different tires. The difference in tire's construction comes from the mechanical structure (radial or bias) and (or) the chemical compounds of the rubber.

The vertical load [14] has a major influence on the tire's grip. The generated amount of lateral force (or longitudinal) is related, in a nonlinear way, to the vertical load on the tire. This means that the gain in lateral (or longitudinal) force from an increase in vertical load will always be smaller than the loss in lateral (or longitudinal) force from a decrease, of the same amount, in vertical load. Because of the constant braking and acceleration (especially in racing applications), the vertical load on a tire changes dynamically due to the longitudinal weight transfer [12]. During braking, the weight shifts from the rear to the front, unloading the rear tire from a certain amount of vertical load and loading the front tire with the exact amount. At a constant slip angle during a corner, the previous vertical load variation result in a bigger grip loss at the rear than the grip gain at the front. This increases over-steer which tends to unstable the vehicle.

Another important condition is the inflation pressure [15]. A low inflation pressure allows more deformation of the contact patch therefore increasing grip. An inflation pressure too low increases dramatically the rolling resistance (increasing fuel consumption) and the steering torque (hard steering for the driver). High inflation pressure resolves the rolling resistance and steering torque problem but it reduces the contact patch leading to less grip (less stability) and less damping (less ride comfort). The optimal inflation pressure varies from tire to tire.

Tire's temperature [16], [17] is also an interesting condition since every tire operates best at its optimal temperature where the rubber becomes soft and sticky. In revenge, a low temperature makes the rubber harder resulting in some loss of grip. This is why, in racing, the tire is preheated at its optimal temperature in order to deliver the maximum grip. Also temperature and pressure are related to each other by the gas laws. Therefore an excessive variation in temperature results in a variation of the inflation pressure which influences the tire's behavior.

All the above justifies the importance of tire testing [18]. A tire testing machine intends to reproduce, indoor, the tire's behavior on the road while varying the several factors mentioned earlier (Vertical load, inflation pressure, temperature...) and others (like the speed for example). The machine is equipped with load cells that measure the forces and torques during the test session. The

measurements are then elaborated by mean of a software in order to analyze the characteristics of the tested tire.

Many engineering firms present various and competitive tire testing machines which all share in common the high cost. Below are listed some of the most interesting machines in today's market.

1.1 The FlatTrac III Classic from MTS

The Classic features the capacity and capability for testing passenger car and light truck tires under a wide range of conditions. You can dynamically change tire attitudes and loads on its continuous flat surface, while simultaneously measuring tire-generated forces and moments. You can take data under steady state or slowly changing conditions. The Flat-Trac III Classic system can also be used for running simple roadway simulations. Drawing on the Flat-Trac heritage and patents from all earlier designs, the FlatTrac III Classic system provides you with a wide range of capabilities not available with tire test systems of other manufacturers. One reason is the performance of its continuous-loop stainless steel belt tensioned between two drums. Testing is performed on the flat portion of the belt that is supported by a hydrodynamic water bearing. The tire spindle assembly is mounted on an A-frame positioned over the belt. This design allows the tire assembly to be steered (slip angle) about the center of the tire, and also to be cambered (inclination angle) about the tire patch.

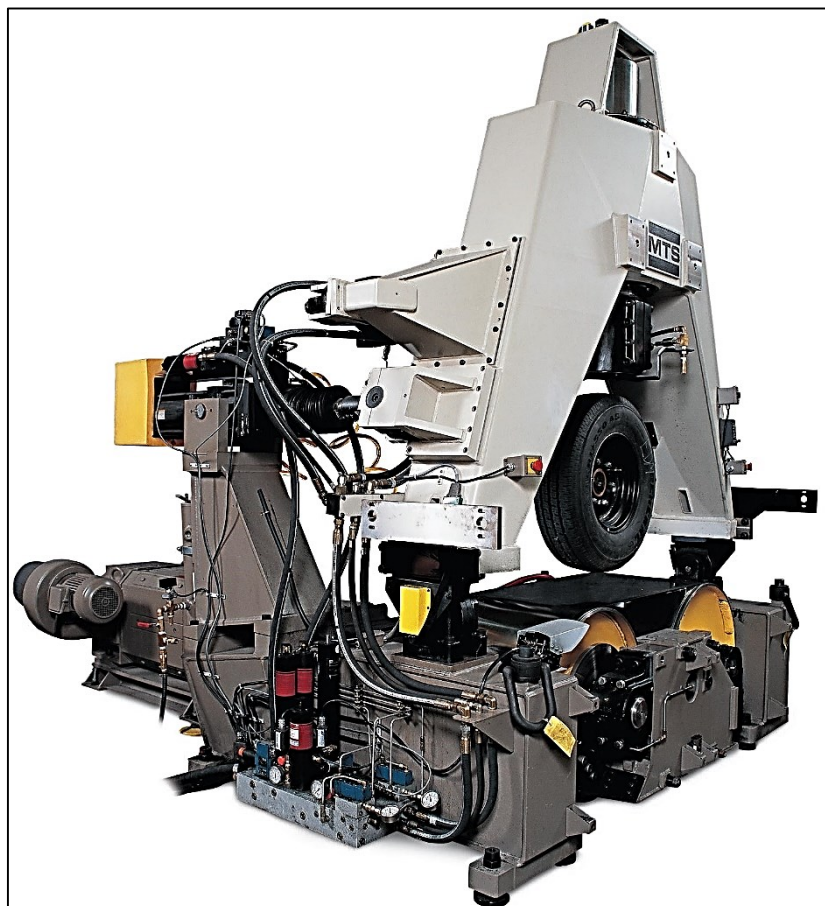


Figure 2: The FlatTrac III Classic from MTS

1.2 Calspan tire test machine

Calspan's Force and Moment Testing is performed onsite at the test facility, which is the most premier indoor tire test facility of its kind in the world. The facility's unique combination of speed and torque enables cutting-edge research and robust data quality. An experienced tire test team helps customers select load, velocity, slip angle, inclination angle, slip ratio, and other test conditions to maximize the effectiveness of their test programs.

The test bench allows to measure dynamic force and moment characteristics of a tire to predict how its performance will affect vehicle behavior. It controls the vertical load, slip angle, inclination angle, slip ratio, inflation pressure and speed to understand how a tire responds to different inputs. Force and Moment data provides detailed insight into how the tire interacts with the road surface and how the resulting forces and moments influence tire and vehicle performance attributes such as braking and cornering.

The continuous flat belt machine is capable of delivering road speeds in excess of 200 MPH (320km/h) and tire loads up to 12,000 pounds (53kN). It can accommodate large test articles and is well suited to truck tires, racing tires, small aircraft tires, and more. Finally, the machine can perform high torque (braking and driving) with high precision thanks to high power electric drives.

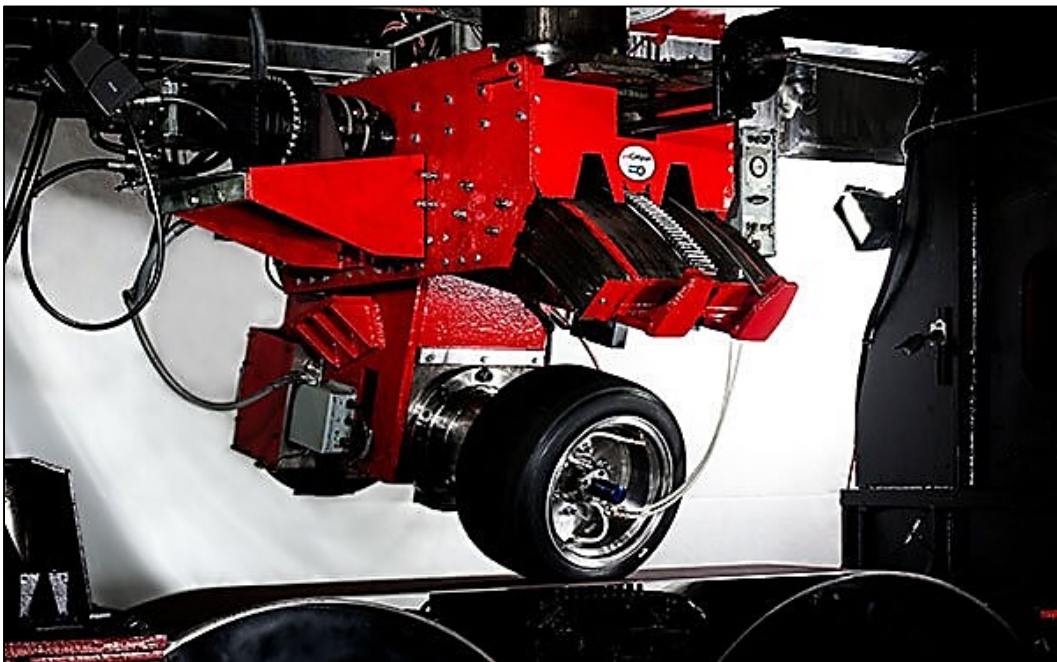


Figure 3: Calspan tire test machine

1.3 Delft-tire test from TASS International

TASS International offers an interesting and profound test facility. The on-road test lab measures tire performance at any road surface and almost any condition. The test trailer is completely designed to measure the forces and moments that arise when placing a tire on the road in various situations. By default, two towers are mounted. On one side there is a car tire measurement setup, on the other side, there is a motorcycle tire measurement setup, with the possibility to measure tires at camber angles up to 70 degrees. Measurements with the tire test trailer is usually performed at proving grounds ATP in Germany or IDIADA in Spain, but can be conducted at any other test track. Such test benefits from extremely realistic, on-road, testing of tire slip characteristics. In addition, it is flexible in timing and location.



Figure 4: Delft-tire test trailer

1.4 Our tire testing machines

All of the above machines, and many more, are leaders in the field of tire testing. These machines share in common the highly accurate and realistic tire measurements as well as the high cost which makes it nearly impossible to afford one. This is why, the majority of the clients pay huge amount of money for testing facilities in order to perform tires tests for them.

On one hand, tire testing became indispensable for the development of any vehicle (two and four wheels) but on the other hand it is very expensive. From this dilemma did rise our urge to design, build and develop tire testing prototypes that can provide accurate results at a very low price, almost negligible compared to the machines mentioned above. The Mototiremeter was the first tire machine developed in our laboratory. The measurements were compared with other machines in the market and the results were satisfying. Such machine was completely updated (Chapter 2) during my thesis and was, as well, used to perform a large amount of tests (Chapter 3) for several clients.

Another prototype (Chapter 4) has been designed and built at our laboratory. This prototype is an improvement over the Mototiremeter, and it offers a lot of advantages and new features in order to improve tire testing accuracy and safety, as well as decreasing tire testing time.

Chapter 2 - Mototiremeter

This particular testing rig (Figure 5) was developed for testing motorcycle and scooter tires. The wheel is mounted on a hinged arm that creates the side slip angle ($\pm 9^\circ$) and/or the camber angle ($\pm 50^\circ$). The wheel rolls freely on a rotating disc (diameter 3m) covered by a high friction material (safety walk) to simulate the road. Data are collected by means of three load cells mounted on the arm.

The first load cell is mounted in the lateral direction, locking the hinged arm and therefore measuring the lateral force component. The two other load cells measure the moment around the diametrical axis that passes through the contact patch and the moment about the wheel spin axis (Figure 6). The load cells are then connected to the computer through a data acquisition system composed of some specific modules (NI-9237 and NI-CDAQ 9188) to convert the signals.

Side slip tests are performed by varying the side slip angle while fixing the camber angle at zero. The resulting curves are the side slip force and self-aligning torque.

The self-aligning torque results from the non-symmetric distribution of stresses along the contact patch and it tends to align the wheel to the direction of speed if a perturbation takes place.

Camber tests are performed by varying the camber angle while fixing the side slip angle at zero. The resulting curves are the camber force and the twisting torque. The twisting torque represents the tendency of the cambered wheel to move along a trajectory with a curvature radius smaller than the one demanded by the steady turning manoeuvre; it does not tend to align the wheel.



Figure 5: Mototiremeter testing machine

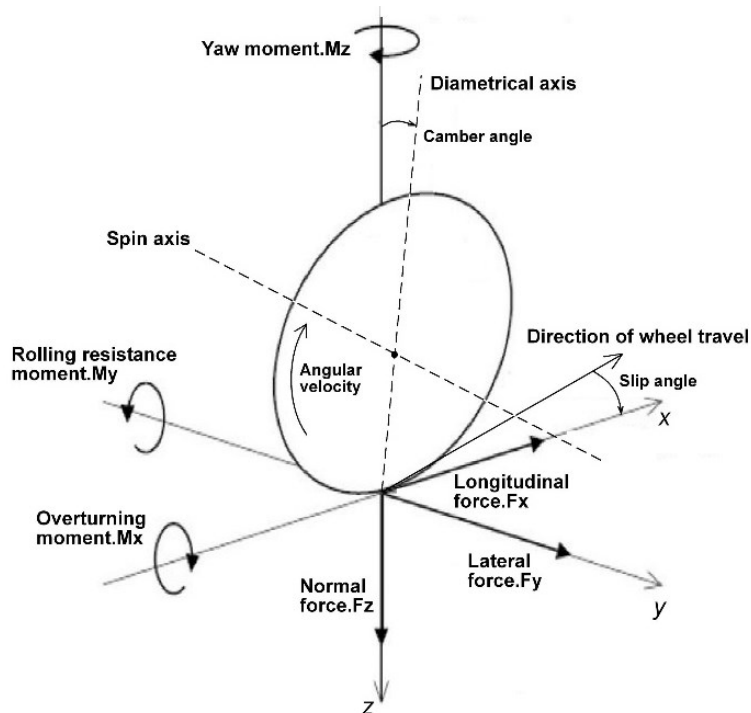


Figure 6: The coordinate system for the definition of tire forces and torques

The tests are carried in steady-state condition, which is achieved by keeping the hinged arm firm for a specified interval of time (5s by default) for each assigned value of side slip (or camber) angle. During this interval some measurements are made and the mean value for each slip (or camber) angle is calculated later by the elaboration software.

The first load cell (responsible of lateral force measurement) measures the actual lateral force with an additional force generated by the curvature of the track.

This additional force is cancelled by carrying out measurements for positive and negative range of side slip (or camber) angle. The resulting measurements have the same curvature force (which depends on the position of the contact point on the disc) and side slip (or camber) forces with the same absolute

value but opposite signs. The elaboration software calculates the half difference between forces corresponding to the positive and negative range of side slip (or camber) angle. This is a good estimate of the real side slip (or camber) force, because the curvature forces cancel each other. The side slip (or camber) force at zero side slip (or camber) angle is simply set to zero, since the measured value results only from the curvature force.

To perform the correction, measured data are processed by means of a MATLAB code that generates the curves for side slip force, camber force, self-aligning and twisting torque with their fittings based on the Magic Formula [19].

2.1 Hardware problems

The “Mototiremeter” is an old thesis project [20] built in the past. It incorporates two systems; the motion control and DAQ (data acquisition). Both were subjected to various unsystematic adjustments which led to a complicated and time consuming test procedure. In addition the control and DAQ system were engaged independently which increases the chance of mistakes.

The motion control is executed by a PCI-7344 board which is a motion controller, from National instruments, integrated in the desktop computer (Figure 7). It represents the brain which takes the motion request from the user, by way of a Labview code [21], and convert it into the proper command for the step motor. Meanwhile data were acquired by connecting a laptop to the load cells on the machine through some modules from National Instruments.



Figure 7: Old Control Unit of the Mototiremeter

The motion control hardware was not established properly. The cables and wires (Figure 8) were disordered and not labeled making it difficult to identify. The step motors switches (Figure 9) were exposed and hard to reach which was problematic since their main function is safety. The DAQ hardware suffered from the same inconvenient and contained unnecessary equipment (Figure 10). In addition to the unprofessional appearance of the machine, it was hard to perform any kind of modification or maintenance.

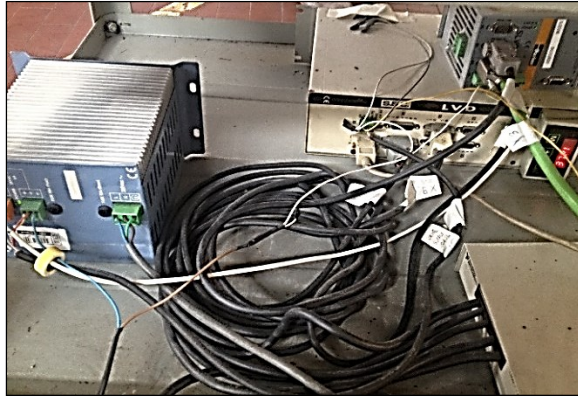


Figure 8: Bad wiring



Figure 9: Roll switch (left side) and Slip switch (right side)



Figure 10: Useless hardware

2.2 Hardware update

Updating the system requires a full understanding of its components and connections. For this reason the hardware was completely dismantled and then reassembled after removing unnecessary components (Figure 11). Cables and wires were labeled and organized (Figure 12) In order to simplify future work like update or maintenance.



Figure 11: Removal of useless hardware



Figure 12: Proper wiring

The old desktop computer (Figure 7) was replaced with a recent one (Figure 13) while the rest of the motion control system remained interchangeable. The same motion controller (PCI-7344) was integrated in the new computer with the installation of its drivers.



Figure 13: New workstation – Front view

The new DAQ system is formed of a NI-CDAQ chassis, from National Instruments, which is connected to the desktop computer via Ethernet cable. On the chassis is inserted a NI-9237 module that is an analogue equipment connected to the three load cells. Therefore both system are connected to the same workstation (Figure 13 and Figure 14).

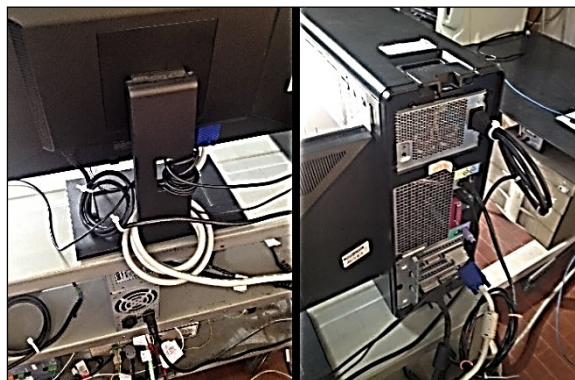


Figure 14: New workstation – Rear view

The problem of the exposed switches (Figure 9) was resolved by building a switchbox (Figure 15). The switchbox is placed on the top next to the computer allowing easy reach in case of emergencies or malfunctioning.



Figure 15: New switchbox

2.3 Software problems

Since the motion control and DAQ were two separate systems, they were running on different software which resulted in two different output files. The motion file contained the performed motion (slip and camber angles) while the DAQ file had the measured forces and moments.

Previously it was required to merge both output files together in order to associate every motion angle (slip or roll) with the appropriate measurements. This was possible through an intermediate Matlab code which was time consuming. The software associates the angles to the measurements by dividing it into steps based on the variation in value, leading to inaccurate results.

In addition, the motion control software was running on Labview 7.5 which is out of date. The front panel had unnecessary buttons and switches (Figure 16) and the block diagram (software's code) was incomprehensible making it hard to modify or update. The user interface was not friendly and did not allow the possibility of combined slip-roll tests (¶ 3.1.7).

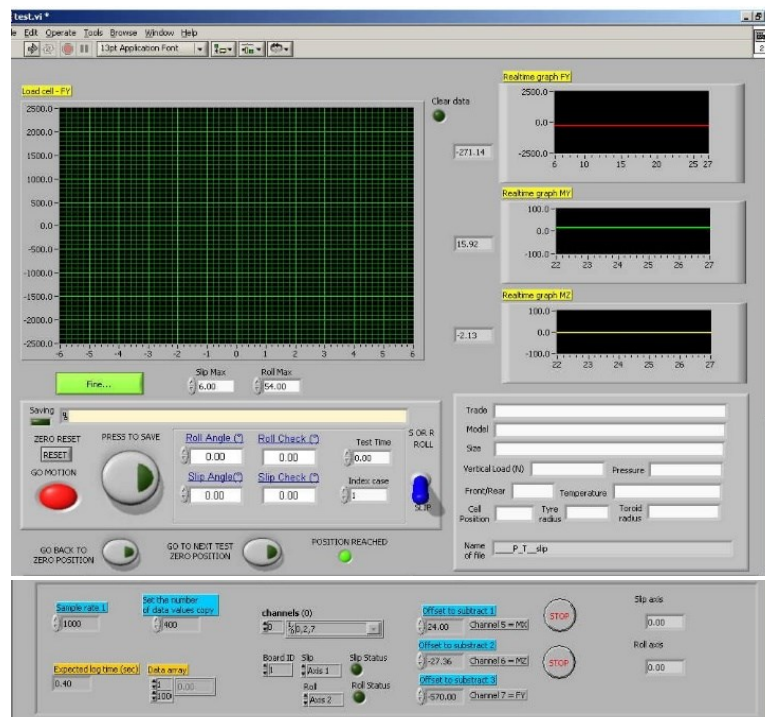


Figure 16: Front panel of the old software

2.4 Software update

2.4.1 First stage

It focused on simplifying the test procedure and reducing the time. The motion control and DAQ software were joined together into one unique program. It was built using Labview 2012 (the latest available version) to benefit from the new features and simplify the code. The motion control code was rebuilt from zero, using the new features of Labview (Figure 17) while the DAQ code [22] remained almost the same with some minor adjustments (Figure 18).

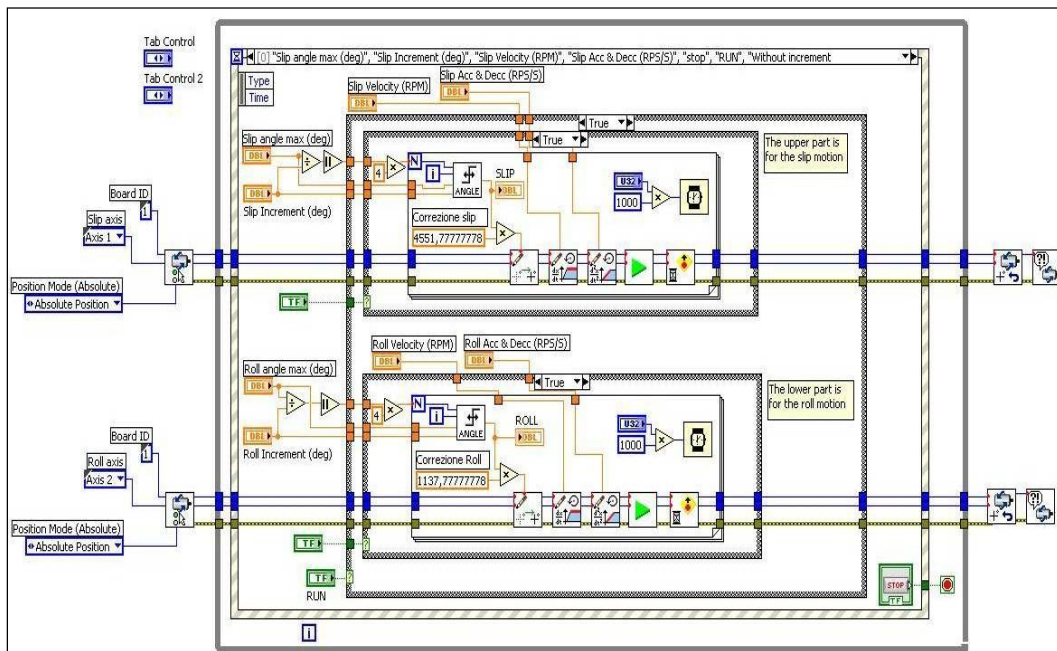


Figure 17: New control block diagram.

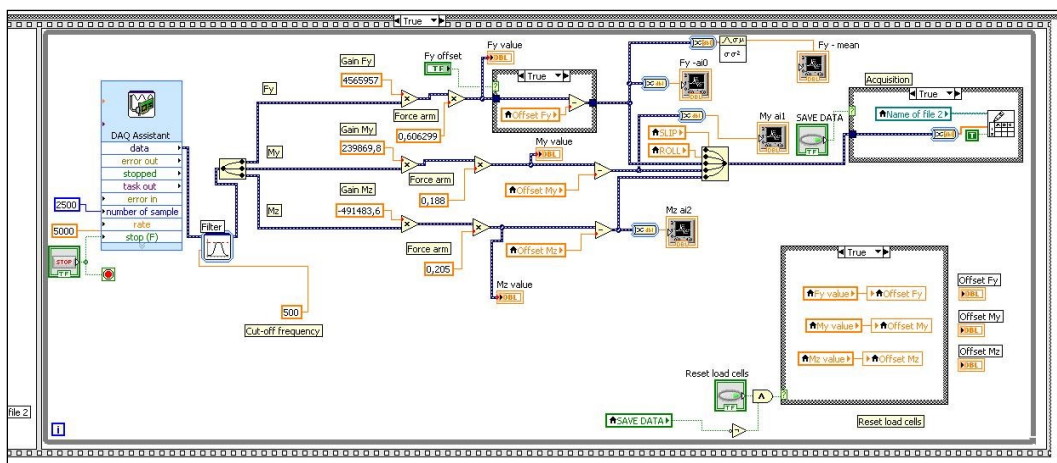


Figure 18: New DAQ block diagram

The front panel was redesigned (Figure 19) to be user friendly since it represents the interface between the user and the machine. An update history was created to allow the user to track and understand every modification in the code.

This software version asks the user to insert some inputs related to the tire characteristics (such as toroid radius and rolling radius) and others related to the test (such as the vertical load, height of the M_y load cell, the slip and or roll angle).

The output file (.txt file) contains the inserted input, the motion angles (slip or camber) and the measured data (F_y, M_y, M_z) from the test session. The file is directly imported in Matlab for data elaboration.

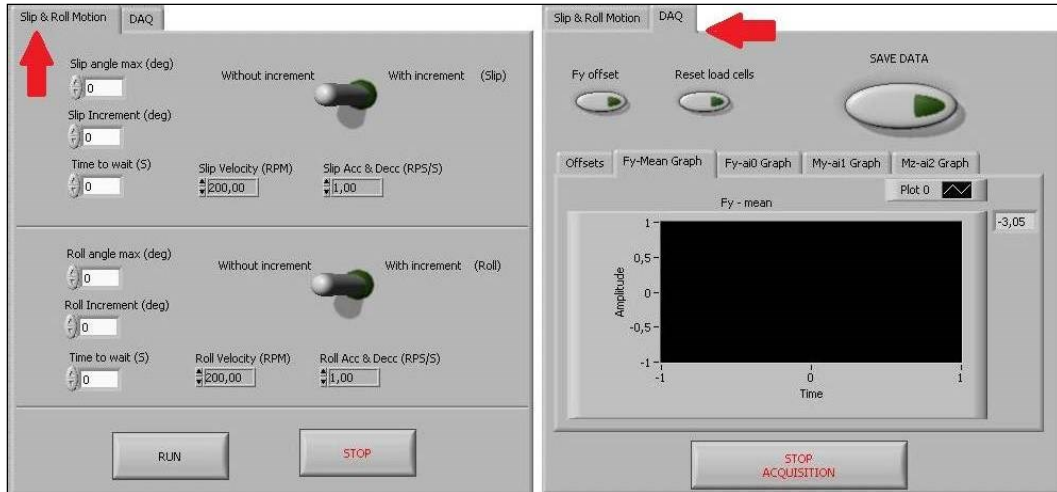


Figure 19: New front panel – First stage

2.4.2 Final stage

The front panel was organized and divided into four sections (Figure 20) to prevent the user from forgetting any necessary step in the procedure. A message box appears directly after launching the application, to remind the user of all the precautions and steps to do before starting a test run. Safety switches were added to avoid running the wrong test.

The graphs on the front panel allows the visualization of the measurements in real time during the test session. A red led is enabled every time a test runs which helps the user to identify the end of the test.

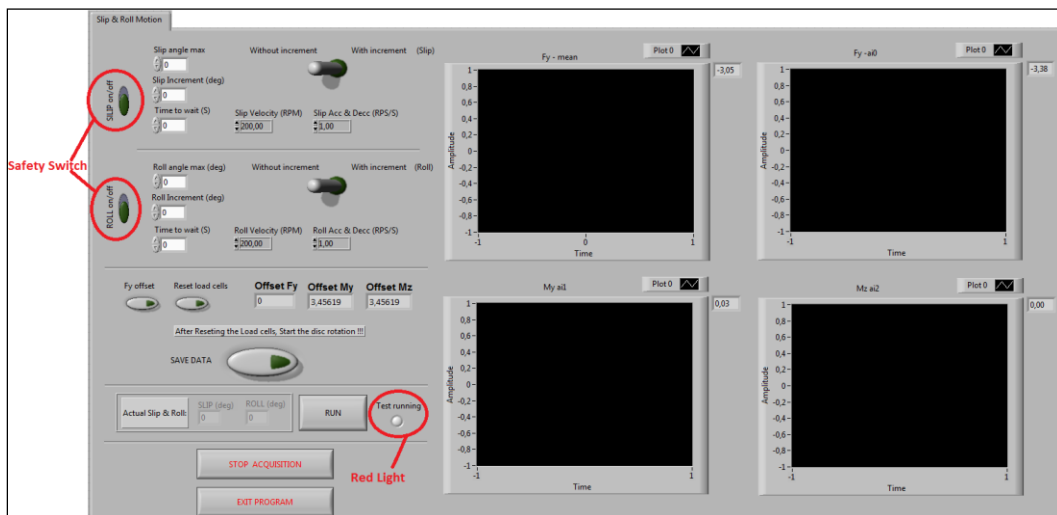


Figure 20: New front panel – Final stage

2.5 Instructions

The instruction manual is found on the server in the “Mototiremeter” folder and also on the desktop of the workstation’s computer. It explains the major precautions and steps for new users to prevent damaging the machine or performing wrong tests.

2.5.1 Hardware

- Switch the power on (the black switch on the metallic box hanged on the wall).
- Power on the NI-DAQ chassis and the power supply by switching on the red switch (Figure 21).

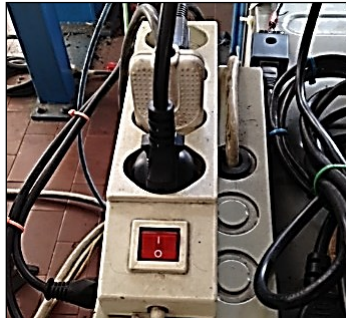


Figure 21: Switch to power the hardware

- Connect the Ethernet cable of the NI-DAQ chassis to the computer (Figure 22).



Figure 22: Ethernet cable for NI-DAQ chassis

- Make sure the sensors cables numbered 0, 1 and 2 are respectively connected to the slots CH0, CH1 and CH2 of the first NI-9237 module on the NI-DAD chassis (Figure 23).



Figure 23: Cable connections to the NI-9237 for “Mototiremeter”

2.5.2 Software

- Start the NI-MAX software to make sure that the hardware is functioning properly.
- In NI-MAX go to the tree on the left and deploy the section **devices and interfaces**, click on **network devices** followed by **NI-cDAQ-9188**. This is the chassis which contains the modules, normally it is already reserved in NI-MAX (in case it is not, click on the **reserve chassis** button) so just click on the reset button to activate it and make sure that it recognize the two modules plugged in.
- Back to the tree on the left, deploy the section **NI motion devices** and then click on **PCI-7344**. Click on **reset device** followed by **initialize**. This defines the new reference of the motion controller, so be sure to perform this step after making sure that the wheel is centered at zero slip and zero camber angle.
- Switch on the step motors from the small switchbox on the table (Figure 15).
- Start Labview and choose the latest version of the software which is found in the "Mototiremeter" folder on the Local disk (Figure 24).

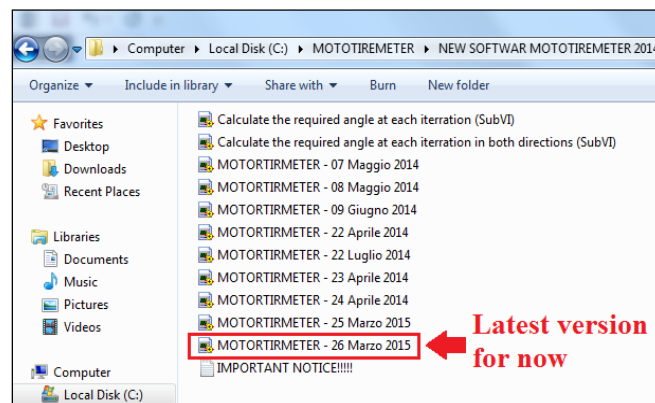


Figure 24: Path of the software for current machine

- Once the software is open you can directly run it, at the beginning it reminds you to check the previous steps before testing, as a precaution, then it ask you if you want to enable data acquisition. Press yes and choose the location to save (the file format will be .txt).
- Enter the values for the vertical load, toroid radius, rolling radius and the height of the load-cell that measure the M_y component.
- The software layout is divided into four sections to prevent you from forgetting any step. Start by switching on the slip (or roll) switch to activate the desired panel.
- Choose between the test with or without increment
- Enter the desired values for maximum angle, increment angle and time interval.
- Go to the second step and reset the load cell until you see approximate zeros on the graphs.
- After resetting, turn on the rotating disk to the desired speed. (It is important to reset before turning the disk on in order to know the value of the lateral force due to the curvature).
- Go to third step and press the "SAVE DATA" button to record data.
- Press RUN to start the test.
- The led "test running" will enable (red color) until the end of the test run.
- When the red led is disabled go to the fourth step and press "STOP ACQUISITION" followed by "EXIT PROGRAM".

Chapter 3 - Tire tests & Data elaboration

During the thesis, many tires were tested for different applications ranging from scooters to racing. Section 3.1 describes the various tests procedures while section 3.2 illustrates some results for three tested tires; Michelin, Dunlop and Brembo. The tires size and type are not mentioned, for confidentiality purposes, as well as the measurements values. The tires are not in the same category and not for the same application so it is impossible to compare them. The objective of section 3.2 is just to explain the general idea behind the graph and its purpose.

Sections 3.3, 3.4 and 3.5 explain, in depth, the evolution of the Matlab code developed for the data elaboration software used to process the tire measurements from the testing session.

Finally section 3.6 describe briefly the written articles that involved tire testing on the Mototiremeter.

3.1 Test Description

3.1.1 Rolling radius

The rolling radius of a tire is the distance between the center of the wheel and the contact patch. Typically, the larger the diameter of the tire, the greater the rolling radius. The tire behaves as a linear spring in vertical direction therefore the effective rolling radius varies significantly with tire load. The effective rolling radius is used in vehicle dynamics calculations to have the accurate height of the wheel center due to the tire deformation.

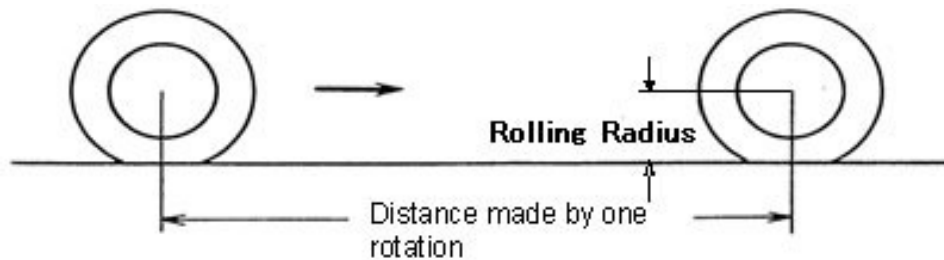


Figure 25: Rolling Radius measurement

Figure 25 explains the procedure for measuring the rolling radius (rr). The measured distance made by one complete wheel's rotation is the perimeter (P) of the tire. Therefore the rolling radius is calculated from the following equation:

$$P = 2 \times \pi \times rr \quad (3-1)$$

At our laboratory, we measure the distance made by five complete wheel's rotation in order to obtain an average rolling radius.

3.1.2 Toroid Radius

A tire's cross section is assumed to be a circle therefore measuring its radius represents the toroid radius (tr). Figure 26 shows the appropriate tool used for such measurement. In case of a used tire, it is important to mount the tool on the less consumed section since the toroid radius vary with tire wear. The tool is centered on the tire by positioning the central tip at the middle of the section. After that, the two vertical sides are adjusted until contact with the tire sidewalls.

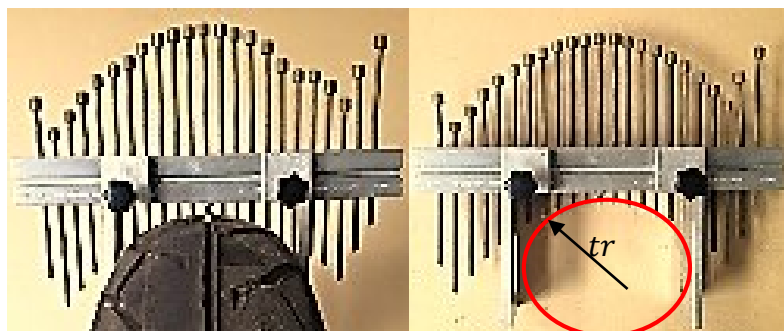


Figure 26: Toroid radius measurement

Once it is mounted and centered on the wheel, the vertical tips are screwed until contact with the tire surface therefore reproducing the tire cross section. Finally the tool is removed and the distance, from the horizontal reference until each extremity, is measured.

The measurements are divided into left and right sets because a tire is not perfectly symmetrical and might be consumed more on one side. The toroid radius is calculated by mean of a small Matlab code. The measurements are inserted in the program which performs a circle fitting for each set and a global fitting for both sets (as shown in Figure 27). This method offers a quality control of the measurements and evaluate if the error is acceptable, the closer the values are, the smaller the error.

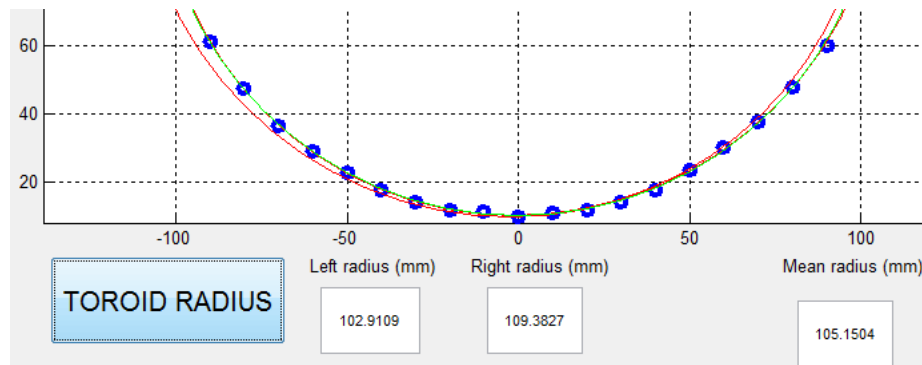


Figure 27: Toroid radius calculation software

3.1.3 Radial stiffness

Pneumatic and solid rubber tires must be considered as elastic components [23]. Thus an applied load (F) in the vertical direction will result in a corresponding global deformation (Δ) in the same direction. Therefore the tire can be described as a spring. The tire's spring constant (K_R) is the radial stiffness. The radial stiffness test (Figure 28) consist of increasing the applied vertical load and measuring the corresponding displacement. The radial stiffness is then deduced from the linear relation between the force and the displacement.

$$F = K_R \times \Delta \tag{3-2}$$



Figure 28: Radial stiffness test

3.1.4 Lateral Stiffness

Similar to radial stiffness (¶ 3.1.3), an applied load in the lateral direction (Figure 29) of the tire will result in a lateral deformation (Figure 30). The resulting tire's spring constant (K_L) is the lateral stiffness.

Both radial and lateral stiffness depend on some tire characteristics like inflation pressure, mechanical structure and type of rubber. In addition, the lateral stiffness varies with the vertical load therefore the test is repeated at different vertical loads.



Figure 29: Lateral stiffness test



Figure 30: Lateral displacement measurement

3.1.5 Side Slip

The side slip test (Figure 31) measures the lateral force, self-aligning and rolling resistance torque in function of the slip angle variation for zero degree camber. The side slip variation is applied in both directions, positive and negative intervals. The interval is defined by the maximum angle (until 9°), the increment angle (usually 0.5°) and the delay time (per default 5 seconds). The test is usually repeated for several vertical load [14], different inflation pressure [15] and sometimes at various speed [24].

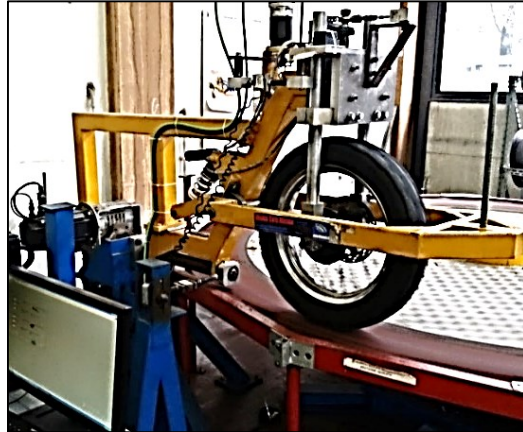


Figure 31: Side slip test

3.1.6 Camber

The camber test (Figure 32) measures the lateral force, twisting and rolling resistance torque in function of the camber angle variation for zero degree side slip. The camber variation is applied in both directions, positive and negative intervals. The interval is defined by the maximum angle (until 50°), the increment angle (usually 2°) and the delay time (per default 5 seconds). The test is also repeated for several vertical loads [14], different inflation pressure [15] and sometimes at various speed [24].



Figure 32: Camber test

3.1.7 Combined Test

The machine's update offers the possibility of performing combined tests (Figure 33) which represent the real case of a motorcycle tire during cornering. The combined side slip test measures the lateral force, self-aligning and rolling resistance torque in function of the slip angle variation for a camber value different than zero. The combined camber test measures the lateral force, twisting and rolling resistance torque in function of the camber angle variation for a side slip value different than zero. The test can also be repeated for several vertical loads [14], different inflation pressure [15] and sometimes at various speed [24].



Figure 33: Combined test

3.2 Test results

The following sections present a qualitative interpretation of the tests carried on three front and three rear tires. For confidentiality purposes, tires size and type are not mentioned as well as the measurements values therefore the comparison cannot reflect the superiority of a tire over another. The aim is to show the trends of the curves and their signification. The three tested tires were a Michelin, a Dunlop and a Brembo. The blue curve is represented as Tire A, the red curve as Tire B and the green curve as Tire C.

3.2.1 Radial stiffness

Figure 34 illustrates the results of radial stiffness measurements (¶ 3.1.3) carried on the three front tires. The dots in the graph, represents the cumulated vertical load applied (in Newton) in function of the total vertical displacement. The values are fitted with a linear regression model where the slope represents the radial stiffness. Tire B shows the highest radial stiffness while Tire A shows the lowest.

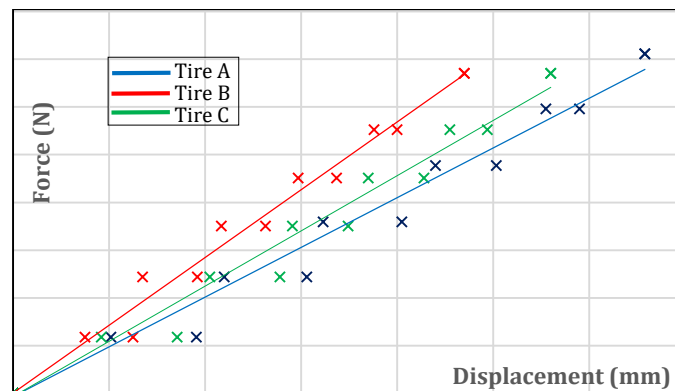


Figure 34: Radial stiffness results for front tires

The same concept applies for the rear tires shown in Figure 35, where Tire B and Tire A present almost equal values for radial stiffness while Tire C has the smallest radial stiffness.

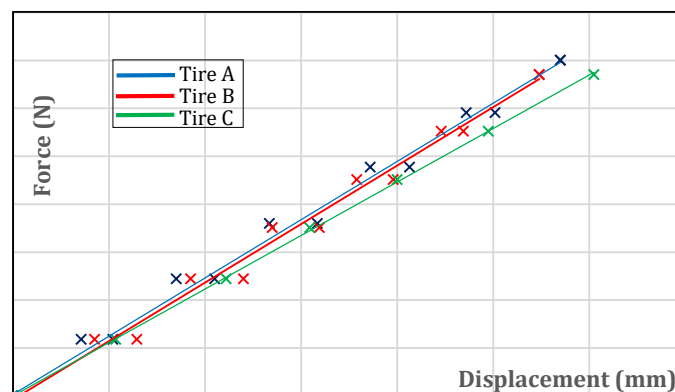


Figure 35: Radial stiffness results for rear tires

3.2.2 Lateral stiffness

Figure 36 demonstrate the results of lateral stiffness measurements (¶ 3.1.4) carried on the three front tires at a vertical load of 1000 N. The dots in the graph, represents the cumulated lateral load applied (in Newton) in function of the total lateral displacement. The values are fitted with a linear regression model where the slope will be the lateral stiffness. Tire B and Tire C show almost equal values of lateral stiffness while Tire A has a much smaller lateral stiffness.

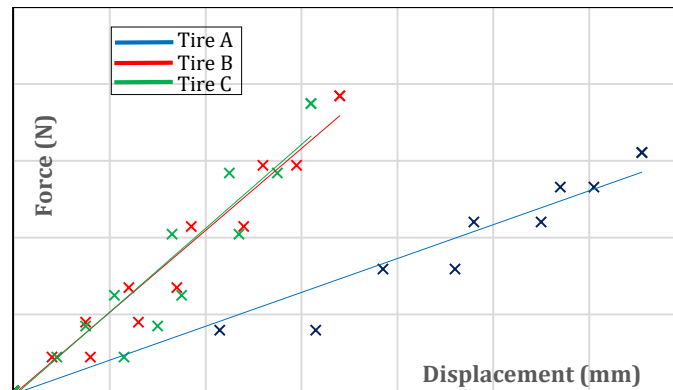


Figure 36: Lateral stiffness results for front tires

The rear tires results are shown in Figure 37 where the test was also carried at a vertical load of 1000N. Tire B presents the highest lateral stiffness and Tire A presents the smallest lateral stiffness. The lateral stiffness of Tire C comes in between.

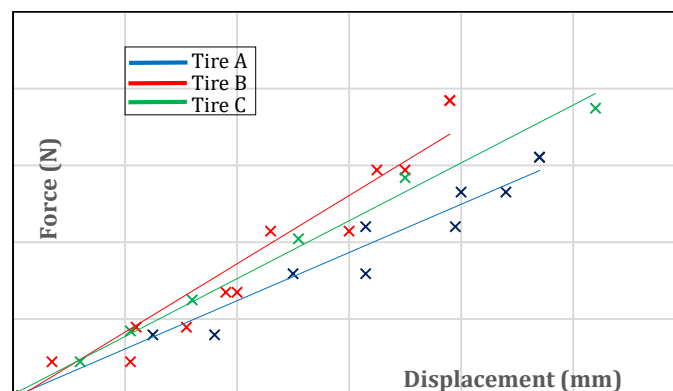


Figure 37: Lateral stiffness results for rear tires

3.2.3 Side Slip

The results in Figure 38 are the lateral force in function of side slip variation (¶ 3.1.5), under a vertical load of 1000 N, for the three front tires. The dots and curves are respectively, the raw data and the Pacejka fitting (¶ 3.3.4). The slope of the linear part is associated to the side slip stiffness of the tire.

Tire A shows the smallest side slip stiffness as well as the smallest side slip force at all tested slip angles. At the linear part of the curve, Tire B and Tire C present equal values of side slip stiffness, however after a specific value of slip angle, Tire B delivers higher side slip force than Tire C for the same side slip.

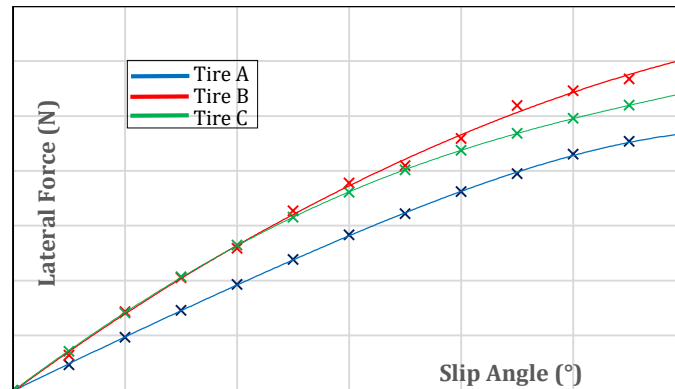


Figure 38: Side slip force for front tires at vertical load 1000N

Figure 39 shows the results of the same test performed on the three rear tires under the same conditions. Tire C shows the highest side slip stiffness and delivers the highest side slip force at all slip angles. On the other hand, Tire B seems to be slightly inferior to Tire A in terms of side slip stiffness and side slip force.

For this interval of slip angle, the trend of Tire A starts to become flat which indicates the beginning of saturation. It implies that a larger increment in slip angle will induce a smaller gain in lateral force. However Tire B does not show saturation yet, which suggest that it might deliver higher side slip force than Tire A for bigger slip angles.

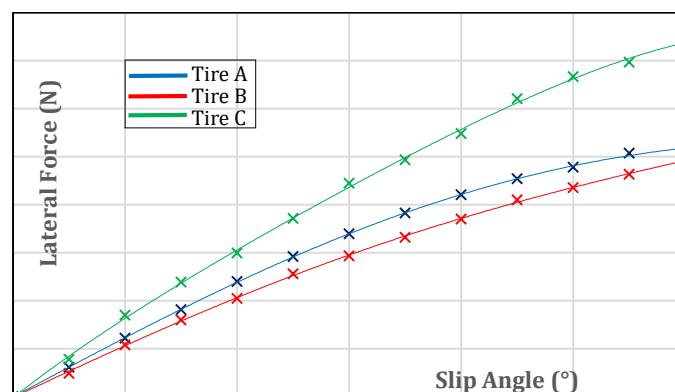


Figure 39: Side slip force for rear tires at vertical load 1000N

3.2.4 Camber

The results in Figure 40 are the lateral force in function of camber variation (¶ 3.1.6), under a vertical load of 1000 N, for the three front tires. The dots and curves are respectively, the raw data and the Pacejka fitting (¶ 3.3.4). The slope of the linear part is associated to the camber stiffness of the tire.

Tire C demonstrates the highest camber stiffness as well as the highest camber force at all camber angles. In contrary, Tire A shows the lowest camber stiffness and also the lowest camber force at all tested camber angles. Tire B fits in between the two in term of camber stiffness and camber force at all tested camber angles.

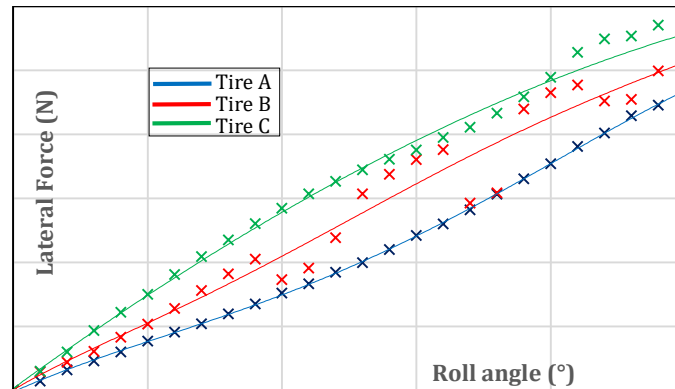


Figure 40: Camber force for rear tires at vertical load 1000N

3.3 TIRE_FITTING_V1

3.3.1 Purpose

The exported file from the tire measurements holds the necessary data for the elaboration. Such data are the measured forces and moments with the corresponding slip and camber angles from the test sessions, as well as the applied vertical load and the tire characteristics like rolling radius (¶ 3.1.1) and toroid radius (¶ 3.1.2).

In order to analyze the test measurements, the program must cancel the turn force (Figure 41) generated by the curvature effect of the rotating disc. Once the curvature effect is removed (¶ 3.3.3), the program generates the necessary graphs of the measurements. It calculates the necessary tire parameters by fitting the curves with the magic formula [19]. Finally all graphs are saved and the results are exported in an excel file.

The previous data elaboration was performed by mean of an excel file that was a black box. It initiated the need of a simpler, more advanced program which was built using Matlab [25].

3.3.2 Inputs

This version of the software asks the user to import the measurements files (Table 1) from the test sessions. Each desired vertical load requires a side slip test (¶ 3.1.5) and a camber test (¶ 3.1.6). The program guides the user towards the correct order of importing the data.

Fz (vertical load)	Slip angle	Roll angle	Fy	My	Mz	tr	rr	h

Table 1: Measurement file from test session

"tr" and "rr" are respectively the toroid and rolling radius of the tire, both expressed in millimeters, and "h" is the "M_y" load cell height from the surface of the rotating disc.

Before initiating the Pacejka fitting, the program asks the user to choose the limit slip and camber angle for fitting based on the visualization of the raw measurement curves. This step was added in order to neglect the data at high angles in case of bad measurements due to excessive vibration therefore allowing a more accurate curve fitting.

3.3.3 Outputs

Based on the delay time specified by the user for the test session, the DAQ system records many measurements for each slip (or camber) angle depending on the measurement frequency of the system. The result is a large number of data which is why the program calculates the average of the measured force and moments for each slip (or camber) angle. After reducing the number of data, the turn force generated by the curvature effect of the rotating disc must be cancelled.

Figure 41 illustrates the turn force during a positive and a negative slip angle without camber angle ($\gamma=0^\circ$). The turn force aims always to the outside of the rotating disc independently from the sign of the slip angle. Therefore it adds up to the side slip force in case of negative slip angle and subtract from it in case of positive slip angle.

$$F_{y_{\text{measured } (+\alpha)}} = F_{y_{\text{side slip}}} - F_{\text{turn}} \quad (3-3)$$

$$F_{y_{\text{measured } (-\alpha)}} = -F_{y_{\text{side slip}}} - F_{\text{turn}} \quad (3-4)$$

Subtracting the measured force of negative slip angle from the one of positive slip angle and dividing the total by two will arbitrarily cancel the turn force. This method assumes that the tire is perfectly symmetrical therefore the sideslip force generated in case of positive and negative slip angle is equal in absolute value but opposite in sign.

$$F_{y_{\text{slip}}} = \frac{F_{y_{\text{measured } (+\alpha)}} - F_{y_{\text{measured } (-\alpha)}}}{2} \quad (3-5)$$

The same calculation is valid for the measured moments and also in the case of varying the camber angle without slip angle ($\alpha=0^\circ$).

Once the turn force is cancelled, the measurements and the appropriate fitting curves can be presented for further analysis. Figure 42 illustrates the raw data, in dots, with the appropriate fitting curves for the normalized side slip force at three different vertical loads.

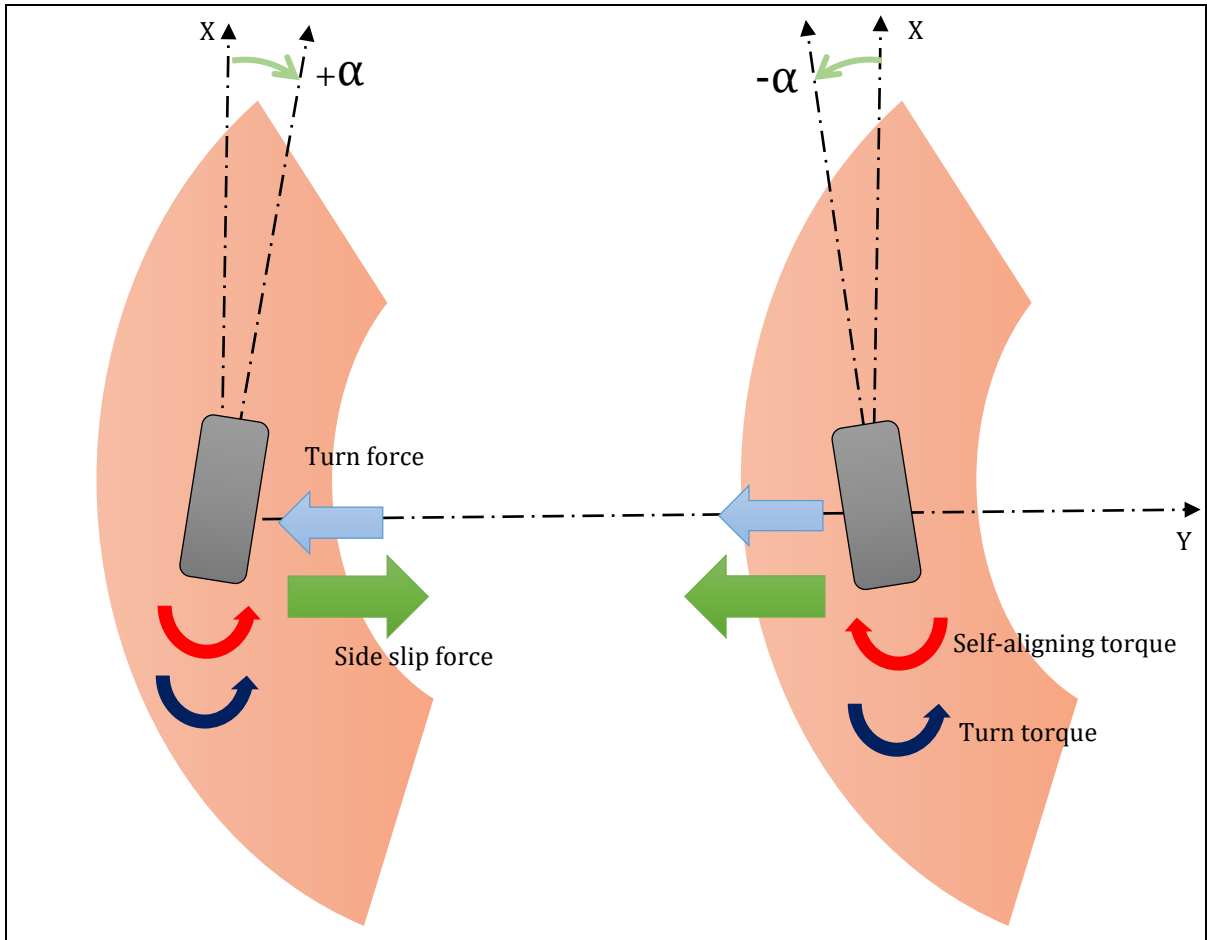


Figure 41: Curvature effect in case of positive and negative side slip angle (α)

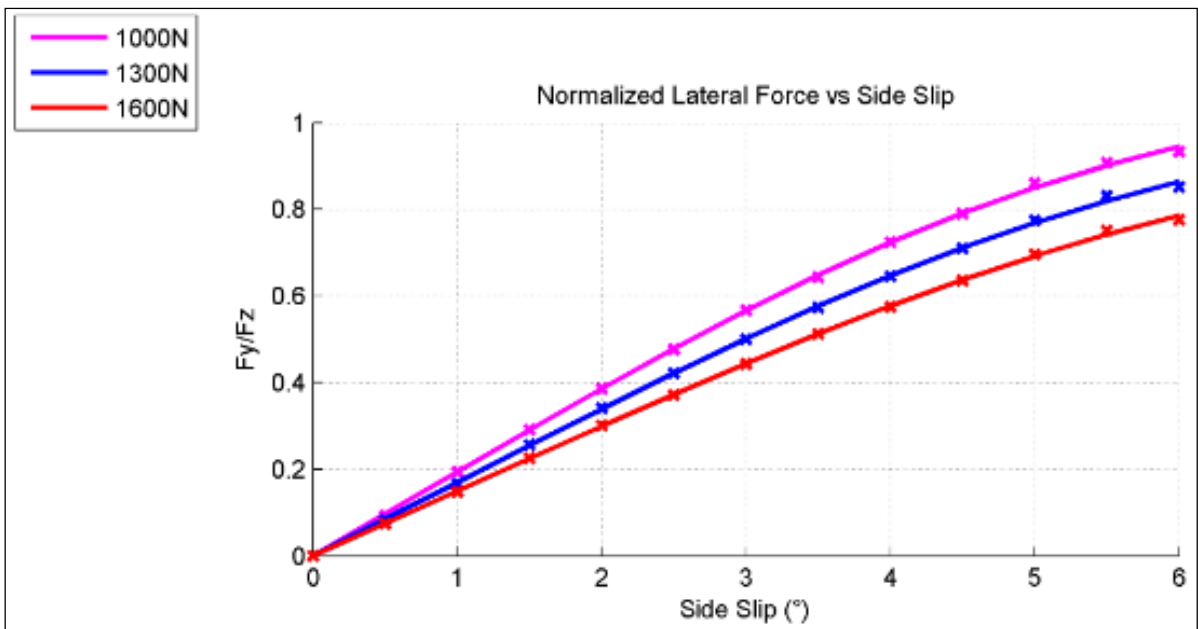


Figure 42: Corrected curvature data (dots) with Pacejka fitting curves

Finally the graphs are automatically saved and the results are exported into an excel file. The first excel sheet holds the measurements results after cancelling the turn force, for side slip and camber tests and at all vertical loads (Figure 43). The second excel sheet is identical to the first one, but it contains the data for the fitting curves. The last excel sheet provides all the Pacejka coefficients (Figure 44) which are used to build tire models later on.

	A	B	C	D	E	F	G	H	I	J	K	L	M	N
1	1000 N	1000 N	1000 N	1000 N	1500 N	1500 N	1500 N	1500 N	2000 N	2000 N	2000 N	2000 N		
2	Slip	F _y	M _y	M _z	Slip	F _y	M _y	M _z	Slip	F _y	M _y	M _z		
3	0,0	0,00	0,00	0,00	0,0	0,00	0,00	0,00	0,0	0,00	0,00	0,00		
4	0,5	155,02	-0,17	-2,40	0,5	170,11	-0,08	-3,87	0,5	200,00	0,01	-4,61		
5	1,0	339,84	0,00	-5,23	1,0	379,44	-0,06	-8,64	1,0	341,00	0,04	-9,42		
6	1,5	476,37	-0,02	-6,62	1,5	531,52	-0,16	-11,31	1,5	517,88	0,12	-14,57		
7	2,0	598,06	-0,23	-7,79	2,0	667,37	-0,52	-14,27	2,0	722,49	0,17	-18,38		
8	2,5	742,57	0,05	-9,22	2,5	846,29	-0,67	-15,99	2,5	860,21	0,32	-22,34		
9	3,0	889,50	0,10	-8,93	3,0	1020,74	-0,97	-16,14	3,0	1020,91	0,51	-26,20		
10	3,5	986,73	0,09	-8,04	3,5	1142,43	-1,07	-16,88	3,5	1209,44	0,65	-28,12		
11	4,0	1095,83	0,25	-8,33	4,0	1282,17	-0,91	-18,17	4,0	1373,86	0,72	-26,04		
12	4,5	1240,66	0,58	-7,49	4,5	1450,63	-0,67	-17,01	4,5	1501,96	0,98	-27,85		
13	5,0	1332,86	0,27	-5,38	5,0	1565,30	-0,56	-16,30	5,0	1681,19	1,09	-25,86		
14	5,5	1392,93	0,58	-3,67	5,5	1649,04	-0,39	-15,31	5,5	1856,17	1,31	-23,30		
15	6,0	1479,25	0,76	-3,23	6,0	1760,61	0,34	-13,17	6,0	1988,87	1,18	-18,15		
16	6,5	1575,75	1,43	-1,49	6,5	1900,10	0,33	-10,98	6,5	2113,00	1,43	-16,38		
17	7,0	1634,43	1,11	0,91	7,0	2010,70	0,45	-10,53	7,0	2231,22	1,51	-14,92		
18	7,5	1669,23	1,42	-0,37	7,5	2098,93	0,55	-9,26	7,5	2340,46	1,70	-15,28		
19	8,0	1733,45	1,42	3,96	8,0	2198,32	0,56	-6,54	8,0	2403,84	2,44	-17,00		
20	8,5	1807,54	1,70	3,24	8,5	2294,30	0,84	-2,90	8,5	2453,50	3,23	-21,47		
21	9,0	1806,00	1,55	3,82	9,0	2312,40	0,28	-2,03	9,0	2528,44	3,70	-24,02		
22														

Figure 43: Exported data in Excel

	A	B	C	D	E	F	G	H	I	J	K	L	M	N
1		1000 N	1000 N	1000 N	1000 N			1000 N	1000 N			1000 N	1500 N	2000 N
2		B	C	D	E			mr	tw		Mean My (N.m)	-0,04	1,05	2,81
3	Fy Slip	3,66413	2,87481	1,69938	0,06019		My Slip	0,00371	25,09295					
4	Fy Roll	0,91129	1,09320	1,69938	0,25264		My Roll	0,00049	-4,60118					
5	Mz Slip	3,93356	0,68145	-0,08440	18,07877		Mz Roll	0,02409	0,41346					
6														
7														
8		1500 N	1500 N	1500 N	1500 N			1500 N	1500 N					
9		B	C	D	E			mr	tw					
10	Fy Slip	4,19525	2,27257	1,40485	-0,99748		My Slip	-0,00607	-35,45288					
11	Fy Roll	0,35663	3,08575	1,40485	-0,01002		My Roll	0,00210	1,39739					
12	Mz Slip	3,80731	0,62500	-0,11192	14,54341		Mz Roll	0,02675	0,23569					
13														
14														
15		2000 N	2000 N	2000 N	2000 N			2000 N	2000 N					
16		B	C	D	E			mr	tw					
17	Fy Slip	2,59602	2,37793	1,61818	-2,14668		My Slip	0,00516	11,95978					
18	Fy Roll	0,20618	3,99669	1,61818	-9,99982		My Roll	0,00252	2,62266					
19	Mz Slip	3,08201	0,62904	-0,15260	21,42623		Mz Roll	0,02880	-0,56668					
20														

Figure 44: Exported Pacejka coefficients in Excel

3.3.4 Fitting formulas

The side slip and camber force are respectively the lateral force in function of the side slip and camber variation while the self-aligning torque represents the moment around the axis "z" in function of the side slip. The three are fitted by mean of the general form of the Magic Formula [19], [26], [27]. In the future it might be interesting to use more advanced magic formulas which take into consideration with tire pressure and even tire temperature.

$$F_y = D \times \sin (C \times \operatorname{atan} (B \times x - E \times (B \times (x - \operatorname{atan} (B \times x)))))) \quad (3-6)$$

B	Stiffness factor
C	Shape factor
D	Peak factor
E	Curvature factor
x	Slip or Camber angle (rad)

Table 2: Magic formula coefficients

The twisting torque is defined by the moment around the axis “z” in function of the camber angle and it is fitted using the following equation.

$$M_z = m_r \times \gamma \times (1 + t_w \times \gamma^2) \tag{3-7}$$

m_r	Stiffness factor
t_w	Curvature factor
γ	Camber angle (rad)

Table 3: Twisting torque coefficients

The rolling resistance torque is defined by the moment around the axis “Y” in function of side slip and camber. It is generated by the longitudinal force from the rolling resistance. The fitting curve uses the same formula of the twisting torque with the addition of the constant M_{y0} .

$$M_y = m_r \times x \times (1 + t_w \times x^2) + M_{y0} \tag{3-8}$$

m_r	Stiffness factor
t_w	Curvature factor
M_{y0}	Rolling resistance torque at zero angle
X	Slip or Camber angle (rad)

Table 4: Rolling resistance torque coefficients

3.3.5 Fundamental elements

This section describes the principal matrices created in the Matlab code in order to help understanding how the programs works. The side slip test and camber test measurements, for a vertical load, are imported and stored respectively in “SLIP_DATA” and “ROLL_DATA” (Table 1).

As mentioned previously, the program calculates the average measurement for each side slip angle and stroes the values in “ALL_SLIP” (Table 5). The same concept is applied for camber angle and the values are stored in “ALL_ROLL”. Both are three dimensional matrices in order to store the data for several vertical load.

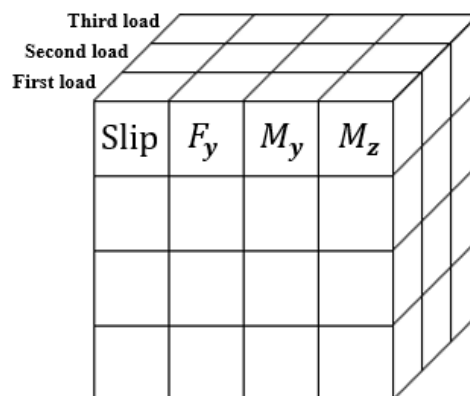


Table 5: ALL_SLIP

The program cancels the turn force generated from the curvature effect and stores the data in “ALL_SLIP_C” and “ALL_ROLL_C”. Once the turn force is cancelled, the fitting curves are generated and the data are stored in “ALL_SLIP_F” and “ALL_ROLL_F”. These four matrices have the same layout of “ALL_SLIP” (Table 5).

The Pacejka coefficients from the curves fitting are later on stored in “PACEJKA” and “PACEJKA_MYMZ” which are three dimensional matrices in order to store the coefficients for all the vertical loads.

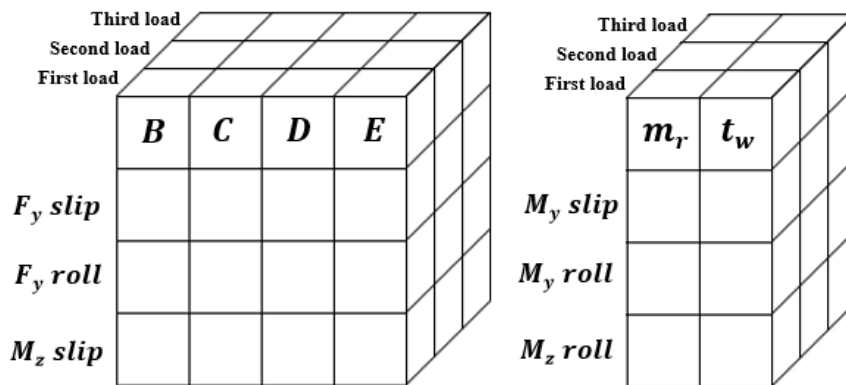


Table 6: PACEJKA & PACEJKA_MYMZ

3.3.6 Advantages

This version offers many advantage over the previous software. It imports, at once, all the measurements files for the different vertical loads and outputs all the results into one excel file and two figures. The program is user friendly and prevent the new users from making mistakes. Finally the code was built properly and comes along with an update history to allow future improvements.

3.4 TIRE_FITTING_V3

3.4.1 Purpose

The new tire machine (Chapter 4) is equipped with a load cell capable of measuring the six components at the wheel therefore the measurements files will contain more data. The aim of the modification is to adapt the Matlab code for the new format in order to have a unique software for both tire machine.

3.4.2 Inputs

The user shall indicate the machine used for the test session by entering the number one if the tests were carried on the old machine (Chapter 2) or the number two for the new machine (Chapter 4). Then he specifies the number of vertical load tested, he can reach up to five vertical loads which is more than necessary. The rest of the inputs remained identical.

3.4.3 Outputs

The two figures contain additional graphs for the overturning moment (M_x) in function of side slip (α) and camber (γ) and also the longitudinal force (F_x) in function of slip ratio (S_r). The layout of the excel file remained identical to the previous version (§ 3.3). The additional measured components are simply added.

3.4.4 Fitting formulas

The slip ratio (S_r) is defined as the percentage of longitudinal slip created by the difference between the rotational speed (Ω_w) of the wheel and its longitudinal speed (V_l).

$$V_l \neq \Omega_w \times rr \tag{3-9}$$

$$S_r = -\left(\frac{V_1 - \Omega_w * r r}{V_1}\right) \quad (3-10)$$

The longitudinal force (F_x) is defined by the force along the axis "x" in function of the slip ratio and it is fitted with a curve using the same Magic Formula used for the side slip force (¶ 3.3.4).

$$F_x = (D_x \sin[C_x \arctan(B_x \times S_r - E_x(B_x \times S_r - \arctan(B_x \times S_r)))] \quad (3-11)$$

$$D_x = (\mu_x \times F_z) / F_z \quad (3-12)$$

$$C_x = P_{Cx1} \times \lambda_{Cx} \quad (3-13)$$

$$B_x = \frac{P_{Kx1} \times F_z \times \lambda_{Kxk}}{C_x \times D_x \times F_z} \quad (3-14)$$

$$E_x = P_{Ex1} \times \lambda_{Ex} \quad (3-15)$$

The overturning moment (M_x) is defined by the moment around the axis "X" in function of side slip and camber angle. In the case of side slip without camber, due to the lateral deflection connected with the side force (F_y), the point of application of the resultant vertical load moves in the direction of the side force and as a result generates the overturning moment [19], [28].

$$M_x = -F_z \times \left(\frac{F_y}{K_L}\right) \quad (3-16)$$

During the test session, the vertical load (F_z) and the lateral stiffness (K_L) are assumed to be constant therefore the overturning moment is related to the side slip force by a linear equation. This means that it can be fitted with the same magic formula as before (¶ 3.3.4).

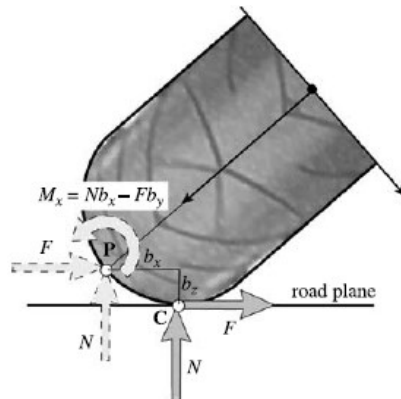


Figure 45: Overturning moment

With camber change (Figure 45) the induced overturning moment comes from the vertical load and the lateral force, and since it seems to be related to the lateral force by a linear equation therefore it also can be fitted with the same previous magic formula [29].

$$M_x = F_z \times \left(\frac{F_y}{K_L}\right) - F_y \times \left(\frac{F_z}{K_R}\right) \quad (3-17)$$

3.4.5 Additional elements

When tests are carried on the new tire machine, the data files contain additional measurements therefore the matrices “SLIP_DATA” and “ROLL_DATA” were modified (Table 7) in order to store the additional data.

Fz (vertical load)	Slip angle	Roll angle	Fx	Fy	Mx	My	Mz	tr	rr	h

Table 7: Modified SLIP_DATA and ROLL_DATA

A “SLIP_RATIO” has been created to store the slip ratio values which are used later on to plot the longitudinal force. Two extra columns were added to the matrices “ALL_SLIP” and “ALL_ROLL” (Table 5) in order to store the longitudinal force and the overturning moment.

Three additional columns were also added to the matrix “PACEJKA” to store the coefficients for the longitudinal force and overturning moments (§ 3.4.4).

3.4.6 Advantages

This version offers a unique program for processing the measurements from both tire machines. It avoids the user from confusion and it is more user friendly. It can import data consecutively until five vertical load.

3.4.7 Instructions

- Open TIRE_FITTING_V3 in Matlab
- Click on the browse folder icon (Figure 46) on the left, and choose the proper directory where the measurement files are located.

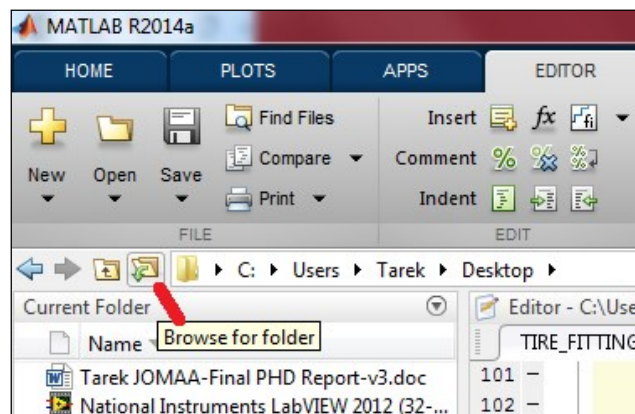


Figure 46: Tire fitting software - Browse folder

- Run the Matlab code
- Enter number one if tests were carried on the old machine and number two for the new machine
- Specify the number of vertical load tested (the maximum is five)
- The program guides you through the sequence for importing the measurement files
- Once all files are imported, the program plots the corrected curvature data (§ 3.3.3)
- Enter the desired limits for the slip and camber angle in order to have the best fitting (§ 3.3.4). The program calculates the Pacejka coefficients and plots the fitting curves (§ 3.3.3)
- Choose a name for the export file which will automatically be saved the directory (§ 3.3.3)

3.5 TIRE_FITTING_V6

3.5.1 Purpose

The measurements present sometimes disturbance due to excessive vibrations of the rotating disk. The previous program performed the data fitting automatically without the interference of the user which often resulted in inaccurate curves or even inadmissible coefficients. The objective from this version is to offer a live interaction between the user and the fitting curves. The program computes the data and outcome an initial fitting that can be manually corrected by the user through a friendly interface. Once the coefficients offer satisfying outcomes the user saves it and proceed to the following vertical load test.

3.5.2 Inputs

The inputs remains identical to the previous version. The user indicates the machine used for the test and the number of vertical load tested then the Matlab code imports all the measurements files. The need of a limit (¶ 3.3.2) slip and roll angle, previously used to improve the fitting, no longer exists since this version offers the possibility of a manual correction.

The curve fitting uses exactly the same Magic formula (¶ 3.3.4) from the previous version and the matrices (¶ 3.4.5) of the Matlab code remained unchangeable. No modification was introduced on the outputs of the program, it maintained the same excel template and figures layout.

3.5.3 Advantages

A user interface was introduced, making the software user friendly. The front panel is organized in a sequence of four steps, leading the user instinctively through the process. The main advantage is characterized by the manual correction of the fitting curves resulting in more reasonable and accurate outcomes.

3.5.4 Instructions

- Open TIRE_FITTING_V6 in Matlab
- Click on the browse folder icon (Figure 46) on the left, and choose the proper directory where the measurement files are located
- Run the code, the user interface panel automatically appears
- Tick the checkbox (Figure 47) for the corresponding test machine. (MACHINE-1 stands for "Mototiremeter" and MACHINE-2 is for the new one)
- Type in the number of vertical load tested.
- Click "IMPORT DATA" to import the measurement files

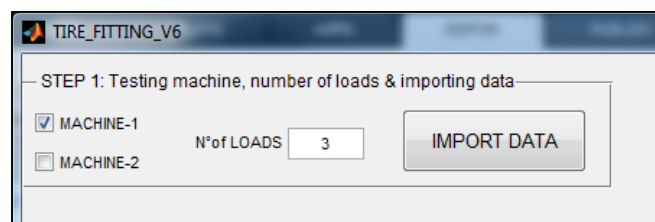


Figure 47: TIRE_FITTING_V6 – Step one

- Click on "FITTING", the program will show the data of the first vertical load, with the initial curve fitting and the Pacejka coefficients (Figure 48)
- In unpleasing fitting, use the sliders on the right side of each graph to adjust the coefficients until satisfactory results (Figure 48).
- Once the correction is finished, Click "Fix Coefficients" in order to save the corrected values
- Repeat the three previous instructions until a message box appears, indicating the last measurement (Figure 48)

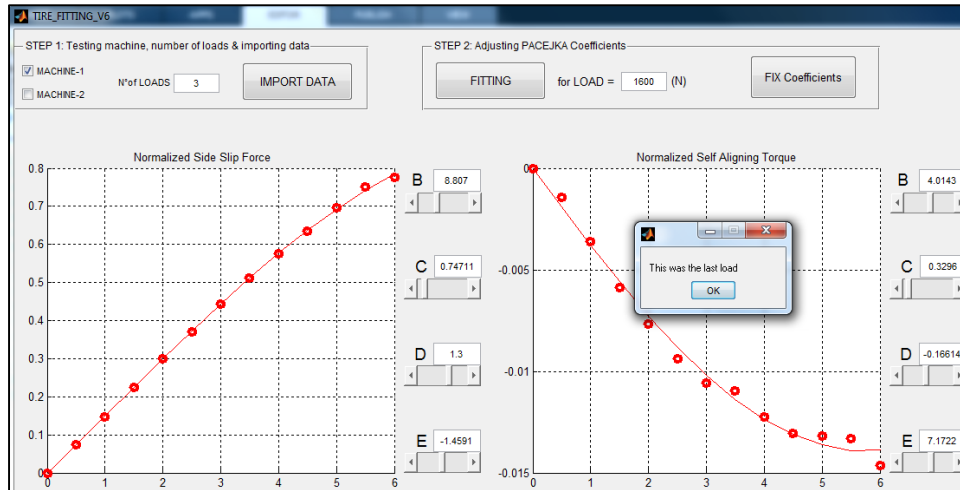


Figure 48: TIRE_FITTING_V6 – Step two

- Once the last measurement is corrected and saved, a message box appears, asking to export the data (Figure 49) therefore click "EXPORT DATA". The results are automatically saved on an excel file, in the directory, under the name "EXPORTED_DATA". A message box will appear to indicate the end of the process.

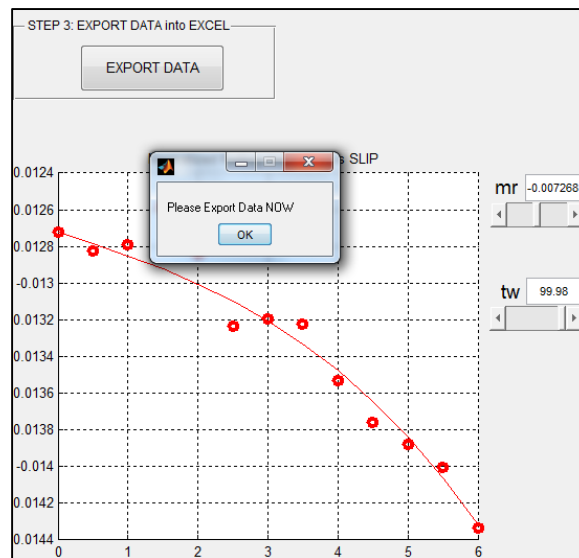


Figure 49: TIRE_FITTING_V6 – Step three

3.6 Issued papers and articles

3.6.1 The effect of the inflation pressure of tires on motorcycle weave stability

The paper [15] focuses on the effect of tires inflation pressure on motorcycles weave stability. Side slip (¶ 3.1.5) and camber (¶ 3.1.6) tests were carried on front and rear tires at different vertical loads and inflation pressures. The desired tire (¶ 3.3.1) parameters are then inserted in an advanced motorcycle multi-body code used for simulations. The simulations results were later on compared with experimental data. The research results show an agreement between tests and simulations where weave stability increases with inflation pressure for the specified range of tire pressure.

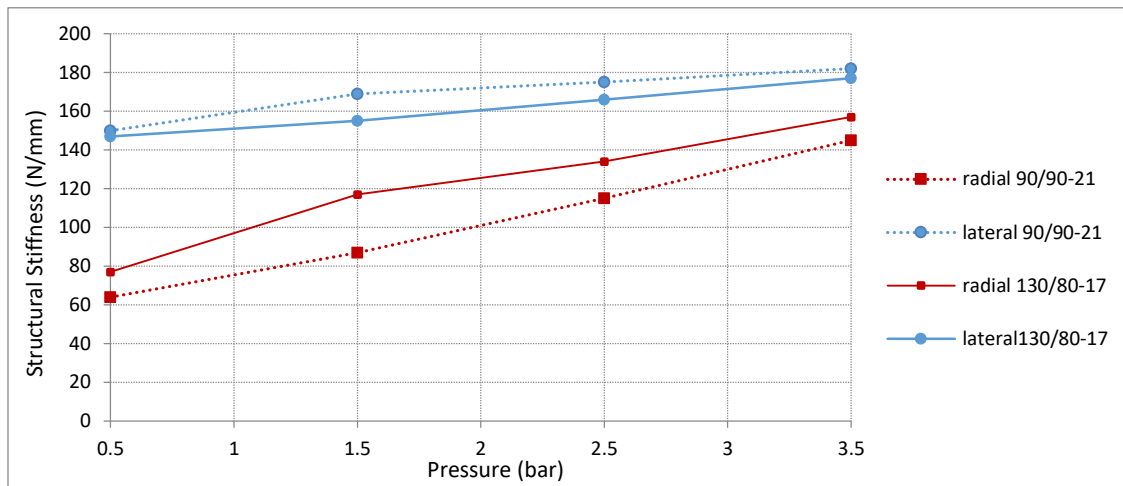


Figure 50: Structural stiffness versus inflation pressure for front (90/90-21) and rear (130/80-17) tires.

Figure 50 illustrates the measurements results of the structural stiffness (¶ 3.1.3 and ¶ 3.1.4) in function of the inflation pressure for front and rear tires. For the tested inflation pressures, both tires shows a higher stiffness in lateral than radial which opposes the test results in [30]. Such difference is mainly due to the tire's carcass construction.

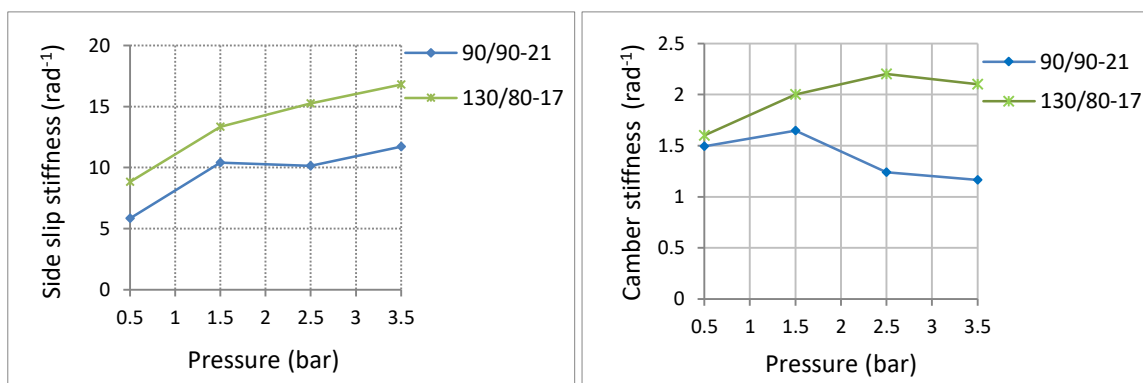


Figure 51: Side slip and camber stiffness in function of the inflation pressure for front (90/90-21) and rear (130/80-17) tires.

Figure 51 shows the plot of the normalized side slip and camber stiffness in function of the inflation pressure for the front and rear tires. It is noticed that side-slip stiffness of the rear tire is always higher than the front for all pressures. Both side-slip stiffness increase with pressure. It is likely that the behavior is related to the nuances and types of tire construction. Indeed the cornering stiffness strongly depends on the lateral structural stiffness and the contact patch size and shape. Therefore, depending on the relative variations in these two factors with pressure, different behaviors may arise.

It is expected that both curves will reach a peak at higher pressure where the stiffness becomes constant or slightly decreases because the tire starts sliding as shown in [30].

The rear tire's camber stiffness increases with the pressure to arrive at its peak at 2.5 bar and then it slightly decreases. The front tire shows a similar behavior with its peak value at an inflation pressure of 1.5 bar. The camber stiffness mainly depends on the lateral deformation of the contact patch. Increasing the inflation pressure will reduce the contact patch. Every tire has an optimal inflation pressure where it reaches its maximum camber stiffness. Above the optimal pressure, the contact patch decreases significantly resulting in the decreasing of the camber stiffness. These results are coherent with [31] and further details about camber force generation are found in [26].

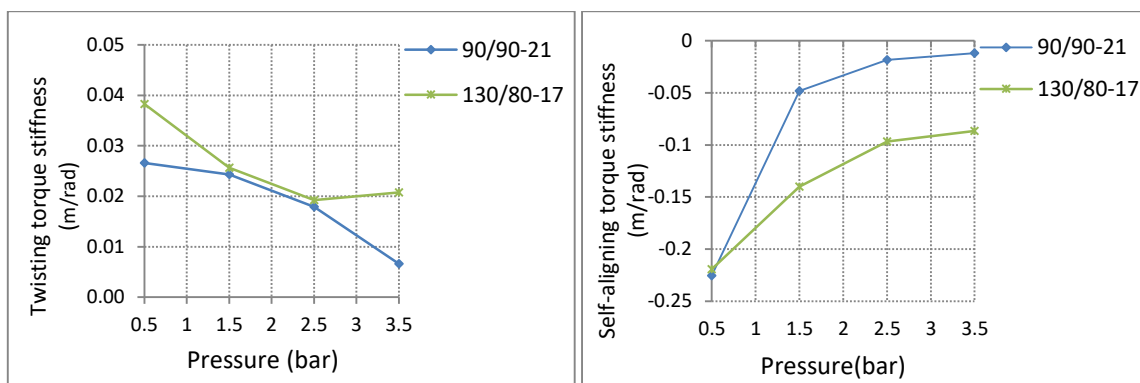


Figure 52: Twisting and self-aligning torque stiffness in function of the inflation pressure for both tires.

Figure 52 represents the plot of the normalized twisting and self-aligning torque stiffness versus tire pressure for front and rear tire. For both tires, the twisting stiffness decreases with the increase of tire pressure. These results were expected since the twisting stiffness is related to differences in the peripheral velocity across the contact patch. The graph shows a higher twisting stiffness for the rear tire at all pressure. Additional details are available in [30] and [31].

For both tires, the self-aligning stiffness decreases, in magnitude, with the increase of the tire pressure. This behavior is expected since the self-aligning stiffness is related to the pneumatic trail which increases with the increase of the contact patch (at low inflation pressure) therefore resulting in the increase of the self-aligning stiffness.

The above results are for the vertical load of 1500N which agree with the results of the other tests performed at vertical loads of 1000N and 2000N.

3.6.2 Identification of the mechanical properties of tires for wheelchair simulation

The paper [24] investigates the capability of the tire testing machine at Padova University to collect data required to develop accurate models for wheelchair tires and analyses the similarities and differences between the behavior of wheelchair tires and bicycle tires. Furthermore, the behavior of wheelchair tires under different working conditions is investigated. Finally, the improvement of wheelchair simulation through this study is discussed. Two tires were tested at different vertical load, inflation pressure and speed.

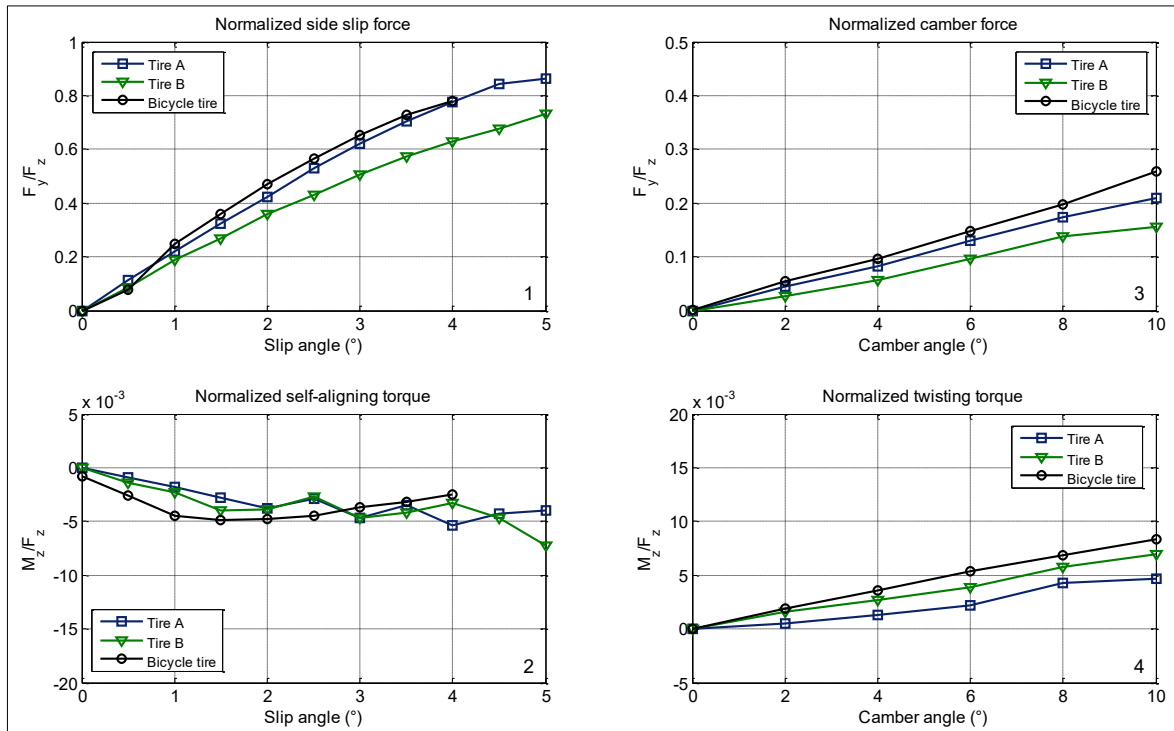


Figure 53: Forces and torques of wheelchair and bicycle tires in reference conditions (vertical load 400 N, inflation pressure 4 bar and disc speed 4 km/h).

The curves of normalized side slip force (Figure 53) show that this component of lateral force increases in monotonic way with side slip angle without reaching a saturation in the tested range of side slip angles. Tire A exhibits larger values of force than tire B for every value of side slip. The curve of tire A is very close to the one of the high performance bicycle tire. The slope of the side slip force curves near the origin is named normalized cornering stiffness. Normalized cornering stiffness may represent tire behavior at small values of side slip angle where the relation between the normalized side slip force and the slip angle is almost linear. This is the case of tires A and B. Cornering stiffness is the product of normalized cornering stiffness and vertical load.

The curves of normalized self-aligning torque are rather close and both show a tendency to saturation above 3° for both tires. The maximum values (in modulus) of self-aligning torques of tire A and B are similar to the maximum value (in modulus) of the self-aligning torque of the bicycle tire, but the bicycle tire shows a steeper slope near the origin and reaches saturation for a lower value of side slip angle. The slope of the curves of normalized self-aligning torque near the origin is named normalized self-aligning stiffness.

The curves of normalized camber force are regular and monotonic for both tires, but tire A exhibits larger values than tire B and its curve is rather close to the one of the high performance bicycle tire. The slope of the curves of normalized camber force near the origin is named normalized camber stiffness. It can represent the behavior of tires A and B, since the curves show a quasi-linear trend.

Finally, the curves of twisting torque against camber angle are almost linear, in this case tire B has a behavior closer to the one of the bicycle tire.

Then the effect of working conditions was analyzed carrying out specific tests in which only one parameter was varied at a time.

Disc speed variations in the range 2÷4 km/h have a negligible effect on the measured tire properties. Figure 54, for example, shows the effect of a decrease in speed on the side slip force generated by tire A, the difference between the two curves is negligible. It is worth remembering that disc speed corresponds to wheelchair speed.

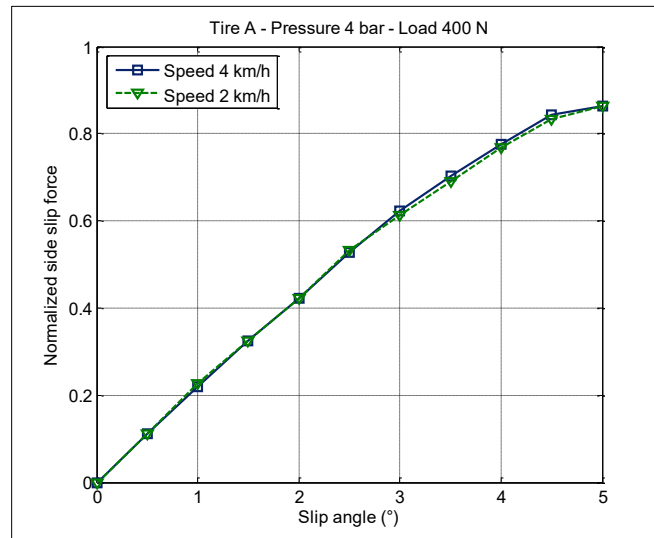


Figure 54: Effect of forward speed on side slip force.

Figure 55 deals with the effect of inflation pressure on tire performance, a strong decrease in tire pressure (from 4 to 2 bar) is considered.

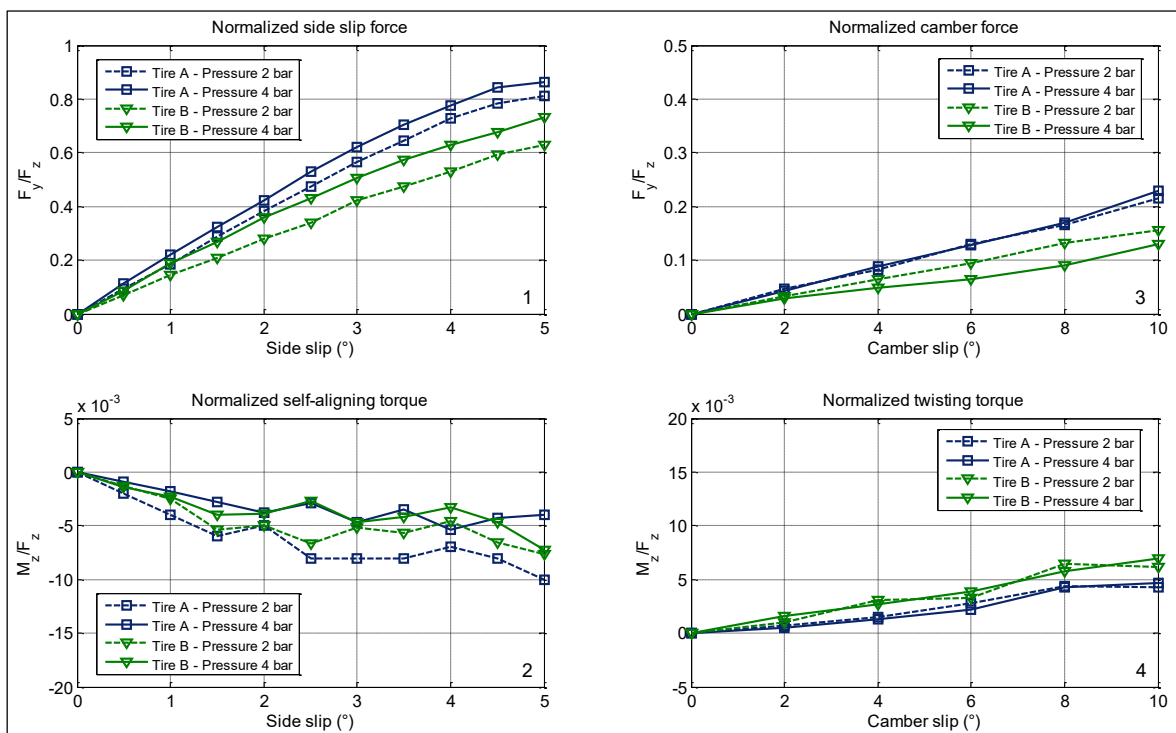


Figure 55: Effect of inflation pressure on tire forces and torques.

Tire properties related to side slip angle are strongly affected by inflation pressure. In both tires a decrease in inflation pressure causes a large decrease in the side slip force generated at the same side slip angle (Figure 55). This trend agrees with the ones measured in bicycle tires [32] and the ones

measured in motorcycle and scooter tires, which sometimes also show a saturation at high pressure [30]. Self-aligning torque increases (in modulus) when inflation pressure decreases, probably because the contact patch becomes larger. This result is in agreement with the ones obtained measuring bicycle and motorcycle tires [30] [32]. Figure 55 shows that camber force generated by tire A is not influenced by inflation pressure, like in bicycle tires [32]; whereas camber force generated by tire B tends to increase when inflation pressure decreases, like in many motorcycle tires [30]. As for the twisting torque, the effect of the inflation pressure appears to be negligible which is similar to the bicycle tires [32].

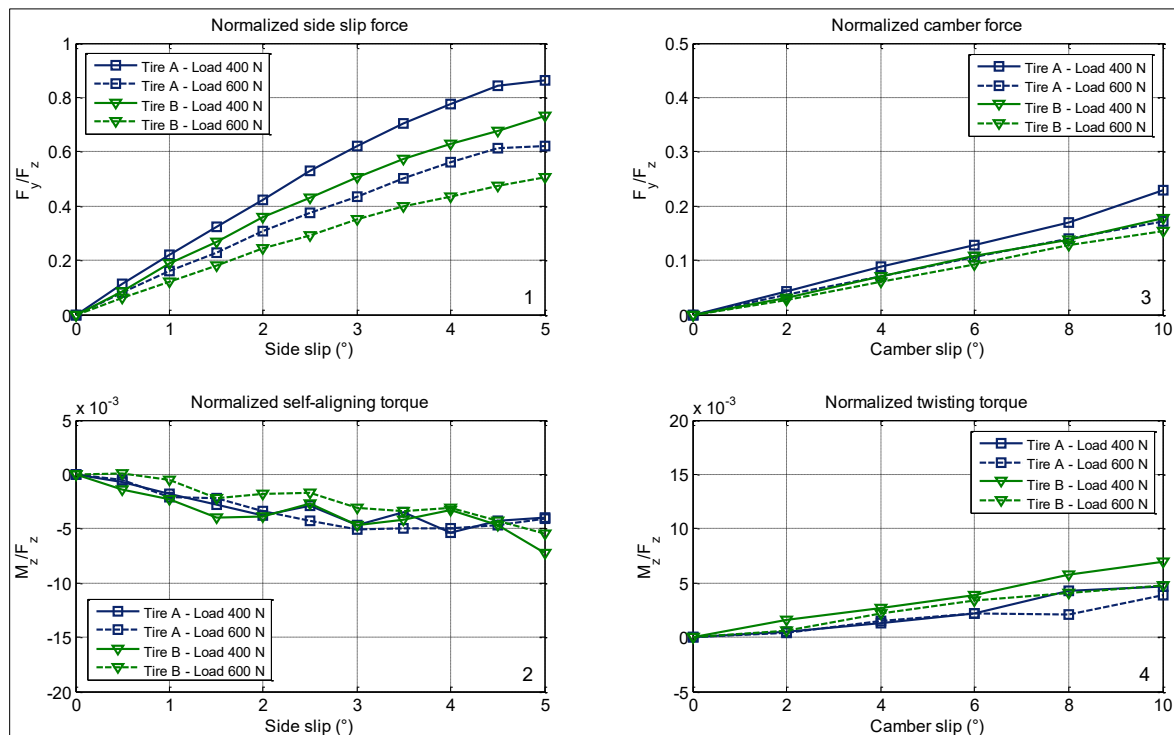


Figure 56: Effect of vertical load on tire forces and torques.

The last parameter here considered is vertical load, its effect is shown in Figure 56. In wheelchair tires, like in bicycle [32] and motorcycle tires [30], when vertical load increases lateral forces do not increase proportionally, because normalized lateral forces decrease when vertical load increases. This effect is particularly important for side slip force (Figure 56). The effect of the vertical load on tire torques is less prominent: in tire A self-aligning and twisting torques are almost unaffected by tire load, whereas in tire B both torque components decrease slightly (in modulus) when load increases.

Chapter 4 - New Tire testing machine

This design offers many improvement over the “Mototiremeter” machine. Several modifications were made during the past years [33] before reaching the actual configuration. The roll arm rotates freely around the universal joints allowing the camber motion ($\pm 50^\circ$). The two universal joints are attached to the roll shafts defining together the roll axis which shall pass through the toroid center of the tire. The machine is intended to test various tire sizes with different toroid radius starting from a bicycle tire (18mm) to a Harley Davidson tire (128mm). The height adjustment is made possible through the vertical movement of the structure which is actuated by two pneumatic pistons, one on each column. In addition the vertical movement is used to apply the desired vertical load which is a major improvement over the “Mototiremeter” where the vertical load was applied by adding weights.

At the center of the roll arm is inserted a splined shaft that holds the slip arm. The splined shaft is the only mechanism available to perform a rotation which is the slip motion ($\pm 10^\circ$), and a translation. The vertical translation is required to adjust the wheel center’s height depending on the tire rolling radius starting from a minimum value of 128mm arriving to 330 mm.

The slip arm holds the wheel’s assembly where the tire is mounted. The wheel’s assembly is equipped with a load cell capable of measuring the three forces (F_x , F_y and F_z) and three moments (M_x , M_y and M_z) at the tire. It can also incorporate a brake disk and caliper to perform tire tests under braking conditions in order to measure the longitudinal force in function of the slip ratio. The load cell and the brake disk represents the major advantages over the previous machine.

Figure 57 illustrates, side by side, the CAD design and real picture of the new tire machine. The machine has been divided into four main assembly depending on the function of each. The design solutions and construction for each assembly are explained in the following paragraphs.

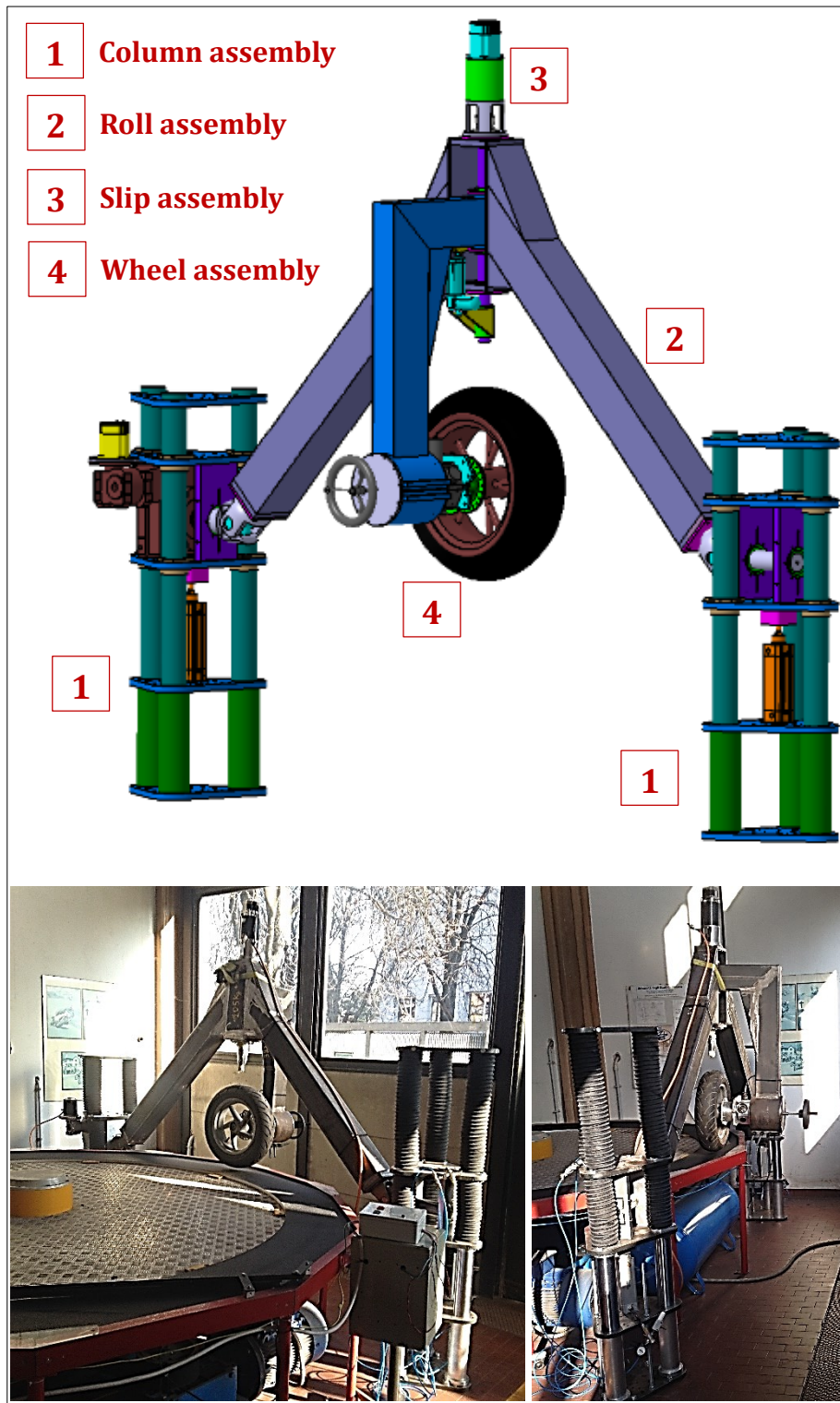


Figure 57 : New tire testing machine (CAD design and real picture).

4.1 Column assembly

The column assembly (Appendix A) represents the structure's support on the ground. It connects the roll shafts to the roll arm by means of universal joints which allows the free rotation of the arm around the roll axis. One column assembly accommodates a step motor with its corresponding speed reducer responsible of establishing the roll motion, while the other column assembly holds the other roll shaft inside two bearings in order to follow the motion. As mentioned earlier, the roll axis height is adjusted through a pneumatic system which actuates the two pneumatic pistons, one on each side. The pneumatic system helps also to apply the desired vertical load on the tire. The assembly is formed of three tubes fixed by five horizontal plates where each plate holds diverse components defining a level (Figure 58).

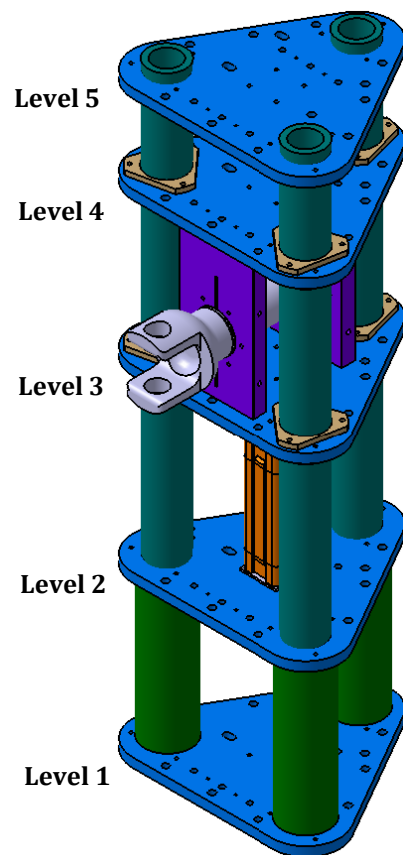


Figure 58: Column assembly

4.1.1 Horizontal plate

There are ten horizontal plates on the machine, each accommodates various parts at different position implying the need of particular fixations at every level (Figure 58). These requirements resulted in a distinctive design for each level which increases the piece machining costs and the chance of confusion. The plates presented a cut at each extremity (green plate in Figure 59) used to clamp the plate on the tube in order to maintain each level at the appropriate height. This method appeared unsafe due to the components weight and the machine vibrations that could overcome the friction force and move the plates.

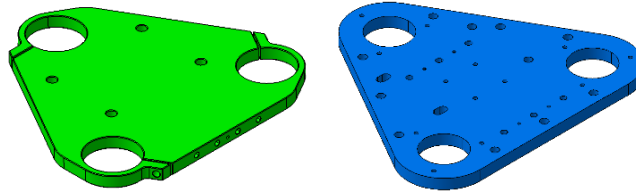


Figure 59: Horizontal Plate designs

For the cited reasons, the design was improved and made unique (blue plate in Figure 59). The plate is made of steel with a thickness of twenty millimeters. It involves all the possible holes configurations for the fixation of the various components. The holes were executed by using plasma cutting technology precision. The technicians at our department's laboratory (Figure 60) performed the final adjustments on the necessary holes for each level.

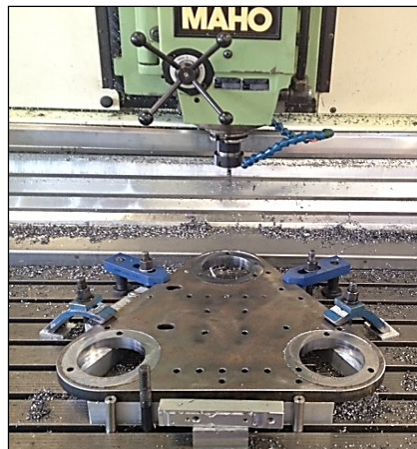


Figure 60: Holes adjustments

The First level serves as the base for the column's assembly. The two base were carefully positioned on the ground according to the measures in the CAD design. The fixation is made using nine threaded bars, of M14, implanted 150 millimeters deep in the ground. The depth was filled by a special fixing resin for such applications. The resin is left twenty-four hours to dry completely, then the plate is inserted and fixed with nuts (Figure 61).

The horizontal level of the base was corrected with three adjustable screw due to ground's imperfection. The two long threaded bars in the middle serve to keep the second level firm, with nuts, in case of vibrations.



Figure 61: Base plate fixed on the ground

Once the base was fixed on the ground, the three tubes were positioned vertically and then welded (Figure 62). Heat is the major concern, during welding, since it can cause an excessive distortion of the tubes which is an issue for the vertical sliding on the columns. The problem was minimized by performing small welding intervals distributed on the three tubes instead of welding each tube continuously. It reduced the rise in temperature therefore minimizing the distortion. A steady sliding check was performed during the welding.



Figure 62: Welding

The height of the second level is maintained in position by three hollow tubes inserted between the first and second plate. The distance shall be equal on the three tubes to insure a vertical position of the pneumatic piston. The welding was made on the top of the base therefore the surface was not horizontal. This issue was resolved by machining a welding cover (Figure 63). It is made of aluminum and has an internal diameter of 81 millimeters in order to be inserted in the tubes. The base diameter (105 millimeters) is larger than the welding surface in order to completely cover it. The second plate settles on the three hollow tubes and is fixed by two nuts to restrain the vertical movement in case of vibrations.



Figure 63: Welding cover

The pneumatic piston holds the third level (Figure 58) with a support fixed by four M8 screws. Actuating the piston causes the vertical translation of the third and fourth levels. These two plates accommodate bushings (¶ 4.1.3) to insure a smooth sliding on the tubes. In between are mounted the speed reducer and the vertical plates (¶ 4.1.2) which hold the roll shafts.

The fifth plate at the extremity keeps the tubes vertical and firm therefore preventing any bending. The height does not need precision, it just requires to be horizontal. The plate is fixed by screws passing through, until contact with the tubes surface. The friction force is enough to maintain it in position since the plates do not hold any component.

However, the other column was preassembled and then welded on a bench (Figure 64). The components mounted reduced the tubes bending during welding which resulted in a better sliding. In

addition, the welding was faster and it was made on the bottom of the base (Figure 65) therefore avoiding the use of welding covers (Figure 63).

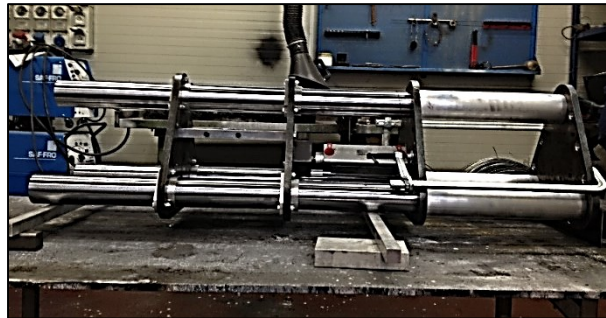


Figure 64: Column welding on bench

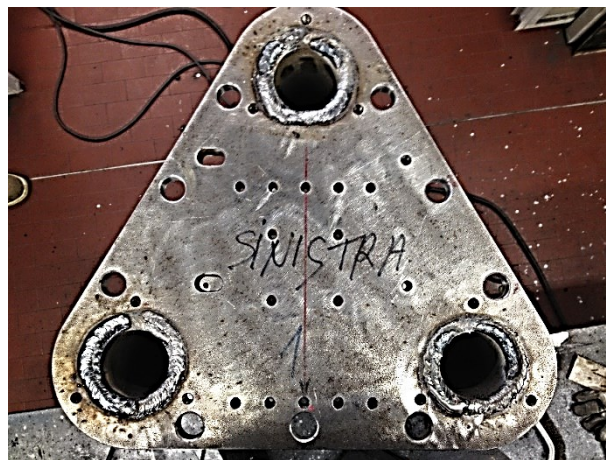


Figure 65: Welding on the bottom of the base

4.1.2 Vertical Plate

The three vertical plates are located between the third and fourth level (Figure 58) of the column's assembly, one on the speed reducer side and the other two on the opposite column. Each vertical plate hosts a bearing holding the roll shaft. The two roll shafts must be aligned in order to form the roll axis of the machine. The initial design was not identical (green design in Figure 66) causing as well the same inconvenient in term of machining time and cost. The design was simplified and made unique for all the plates (Blue design in Figure 66) using the same concept of the horizontal plates. The pieces are made of aluminum and were machined outside our department.

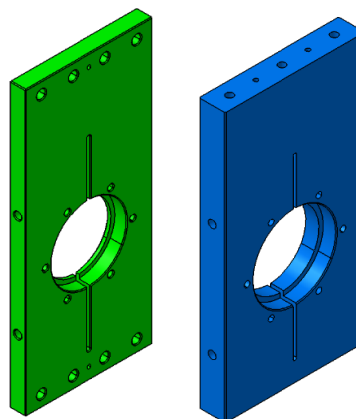


Figure 66: Vertical Plate designs

4.1.3 Bushing

The bushings allow the vertical sliding of the third and fourth level on the tubes. It is made of aluminum with an inner diameter (of 80 millimeters) equal to the tube diameter, and an outer diameter of 90 millimeters. It presents three equidistant holes (Figure 67) in order to be fixed on the horizontal plate with M8 screws. On each plate are mounted three bushings which makes a total of twelve.

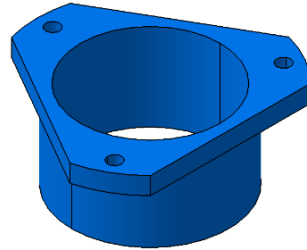


Figure 67: Bushing

The pieces were machined with high precision which created some difficulties in the vertical sliding due to the presence of some distortion in the tubes after welding. The vertical movement intends to adjust the roll axis height and the vertical load therefore it requires a smooth sliding without stick slip. For this reason the inner diameter was augmented of one millimeter to increase the play between the tube and the bushing.

In addition, two sockets were machined in order to fit the guide rings (shown in Figure 68). These rings are manufactured from reinforced acetal resin, a material that is characterized by low coefficient of friction (between 0.05 and 0.1 on steel when lubricated), high mechanical strength and resistance to heavy radial loads. The lubricant used is Silicone grease which protects the guide rings from wear and insure a smooth sliding. Finally the tubes were covered, using flexible air ducts, for protection from dust.



Figure 68: Bushing modification

4.1.4 Speed reducer

The speed reducer associates the step motor with the roll shaft of the machine. Its function is to reduce the motor's speed therefore increasing the torque until the desired amount. It is located between the third and fourth horizontal plate of the left column assembly. The speed reducer was purchased from the manufacturer "Bonfiglioli" (Figure 69).

The speed reducer must rotate a total weight of 180 Kg considering the roll arm, slip arm and wheel assembly. The worst case is at a maximum roll of 50 degrees. Using CATIA V5, the arm length between

the gravity center and the roll shaft was estimated at 0.56 m. Therefore the maximum required torque to move the arm is calculated by the following equation.

$$T_{\text{Roll}} = 9.81 \times \text{Weight} \times \text{Arm} = 9.81 \times 180 \times 0.56 = 990 \text{ N.m} \quad (4-1)$$

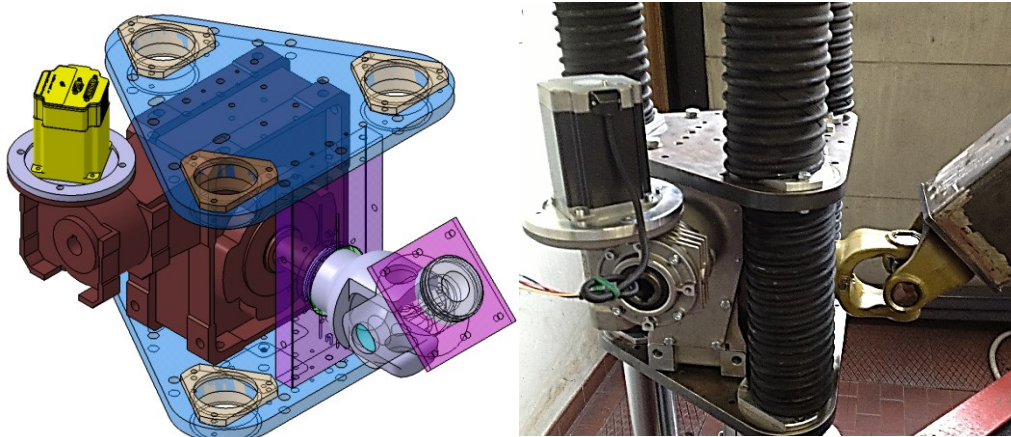


Figure 69: Speed reducer from Bonfiglioli for roll motion

Table 8 shows the characteristics of the chosen speed reducer.

Model	W 110 1/56 + VF 49 7
Gear ratio	392
Efficiency	40 %
Output torque	780 N.m
Recommended Input speed	1400 rpm
Recommended input torque	5 N.m

Table 8: Speed reducer characteristics for roll motion

The equation below shows the relation between the input and output torque of the speed reducer.

$$\frac{T_{\text{output}}}{T_{\text{input}}} = \text{Gear ratio} \times \text{efficiency} \quad (4-2)$$

The above calculations leads to a step motor with an approximate torque of 6.3 Nm (including the safety factor). The recommended input torque is 5 Nm for the safety of the speed reducer. Since the machine will be running for very short period of time and the calculated torque is for the worst case scenario therefore there is no risk on the speed reducer. In addition the speed reducer was already purchased and had an input diameter (where the step motor shaft enters) of 14 millimeters. Therefore the purchased step motor was the "SM 2863-5155" from "R.T.A" which can deliver approximately 5.5 Nm at 1400 rpm. At 600 rpm the step motor can deliver 6.5 Nm. Appendix B provides the detailed specifications of such motor.

The maximum speed input recommended is 1400 rpm, this is not a problem since the rotation speed of the step motor can be controlled through its proper driver. In addition, the high torque of a step motor happens at low rpm speed. The default factory set of the drivers makes the step motors rotates at 800 step/tour which corresponds to 2.22 step/°. Therefore the correction factor to introduce in the Labview software is equal to the product of the gear ratio with the number of step per degree:

$$\text{Correction factor} = \text{Gear ratio} \times \text{number of step/degree} = 392 \times 2.22 = 871.11 \quad (4-3)$$

4.1.5 Piston's Mounting Plate

It associates the pneumatic piston with the bottom of the third level plate (Figure 58). The piston has a threaded head which is directly screwed on the center of the mounting plate. The other side is fixed to the third horizontal plate by four M8 screws (Figure 70). The design was really simple therefore the two pieces were machined in our laboratory.

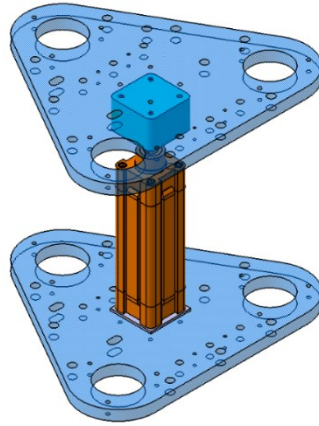


Figure 70: Piston's mounting plate

4.1.6 Pneumatic system

The tire's carcass has circular shape therefore the toroid center (¶ 3.1.2) is assumed to be the theoretical roll center of a given tire. When the toroid center is not aligned with the machine's roll axis, it will migrate during roll motion. Figure 71 show the toroid center's migration for a roll axis bellow (green) and above (red) it. Such migration affects the measurements since the contact patch, as well, follow the toroid center's migration therefore increasing, or decreasing, the contact with the ground.

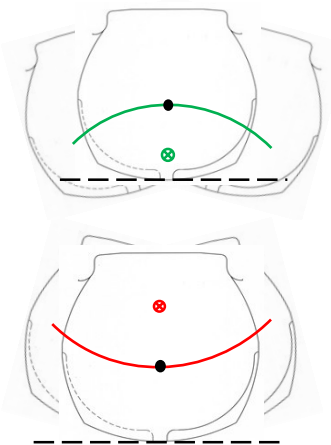


Figure 71: Toroid center migration in function of the roll axis height

Therefore the primary function of the pneumatic system is adjusting the roll axis height depending on the tire's toroid radius starting from 18 millimeters, for a bicycle or wheel chair tire [24], until 128 millimeters for Harley Davidson tires.

Each pneumatic piston must lift half the weight of the structure between the two roll shaft (roll arm + slip arm + wheel assembly) which is approximately 100 Kg in addition to the components above the

piston (2 horizontal plates + 6 bushings + vertical plate + speed reducer + roll shaft) that is around 70 Kg. Therefore each pneumatic piston must be able to lift 170 Kg. Based on the piston’s catalogue in Appendix C, the choice was a piston with a diameter of 63 mm that is capable of lifting 181 Kg.

The pneumatic displacement ($\Delta_{Pneumatic}$) is calculated, in millimeters, by the following formula.

$$\Delta_{Pneumatic} = tr - 20 \tag{4-4}$$

The formula comes from the fact that the minimum roll axis height, for the full piston’s compression, is equal to twenty millimeters.

The other desired function from the pneumatic system is to regulate the vertical load on the tire. The air pressure counteract the weight of the structure until reaching the desired load. Figure 72 illustrates the detailed pneumatic circuit designed with the cooperation of the supplier “PANAR Automation” (Appendix D) using the appropriate pneumatic symbols (Table 9).

The maximum vertical load tested, in our laboratory is 200 kilograms which is less than the weight of the structure applied at the tire. In case of higher vertical loads, the pneumatic system can be modified by incorporating the additional circuit (dashed circuit in Figure 72) therefore the air pressure assists the weight of the structure in order to reach higher vertical load.


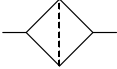
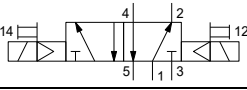
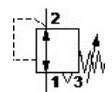
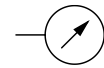
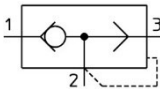
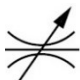
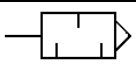
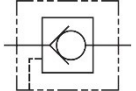
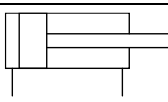
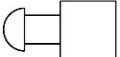
	Reservoir
	Filter
	Solenoid valve 5/2
	Pressure regulator with vent hole adjustment
	Manometer
	Quick exhaust valve
	Speed controller
	Silencer
	Pilot operated check valve
	Pneumatic piston
	Push button

Table 9: Pneumatic symbols

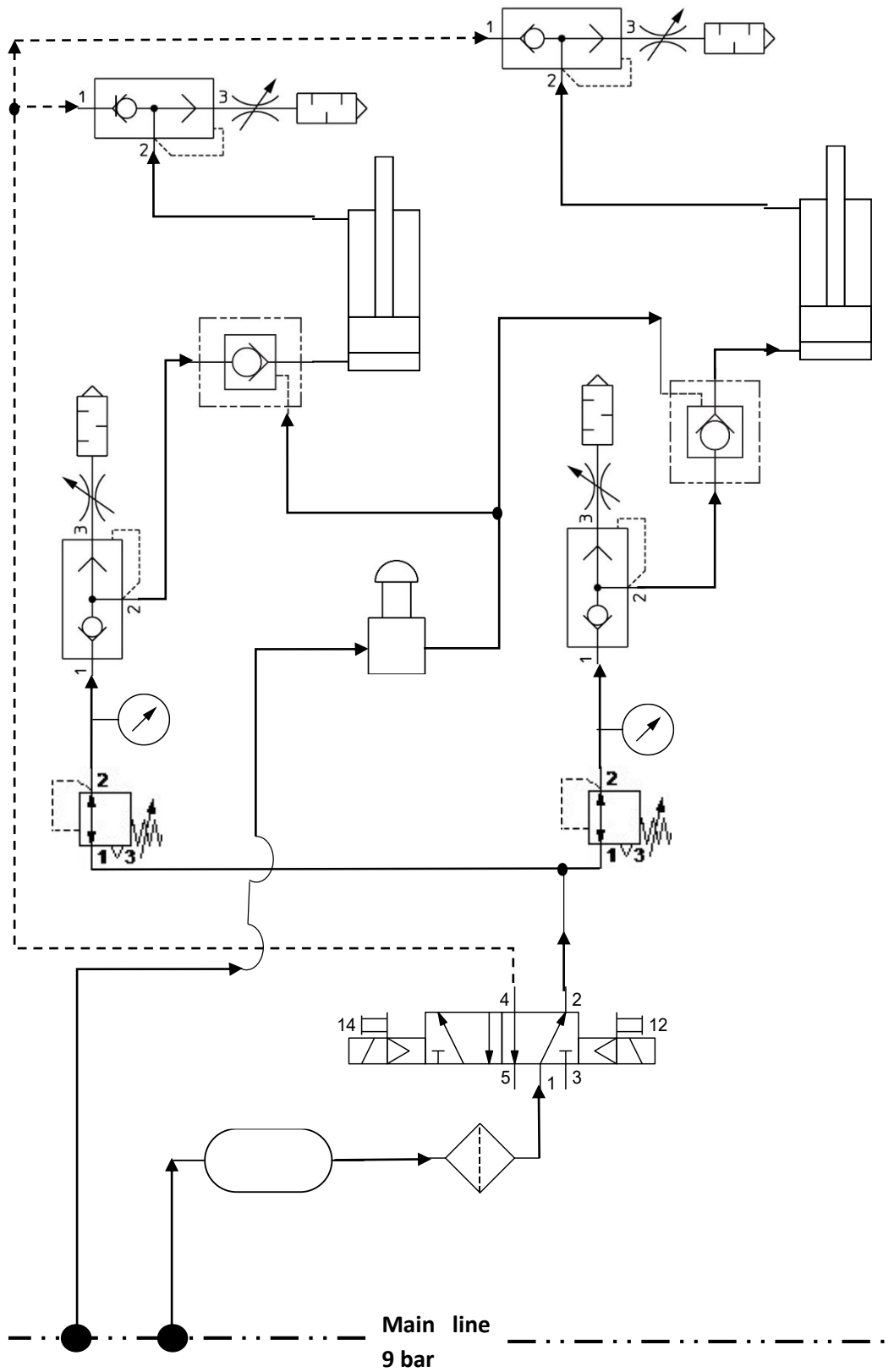


Figure 72: Pneumatic circuit

The pneumatic system was assembled in the laboratory (Figure 73) as well as the appropriate electrical box (Figure 74) for the system's operation.

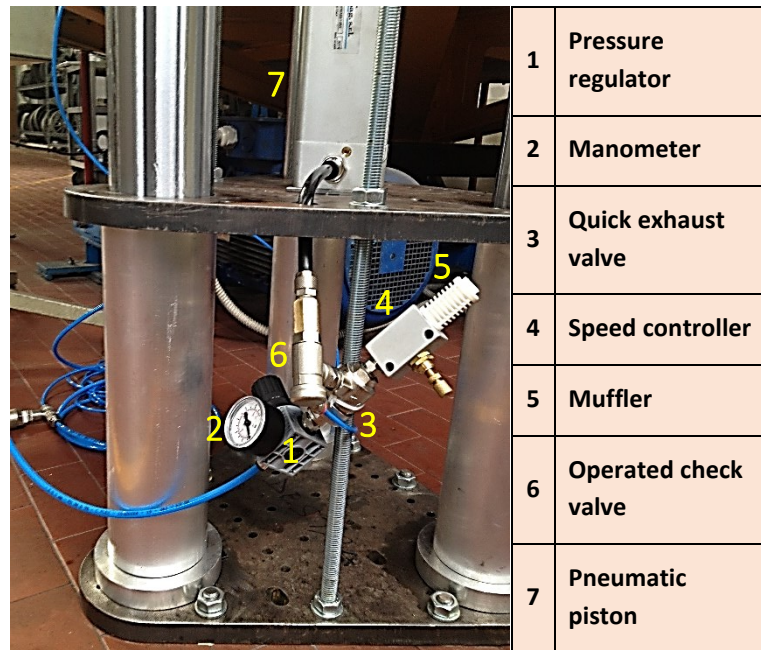


Figure 73: Portion of the pneumatic system

4.1.7 Electric system

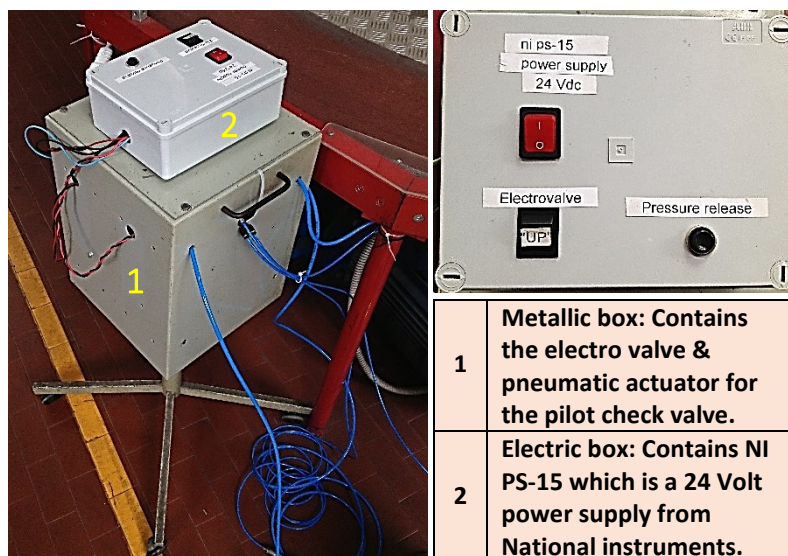


Figure 74: Electric box to operate the pneumatic system

The electric box is composed of three switches. The red switch turns on the power supply, the "Pressure release" switch opens the pilot check valves, and the "Electrovalve" switch opens the port 2 of the electrovalve in order to activate the pneumatic pistons. Therefore pressing on the "Pressure release" button will open the pilot valve and the structure will go down due to its proper weight.

In order to increase the height, the user must press simultaneously the “Pressure release” and “Electrovalve” buttons. Figure 75 illustrate a detailed scheme of the electric circuit inside the electric box while Table 10: Electrical symbols define the electrical symbol used.

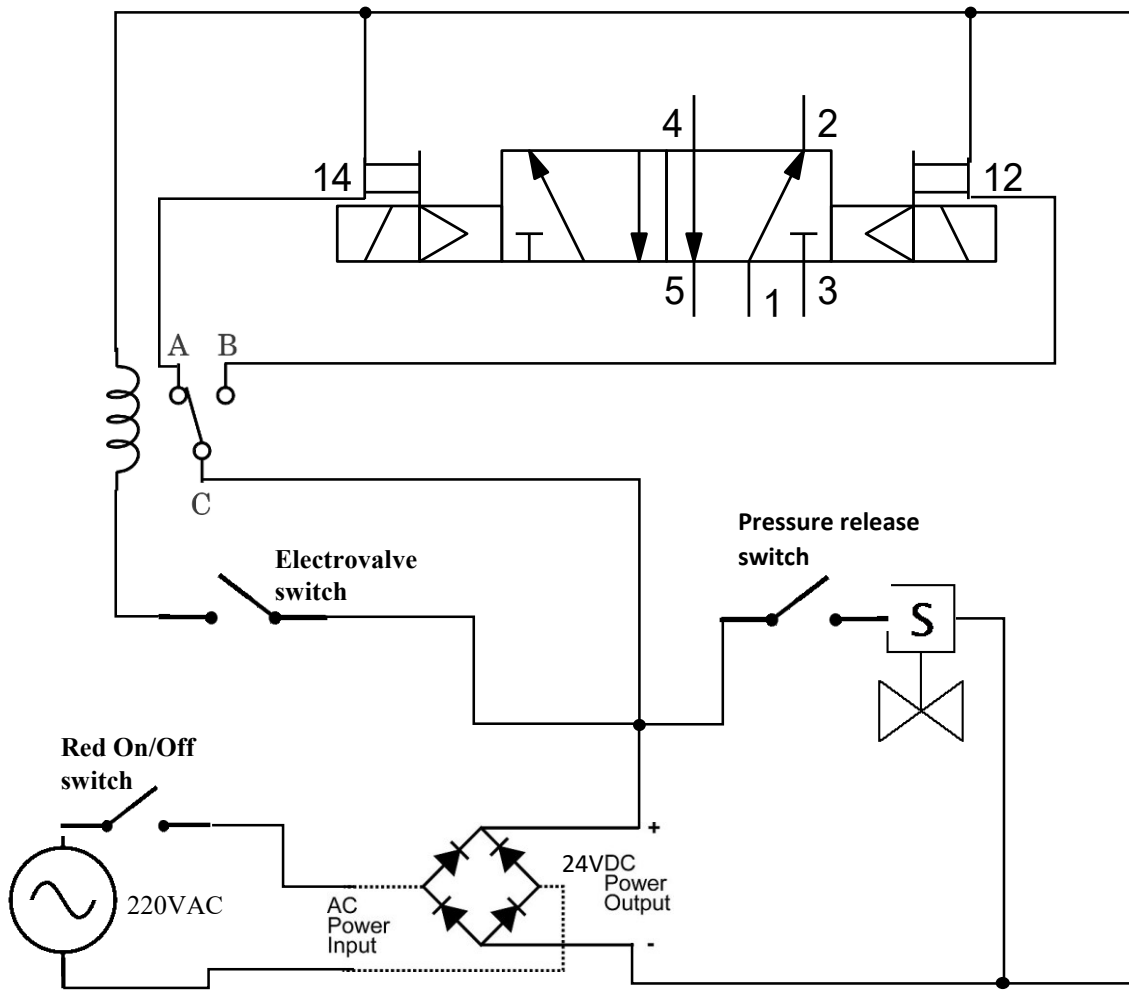


Figure 75: Electric circuit

	Rectifier inside the Ni ps-15 power supply
	Alternative power supply
	Electric switch
	Solenoid operated valve (to control the shut off valves)
	SPDT Relay
	5/2 way Solenoid valve

Table 10: Electrical symbols

4.2 Roll arm assembly

It has an angular shape and it is fixed from both extremities to the roll shafts (Appendix A) by using two universal joints (Figure 76). The structure is responsible of performing the roll motion which can reach $\pm 50^\circ$. The arm is made of steel sheets that were cut and welded according to the specific design.

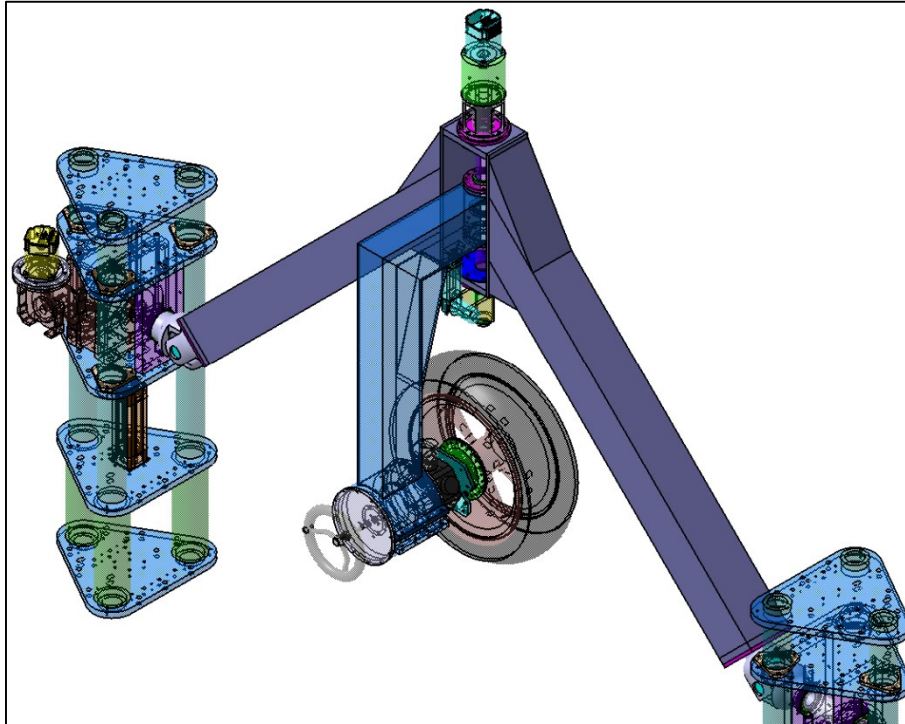


Figure 76: Roll arm assembly

At its center (Figure 77), is inserted a splined shaft to hold the slip arm assembly (¶ 4.3). The shaft's rotation is made possible through two bearings mounted on the top and bottom of the central part of the roll arm. The bearing is held inside a bearing plate (¶ 4.2.1) that is fixed by eight M8 screws. A bearing cover (¶ 4.2.1) is added on the other side of the bearing to protect it from dust and maintain the grease inside.

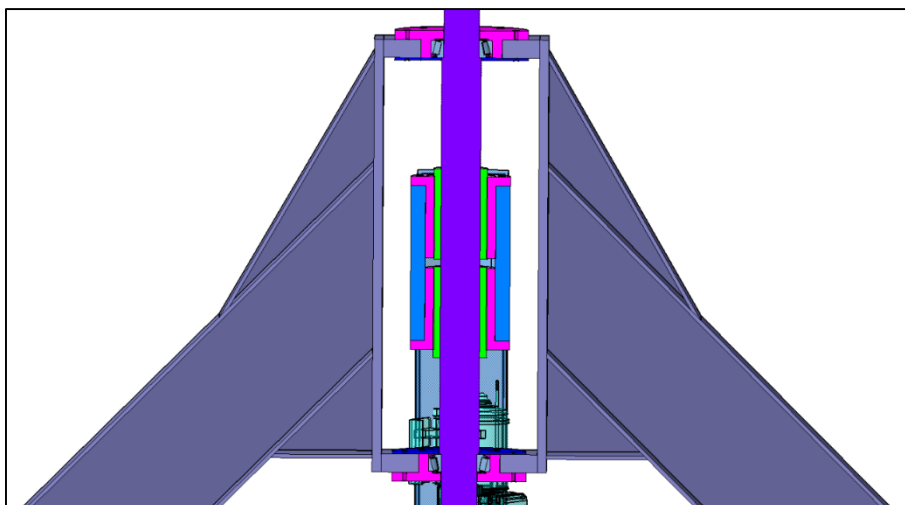


Figure 77: Cross section of the roll arm.

4.2.1 Bearing plate and cover

The bearing plate is mounted on the arm by eight M8 screws. The bearing is inserted inside where it sits on the shoulder of the plate (Figure 78). The other side of the bearing is supported by the shoulder made on the splined shaft therefore it always remains in position.

The bearing cover is a three millimeters disk (Figure 78) which covers the bearing from the other side. It acts as a protection from dust and also keep the bearing's grease inside. The assembly requires a total of two for each piece which are made in aluminum and were machined outside the department.

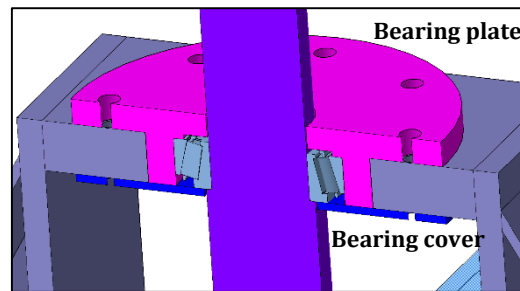


Figure 78: Cross section of bearing assembly

4.2.2 Universal Joint

The joints (Appendix A) connect the roll arm with the two roll shafts located on the columns (Figure 76). The joints are required to have zero play in order to reach an accurate roll angle. The primary joint designed presented a complex shape with two unsymmetrical parts (Figure 79 - first design) which increases dramatically the machining time and cost. In addition, the joint's core was composed of four pieces that might result in some play and less rigidity.

The first design solution (Figure 79 - second image) intended to simplify the joint while keeping the same previous concept. An identical bracket (light blue piece) was designed with respect to the desired clearance. Each joint requires four brackets which are mounted on two rectangular plates (blue plates). The core is a simple cross made of one piece in order to reach maximum rigidity and zero play. The core might present a high machining cost but it remains a very good compromise for the joint in term of rigidity and total cost. The main objective of the second solution (Figure 79 – third image) was to reduce the cost by replacing the brackets with standard brackets from SKF. The core is formed by assembling to cylinders together forming a cross.

The third solution (Figure 79 - fourth image) achieves the best result, which consist of using a standard cardan joint. One fork is fixed on the roll shaft by mean of two steel pins positioned perpendicularly while the other is welded on steel plate that is fixed on the roll arm extremity by mean of six M8 screws. This solution is more expensive but it provides the best compromise in term of rigidity and time.

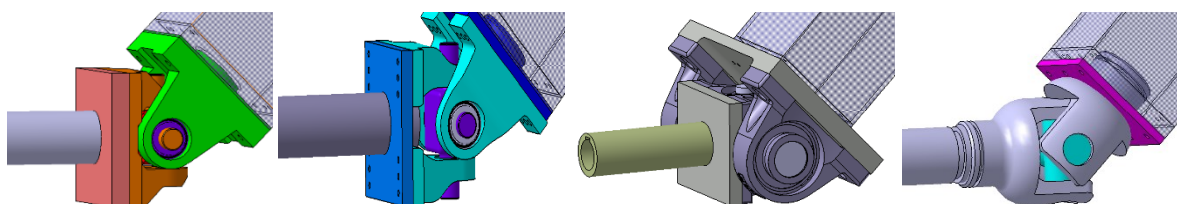


Figure 79: Joint design solutions

4.3 Slip arm assembly

The slip arm assembly (Appendix A) is responsible of the slip motion ($\pm 10^\circ$). It is held by the splined shaft which is inserted at the center of the roll arm (Figure 80). The shaft is supported by two bearings (Figure 77) which allow the rotation around its axis therefore creating the slip motion. In addition, the slip arm must translate vertically in order to adjust the wheel center height depending on the tire rolling radius.

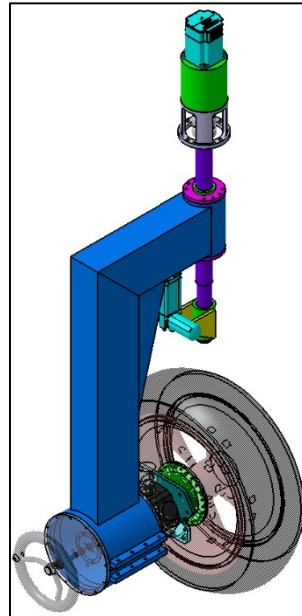


Figure 80: Slip arm assembly

4.3.1 Shaft

The splined shaft with its corresponding sleeves (Appendix A), was the only suitable solution for our specific application since the mechanism must rotate and translate. The shaft had a standard diameter of 44 millimeters therefore the two extremities were reduced until 40 millimeters to fit in the bearings. The splined sleeve (green pieces in Figure 81) was inserted, by press method, inside a housing (Figure 83) which is mounted on the slip arm to serve as a bushing. Two sleeves were used for bushings while the third sleeve was welded on a small rectangular plate (gray plate in Figure 81) and fixed on the shaft, in order to hold the linear actuator.

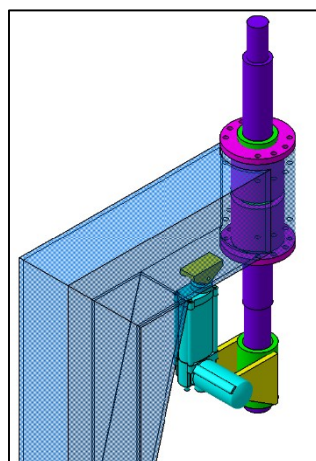


Figure 81: Shaft assembly

4.3.2 Speed reducer

For the same reason mentioned above (¶ 4.1.4) the step motor is associated to the slip shaft by mean of a speed reducer in order to reduce the motor's speed therefore increasing the torque until the desired amount. The speed reducer is located on the top of the splined shaft, joining it to the step motor. Since the slip test requires an increment of 0.5 degrees, it was crucial to carefully choose a speed reducer with the minimum backlash (which represents the play) possible in order to achieve accurate measurements. The only option was the planetary gear unit which is very expensive. The right compromise between precision and cost was found within the "LC" category from the manufacturer "Bonfiglioli" (Figure 82).

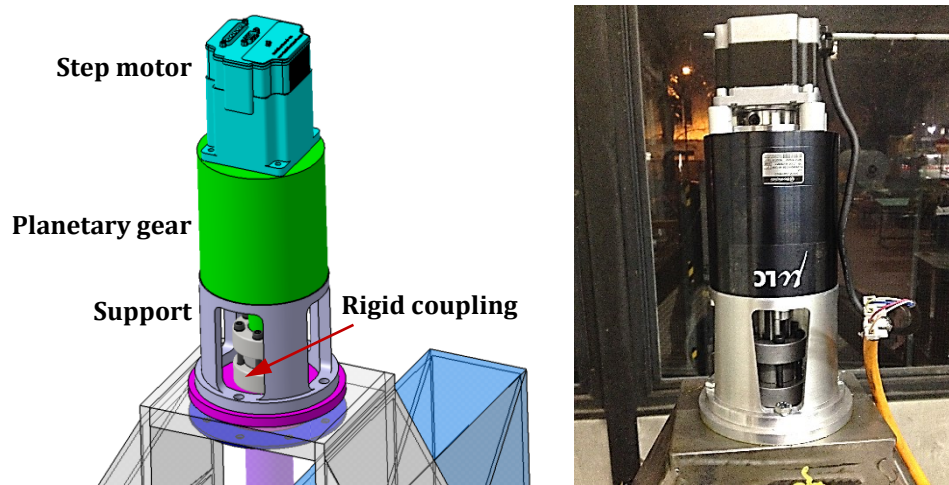


Figure 82: Planetary gear unit from "Bonfiglioli" for slip motion.

The planetary gear unit must rotate a total weight of 70 Kg considering the complete slip arm assembly and wheel assembly. The worst case is at a maximum roll of 50 degrees and a maximum slip of 20 degrees. It is important to mention that we never reach a 20 degree slip during the test but in order to choose the proper speed reducer we have to take into account the worst case which represents the machine's limits which can reach 20 degree of slip. Therefore the maximum force is as follows.

$$F_{\text{slip}} = 9.81 \times \text{Weight} \times \sin(50^\circ) = 9.81 \times 70 \times \sin(50^\circ) \approx 526 \text{ N} \quad (4-5)$$

Using CATIA V5, the arm length between the gravity center and the slip shaft was estimated at 0.28 m. Once again the longest arm will be at a 20 degree of slip angle.

$$\text{Arm}_{\text{slip}} = 0.28 \times \sin(20^\circ) = 0.096 \text{ m} \quad (4-6)$$

Therefore the maximum required torque to move the arm is calculated by the following equation.

$$T_{\text{slip}} = F_{\text{slip}} \times \text{Arm}_{\text{slip}} \times \text{Safety factor} = 526 \times 0.096 \times 2 = 100 \text{ Nm} \quad (4-7)$$

Table 11 shows the characteristics of the chosen speed reducer.

Model	LC 120 2 50
Gear ratio	50
Gear Stage (maximum 3 stage)	2
Maximum Output torque	120 N.m

Table 11: Characteristics of the planetary gear unit for slip motion

As indicated in Figure 82, the output shaft of the planetary gear is coupled with the splined shaft by means of a simple rigid coupling after reducing the diameter of the splined shaft until 32 millimeters (equal to the output shaft's diameter of the planetary gear). The support in Figure 82 allows the fixation of the planetary gear unit on the top of the tire machine. The machined pockets on the support offer the possibility to reach the rigid coupling with the appropriate tool in order to tighten it well. Finally the step motor's shaft is inserted in the back of the planetary gear unit. Based on the above calculations, the purchased step motor was the "SM 2861-5155" from "R.T.A" which delivers a torque greater than 2 Nm until 2100 rpm. Appendix B provides the detailed specifications of such motor.

Applying the same reasoning and calculation of paragraph 4.1.4 we can deduce a correction factor of 111.11 for the slip motion in the Labview software.

4.3.3 Sleeve's housing

The housing (purple piece in Figure 83) is fixed on the slip arm using eight M8 screws. It is made of aluminum with an inner diameter slightly smaller than the outer diameter of the sleeves therefore the two pieces are joined by press method.

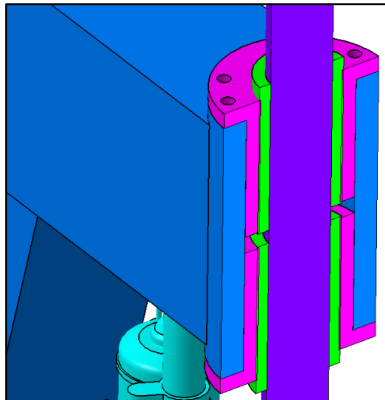


Figure 83: Cross section of sleeve assembly

4.3.4 Vertical motion

The vertical motion is necessary to adjust the wheel center depending on the tire size (3.1.1). The minimum height of the wheel center is 198 mm at a total compression of the pneumatic piston and linear actuator. The linear actuator displacement (Δ_{Actuator}) calculated in millimeters, is expressed, by the following formula, in function of the pneumatic displacement ($\Delta_{\text{Pneumatic}}$) and the tire rolling radius (rr).

$$\Delta_{\text{Actuator}} = rr - (198 + \Delta_{\text{Pneumatic}}) \quad (4-8)$$

The pneumatic system cannot apply accurately the desired vertical load due to the compressibility of air, therefore the vertical motion allows the adjustment with precision.

In the original design, the vertical adjustment was performed manually by a handle bar (Figure 84) mounted on the top of a recirculating screw. The idea was replaced by a linear actuator (light blue piece in Figure 81) allowing a precise and full automated vertical motion. The Desired actuator for such application needs to carry an approximate weight of 1000 Newton at a low linear speed in order to adjust the height with precision.

Therefore the purchased actuator was the LMR 01 from “Linearmech”. Such actuator can carry a maximum weight of 1300 Newton, which is more than necessary, at a low linear speed of 8 mm/s. It has a stroke of 100 mm and it is equipped with two safety switches on both extremities in order to stop the actuator when it reaches the limit. The chosen electric motor was a 24 VDC. For budget reasons, the actuator will be directly controlled by a physical switch instead of controlling it by means of the computer. The main advantage of such actuator relies in its compact size (190 mm when fully retracted) which is important for our application due to the lack of space. The details of the actuator can be found in Appendix B.

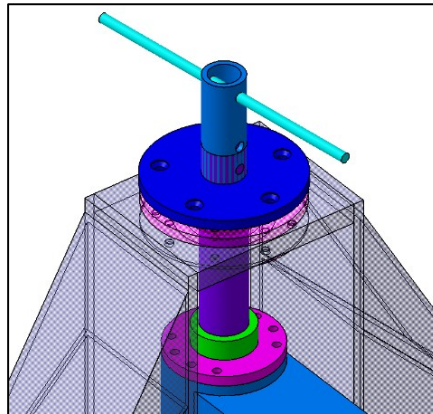


Figure 84: Handle bar for height adjustment

4.3.5 Slip motion

The original design suggested the use of a linear actuator in order to perform the slip motion. The linear actuator was mounted on to brackets joining together the roll and slip arm (Figure 85 – Solution 1). The other low cost solution was to build the linear actuator using a step motor and recirculating screw (Figure 85 – Solution 2).

The vertical travel of the slip arm can reach 100 millimeters which causes a big inclination angle for the linear actuator. This problem can be resolved using ball-joints to allow such inclination but it requires a constant calibration of the linear actuator depending on the inclination angle. For all the above reasons, the design was replaced by implementing a coaxial speed reducer, with the appropriate step motor, directly on the splined shaft (Figure 85 – Solution 3).

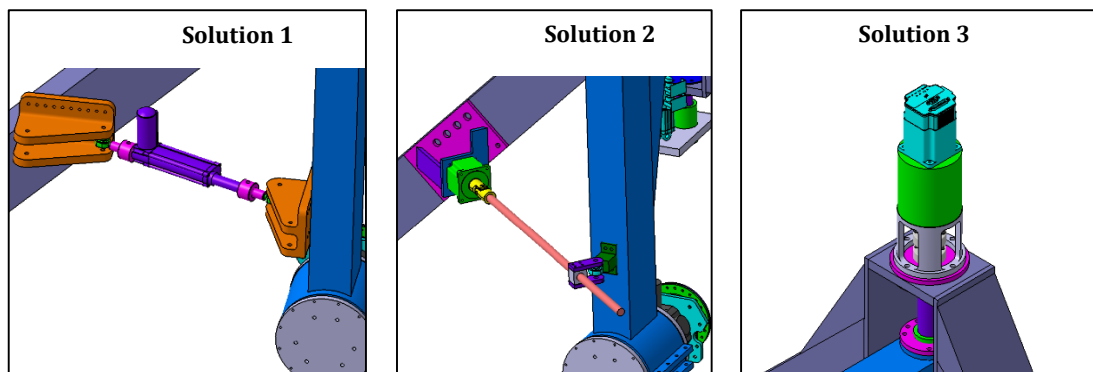


Figure 85: Slip motion solutions

4.4 Wheel assembly

The wheel assembly (Appendix A) connects the tire to the slip arm (Figure 86). The primary function is measuring the forces and moments at the wheel through the load cell (¶ 4.7.1). The wheel hub must allow the free rotation of the tire with minimum friction in order to measure realistic rolling resistance. A braking system can be incorporated, as well, to allow braking test conditions. Finally the wheel assembly must allow the lateral adjustment of the wheel position on the rotating disk.

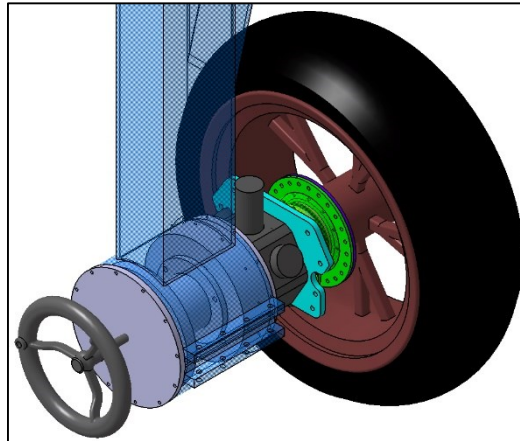


Figure 86: Wheel assembly

4.4.1 Lateral adjustment

The tire and its corresponding rim are directly mounted on the wheel assembly of the machine. Since the width of the rim varies between tires, it will influence the lateral position of the toroid center. A lateral displacement between the roll axis and the toroid center will induce a migration of the toroid center (similar to the previous description in ¶ 4.1.6) creating a tire displacement (Figure 87). Therefore it is important to keep the toroid center on the roll axis. The required lateral displacement ($\Delta_{Lateral}$) is calculated, in millimeters, in function of the rim's width (r_w).

$$\Delta_{Lateral} = 91.2 - \frac{1}{2} \times r_w \quad (4-9)$$

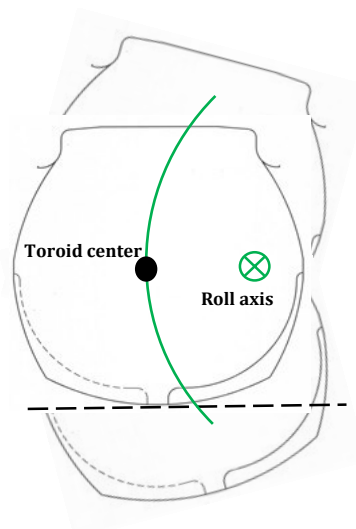


Figure 87: Toroid center migration in function of roll axis lateral position

Figure 88 illustrates the mechanism used for lateral adjustment. It is composed of two cylinders joined by a spacer. The front cylinder holds the load cell by means of six M10 screws and its length (70 millimeters) defines the maximum lateral displacement. A threaded bar is fixed on the rear cylinder by two snap rings (also called seeger) in order to translate the assembly. The other end of the threaded bar is equipped with a knob for rotation. The rear cover is fixed on the slip arm and holds, at its center, a threaded rod coupler in order to convert the rotation into translation. The design of the mechanism was based on the available materials in our department in order to save some cost.

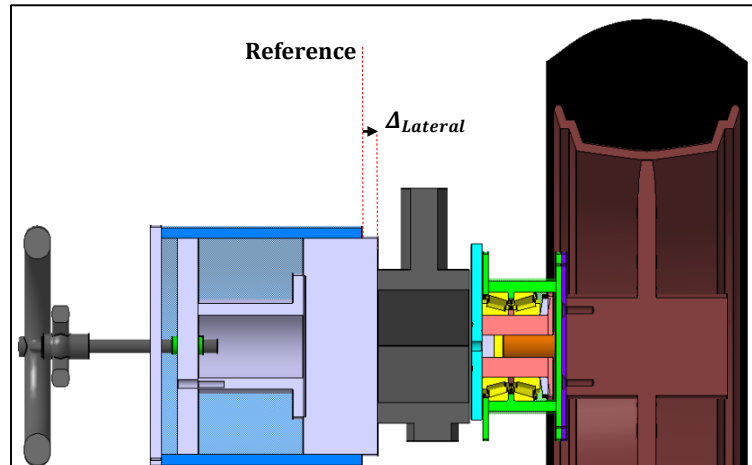


Figure 88: Lateral adjustment mechanism (Cross section of wheel assembly).

4.4.2 Wheel hub

The wheel hub is mounted on the load cell and must allow the free rotation of the tire with minimum rolling resistance. Therefore two tapered roller bearings are mounted inside the hub (Figure 89). The main advantage of such bearings is the ability to support a variety of directional load such axial force (F_y) and radial forces (F_x and F_z). The rim is fixed on a disk (Figure 89 – purple disk) which is then attached to the hub.

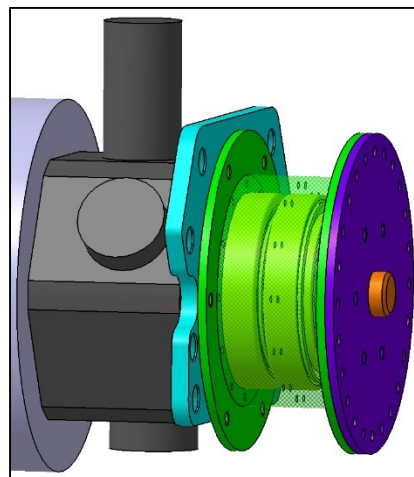


Figure 89: Wheel hub

The wheel hub design was fixed and the components were already machined therefore the remained work was the assembling. The contact surface between the hub and the fixing plate on the load cell (Figure 89 – light blue plate) created a high friction which affects the rolling resistance measurements. The problem was resolved by machining an appropriate washer (2.1 millimeters thick) that was

inserted between the fixing plate and the bearing. The washer is in contact with the inner race of the bearing therefore allowing the hub to rotate freely without touching the fixing plate.

The hub can incorporate a brake disk therefore the clearances were checked by performing some roll simulations. At 55°, the load cell touches the rotating disk and the braking disk clearance is very small. This condition gets worse for smaller tires. The decision made was to use the actual hub without the brake disk for first tests in order to evaluate all possible problems and improve the design in the future.

4.5 Software development

4.5.1 Motion control

Both tire machines are intended for the same application and type of tests therefore the control section of the software remained intact. It uses the first two axes of the motion controller for operating the “Mototiremeter” and the last two axes for the new machine.

The front panel layout was preserved to remain familiar for the user. The safety switch for activating the slip or roll panel are still present as well as the test mode switch (with or without increment). The motion inputs are same as before where the user enters the maximum angle, the increment angle and the time delay.

When the user enters the desired slip (or roll) angle in degrees, it needs to be multiplied by the proper correction factor in order to send the right command to the motion controller. The correction factors calculations, for slip and roll, are based on the number of steps per one rotation and the gear ratio of the speed reducer. Such calculations can be found in paragraph 4.1.4 and 4.3.2.

In the future, it is possible to add a push button on the control panel in order to actuate the linear actuator or even make the actuation automatic by inserting in the code the equation for calculating the required vertical displacement. Therefore the user enters the rolling radius value of the tested tire and the code calculates the corresponding vertical displacement.

Such solution requires an analog output module from national instruments, similar to the NI-9265 but with higher amperage, which is mounted on the NI-cDAQ chassis. Due to our low budget and the expensive price of this module, the priority was given to finish building the machine and therefore this solution was left as a future improvement.

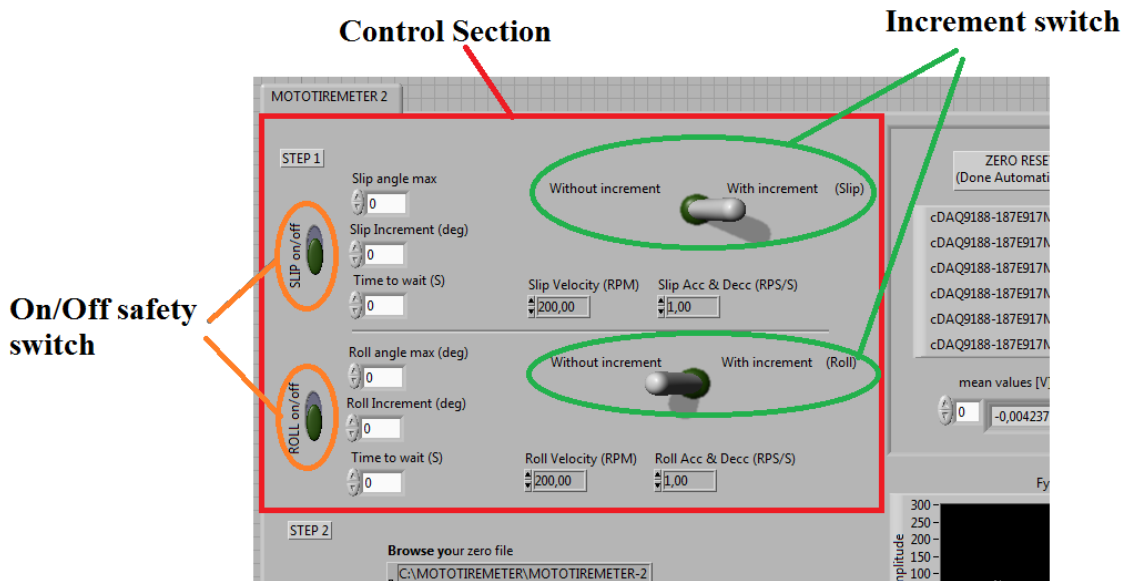


Figure 90: Control section of the new software.

4.5.2 DAQ (data acquisition)

The major portion of the DAQ section remained similar where the “Reset load cell” and “Save data” switches are still present (Figure 91) as well as the monitoring graphs. The program still asks the user to input the toroid radius, rolling radius and the M_y load cell height. In case of the new tire testing machine, the vertical load is no longer an input, it is directly measured by the load cell.

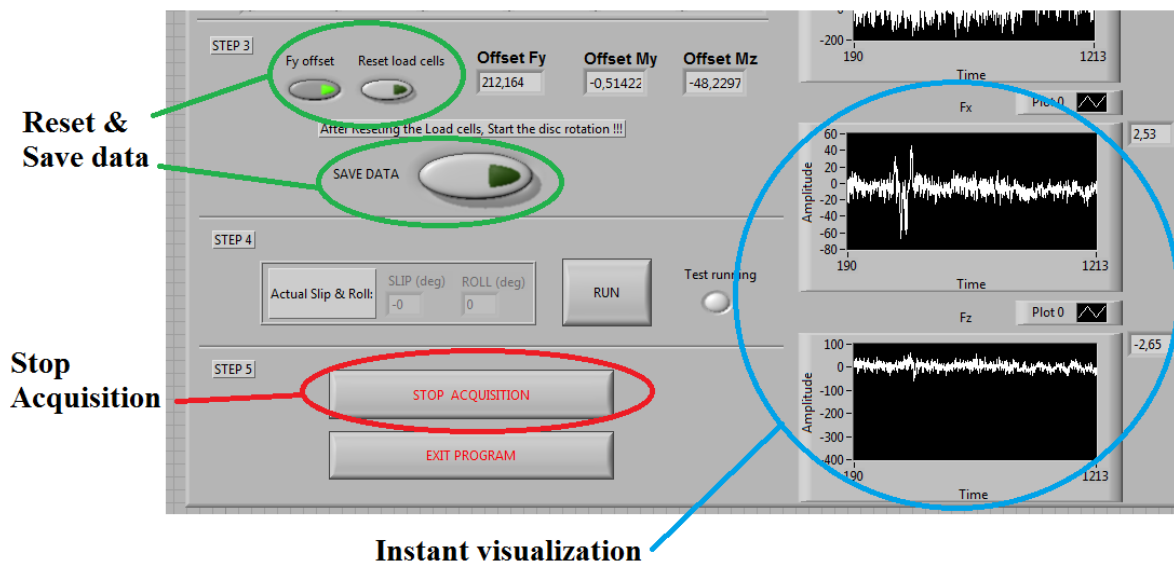


Figure 91: DAQ section – Similar part.

The “Mototiremeter” machine is equipped with three load cells measuring the lateral force F_y , self-aligning torque M_z and rolling resistance M_y . However the new tire machine has a load cell capable of measuring all the tire components (F_x , F_y , F_z , M_x , M_y and M_z) therefore additional graphs were inserted for full measurements monitoring and some columns were added in the output file to record extra data. In addition, the new load cell requires some codes, for reset and calibration, which were implemented in the DAQ front panel (Figure 92).

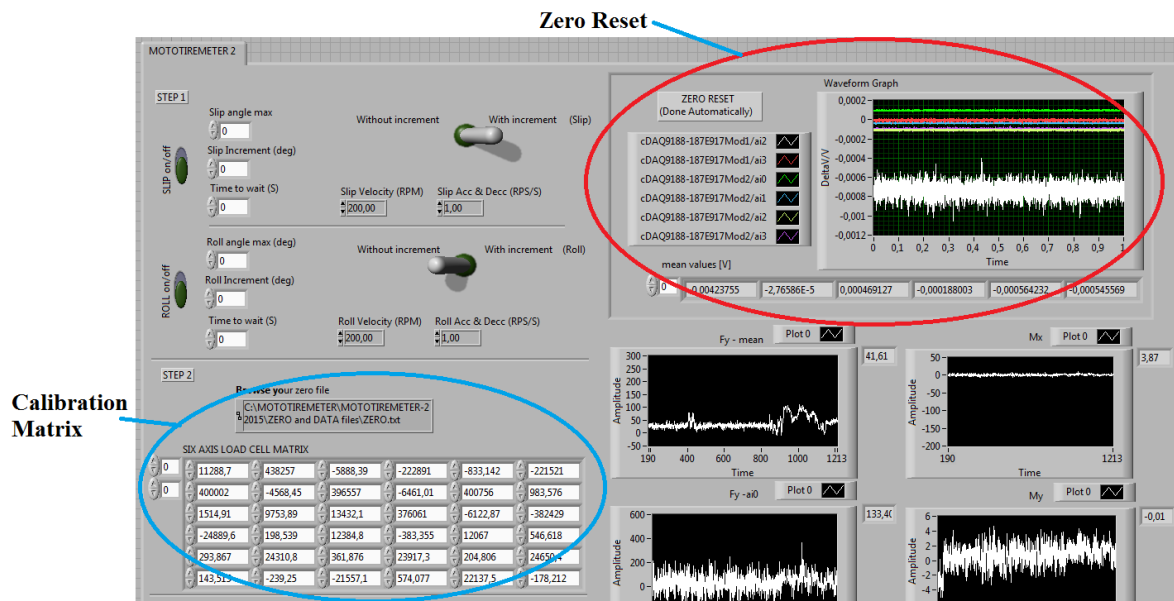


Figure 92: DAQ section – Additional part.

4.6 The control system

The control system represents the network associating the input motion, from the user, to the corresponding movement of the machine. Figure 93 shows a portion of the motion control system for the new tire machine. The two pieces in red are the drivers which are basically the brain of the step motors. The two orange cables are shielded cables and they connect the driver to the step motor.

Due to low budget problems, it was not possible to buy a new motion controller therefore the old PCI motion controller was used for the control of the new machine. The two arrows in Figure 93 represents the commands sent to the drivers from the NI UMI 7764. Since the PCI motion controller and the NI UMI 7764 possess four axis where only two of the them were used to control the “Mototiremeter”, it was therefore possible to use the two remaining free axis and thereby combine the motion control of both machines (Figure 95).

4.6.1 Workstation

It is simply the desktop computer (Figure 13) used by the user to operate the machine by mean of a Labview code (¶ 4.5). The Labview software provides a user friendly interface which allows the user to insert the desired inputs like the desired slip (or roll) angle in degrees, as well as the type of test (with or without increment). The slip (or roll) angle are then multiplied with the corresponding correction factors (¶ 4.1.4 & 4.3.2) in order to convert the input to the proper equivalence in steps. Then, the information is sent to the NI-PCI 7334 motion controller.

4.6.2 NI-PCI 7334 (Motion Controller)

NI 7330 series devices are low-cost stepper motion controllers for point-to-point applications. These low-cost motion controllers provide new solutions for machine builders who need simple, straight forward motion control without a lot of extra features. Unlike other low-cost motion controllers, NI 7330 controllers still have a variety of powerful features including linear interpolation for coordinating multiple axes, real-time system integration for directly communicating with data acquisition or image

acquisition boards and high-performance stepper generation for ensuring smooth motion at high velocities.

In other words, the PCI 7334 represents the brain of the control system. It is equipped with four axes therefore allowing four simultaneous motion, one motion per axis. The first and second axis are already reserved for the slip and roll motion of the “Mototiremeter” machine. Due to budget restriction it was not possible to replace the PCI motion controller with a PXI motion, therefore the third and fourth axis were used for the slip and roll motion of the new tire machine.

4.6.3 NI-UMI 7764 (Universal Motion Interface)

It is a standalone connectivity accessory designed to be used with National Instruments NI 7330 series motion controllers for up to four axes of simultaneous or independent control. Each machine will be using two of the axes. The UMI-7764 connects third-party stepper and servo drives to National Instruments motion controllers PCI-7334.

To work correctly with the UMI-7764, drives must have industry standard interfaces. For stepper systems, the industry standard interface includes step and direction, or clockwise (CW) and counter-clockwise (CCW), pulse inputs. For servo systems, the industry standard interface includes a ± 10 V analog input.

4.6.4 Step motor driver

The driver connects the NI-UMI 7764 to the step motor. Every step motor has its own driver responsible of converting the motion input from the computer to the proper voltage signal for the step motors. The purchased drivers for the new machine control are the X-PLUS B4.1 from RTA. The advantage of such drivers is the simplicity of adapting it to our NI-UMI 7764 since it presents step and direction inputs. Another advantage is the direct plugging to a standard 230 V alternative current. More details about the drivers are available in Appendix B. The detailed connections between the driver and the NI UMI 7764 are illustrated in Figure 94.

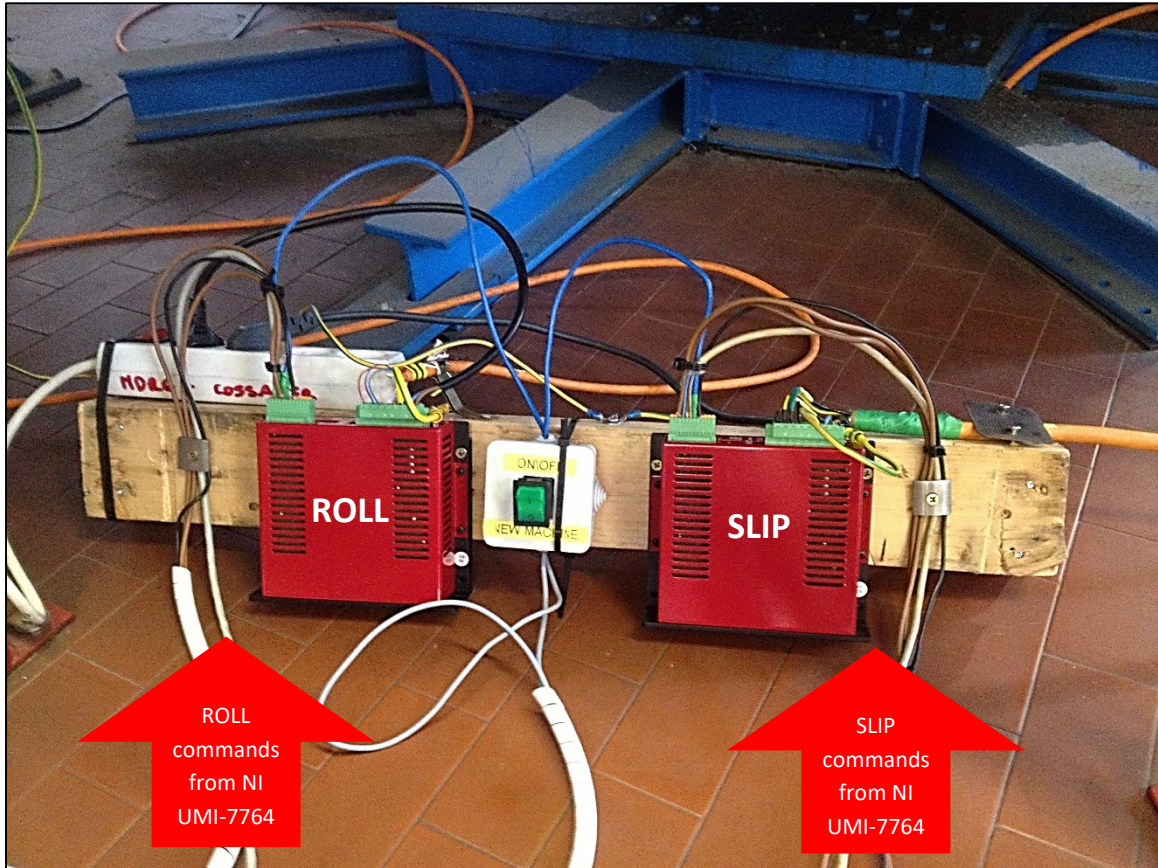


Figure 93: Portion of the motion control system (Drivers).

4.6.5 Step motor

The step motor are the final components of the control system. Every machine is equipped with two step motors, one for slip and the other for roll motion. Figure 94 illustrates the step motor electrical connections to the driver. The details about the step motors calculations are available in the previous sections (¶ 4.1.4 and ¶ 4.3.2) and their specifications are listed in Appendix B.

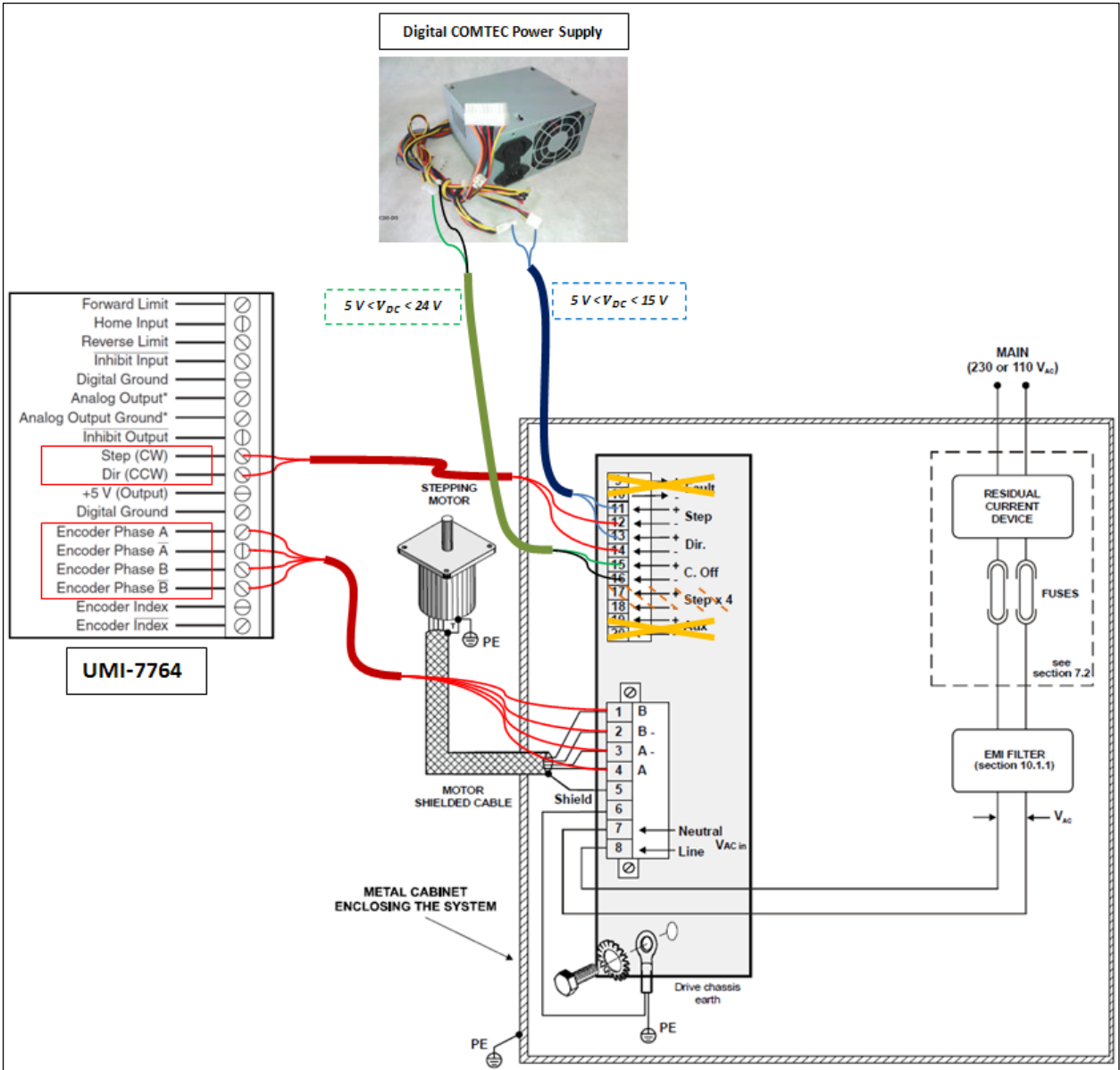


Figure 94: Electric connections between the step motor, the drive and the UMI-7764

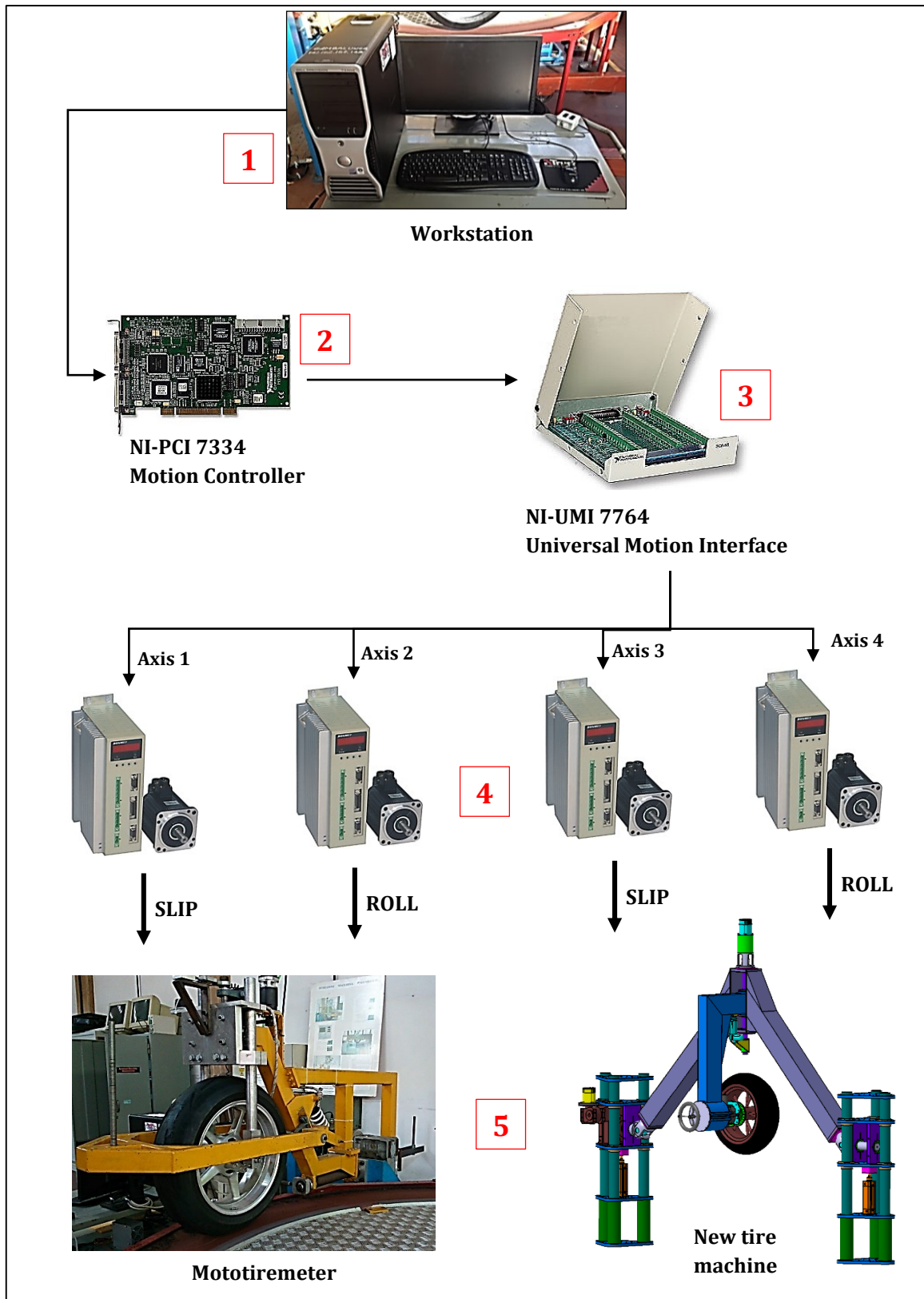


Figure 95: Global motion control system

4.7 DAQ (Data Acquisition) system

The data acquisition on both machine is similar, the difference remains only in the number of measured data since the new load cell measures, in addition, the vertical load, the longitudinal force and the overturning moment. The problem was solved by adding an extra NI-9237 on the chassis in order to increase the number of input channels and the software was adapted to the modifications.

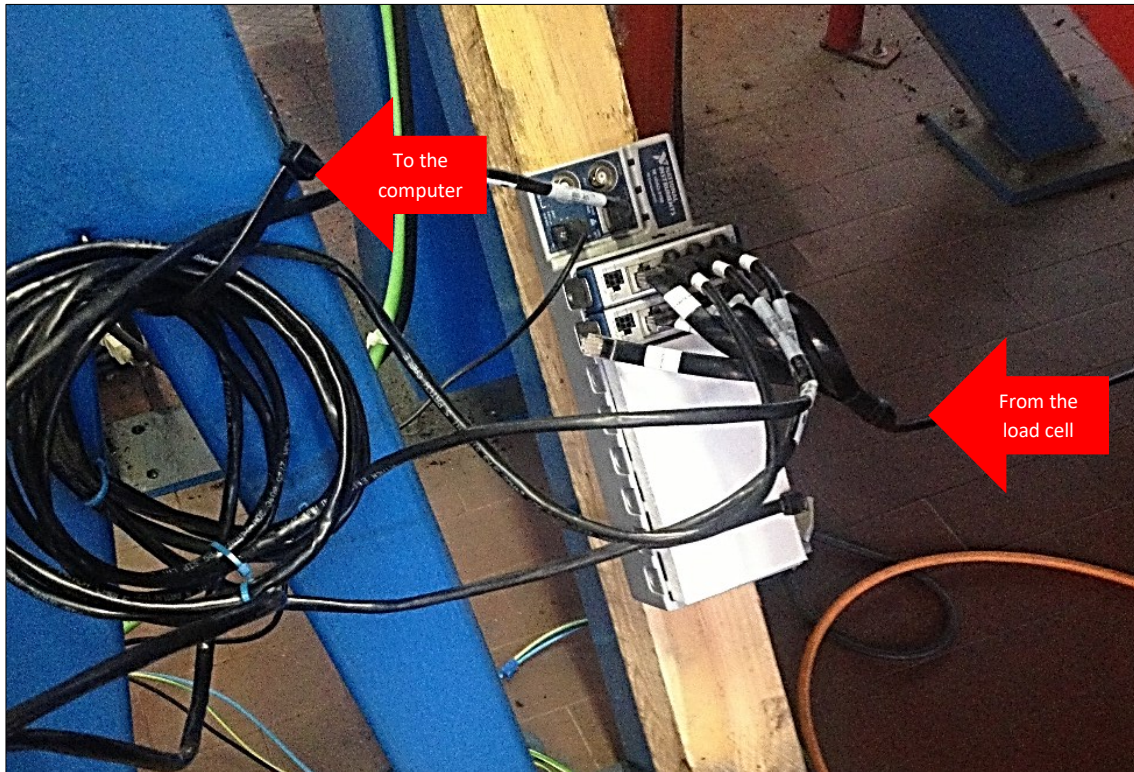


Figure 96: Portion of the data acquisition system (NI cDAQ-9178 and NI 9237).

Figure 96 illustrates a portion of the data acquisition system where we can clearly identify the two modules NI 9237 mounted on the NI cDAQ-9178 chassis. Both modules, together, have a total of eight channels. The “Mototiremeter” requires three channels since we measure three components while the new machine requires six channels for the six measured components. Therefore by interchanging some cables, the DAQ system was made global (Figure 98) for both machines. The chassis was positioned under the rotating disk, so the load cell cable can reach the modules. In the future it is recommended to use a longer shielded cable in order to keep the chassis in a safer location protected from dust and other possible damaging factors.

4.7.1 Load Cell

It is the main reason behind developing a new tire machine. It was purchased from “SMART Mechanical”; a spinoff company born in May 2012 from the University of “Politecnico di Milano”. It is directly attached to wheel assembly (¶ 4.4) of the new tire machine. The load cell is capable of measuring the three force and three moments on the tire (Figure 97). A full detailed user manual of the load cell is available in Appendix E.

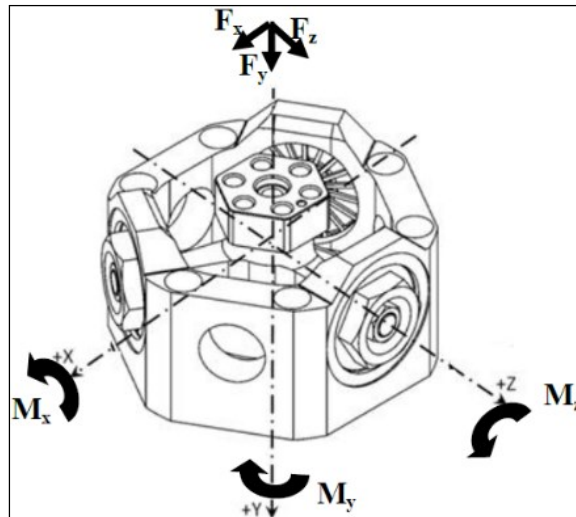


Figure 97: Load cell axes

4.7.2 NI-9237 module

The NI-9237 simultaneous bridge module for use with NI Compact-DAQ and Compact-RIO contains all the signal conditioning required to power and measure up to four bridge-based sensors simultaneously. The four RJ50 jacks provide direct connectivity to most torque or load cells and offer custom cable solutions with minimal tools. The high sampling rate and bandwidth of the NI 9237 offer a high-quality, high-speed strain or load measurement system with zero inter-channel phase delay. With 60 VDC isolation and 1,000 Vrms transient isolation, the NI 9237 has high-common-mode noise rejection and increased safety for both the operator and test system. The NI 9237 can perform offset/null as well as shunt calibration and remote sense, making the module the best choice for strain and bridge measurements.

4.7.3 NI cDAQ-9178

The NI cDAQ-9178 is an 8-slot NI Compact-DAQ USB chassis designed for small, portable, mixed-measurement test systems. Combine the cDAQ-9178 with up to eight NI C Series I/O modules for a custom analog input, analog output, digital I/O, and counter/timer measurement system. The NI 9237 modules are directly inserted on the chassis which itself is connected to the computer by an Ethernet cable.

4.7.4 Workstation

It is the same desktop computer (Figure 13) as before. The Labview DAQ code (§ 4.5) presents a user friendly interface that allows direct monitoring of the measured forces and moments. The data are saved in a text file which is, later on, imported in a Matlab code for data processing (§ 3.5).

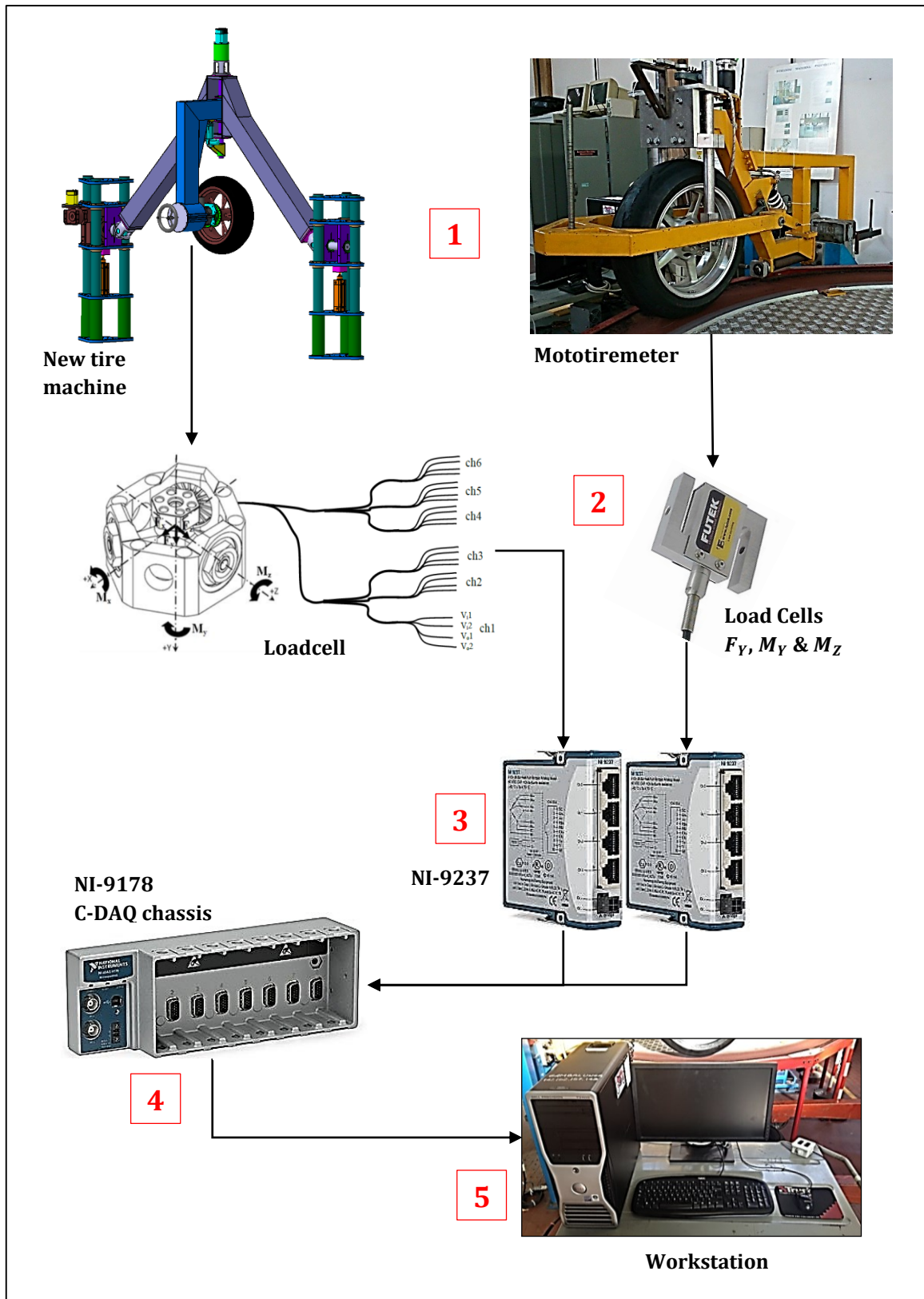


Figure 98: Global DAQ system

4.8 Instructions

4.8.1 Hardware

The hardware instructions for the new tire machine are similar to section 2.5.1. The only difference is in the cable connections between the load cell and the NI-9237 modules. The load cell's cable has six terminals, one for each measurement. Those terminals are connected to two NI-9237 modules following a specific order (Table 12).

Cable number	NI-9237 module	Channel number
Ponte 1	Module 2	CH 0
Ponte 2	Module 2	CH 1
Ponte 3	Module 2	CH 2
Ponte 4	Module 2	CH 3
Ponte 5	Module 1	CH 2
Ponte 6	Module 1	CH 3

Table 12: Load cell's cable connections

4.8.2 Software

- Follow the previous steps (¶ 2.5.2) for the NI-MAX part
- Launch Labview and open the latest version of the program (Figure 99)
- From the calibration and zero rest panel (¶ 4.5) create the zero file which will be the zero reference of the load cell
- The rest of the panel remained identical therefore follow the previous instructions (¶ 2.5.2)

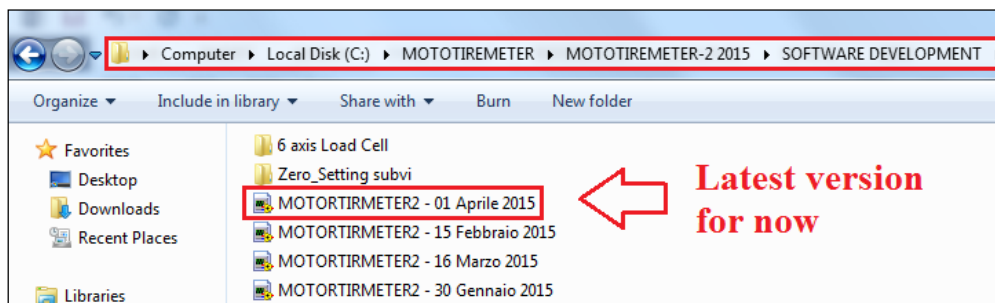


Figure 99: Path of the software for the new machine

4.9 Machine setup

- Measure the rolling and toroid radius of the tire (¶ 3.1)
- Adjust the roll axis height (equal to toroid radius) with the pneumatic system (¶ 4.1.6)
- Adjust the wheel center height (equal to rolling radius) with the linear actuator (¶ 4.3.4)
- Mount the tire on the wheel hub (¶ 4.4.2)
- Adjust the lateral position of the wheel to be at the center (¶ 4.4.1)
- Monitor the measured vertical load in Labview (¶ 4.5.2) and apply the desired value using the pneumatic system.
- If necessary adjust the vertical load, with precision, using the linear actuator (¶ 4.3.4)

4.10 Project management

A project success strongly depends on the management aspect which deals with three main characteristics; specifications, budget and delay. Project management relies on finding the optimal compromise (Figure 100) based on the project priorities. For example achieving higher specifications (higher quality) in a shorter delay (fast result) implies an increase in cost. The opposite scenario is also valid where decreasing the budget and the delay implies reducing the specifications (less quality).



Figure 100: Project management diagram

The tire machine project suffered from a tremendous delay, a large number of misconceptions and a strict budget. In order to achieve a satisfactory result, a considerable part of the design was modified to improve the specifications. As mentioned previously, increasing the quality requires a compromise in budget and/or delay. On the other hand the delay is constrained by the doctorate duration which is divided as follows.

$$T_{\text{Project completion}} = T_{\text{Design}} + T_{\text{Construction}} + T_{\text{Testing}} \quad (4-10)$$

The construction time was hard to predict due to several factors. An extensive amount of time was spent to purchase materials due to the university's bureaucracy. Also the associated technician was not fully available due to his involvement in other activities which restricted more the time factor. The problem was partially resolved by reducing the testing time and incorporating the design time, when it was possible, in parallel to the construction time. The remaining compromise was to increase the budget in order to improve the machine specifications and not sacrifice the product quality.

Table 13 exposes the cost comparison between one of the proposed design (Figure 79 – third image) and the applied design (Figure 79 – fourth image) for the machine universal joints (§ 4.2.2). As a matter of fact, the applied solution shows a higher cost (increment of approximately 27%) over the proposed solution. But on the other hand, such solution did demonstrate a huge amount of time saving and a more rigid joint.

Equipment	Proposed Solution				Applied Solution		
	SKF SYJ_30 KF	SKF SYJ_55 KF	Support plate	Spider	Spider	Forks	Support plate
Quantity	4	4	4	2	2	4	2
Price (in euro)	31	64	15	0	75	97.6	10
Total (IVA Included)	124	256	60	0	150	390.4	20
TOTAL	440				560.4		
% Price increment	27.36						

Table 13: Cost comparison between the design solutions for the machine joints

Table 14 shows another example of cost comparison for the height adjustment mechanism of the slip arm (¶ 4.3.4). In this case the applied solution shows a price increment of 24% but the resulting benefits make it a very good compromise. The height adjustment is fully automatic instead of manual which increase the safety of the user and save time. The linear actuator have a high price since it comes with the proper module (from National Instruments) to control it from the PC by mean of Labview, but of course it is possible to use a simple linear actuator that is directly actuated by a switch and therefore the price drops to 804 € which is lower than the proposed solution. In addition such solution offered the possibility of mounting a step motor on the top of the slip arm, therefore avoiding the use of a linear actuator for slip motion (see ¶ 4.3.5 for the advantages).

Equipment	Proposed Solution			Applied Solution			
	Recirculating screw	Sleeves	Steering wheel	Splined shaft	Sleeves	Sleeves housing	Linear actuator
Quantity	1	2	1	1	3	2	1
Price (€)	158.7	258.6	15.0	102.0	20.5	98.0	500.0
Total (IVA Included)	193.6	630.9	18.3	124.4	75.0	239.1	610.0
TOTAL (€)	842.8			1048.6			
% Price increment	24.41						

Table 14: Cost comparison between design solutions for the vertical adjustment mechanism of the slip arm

Let us define the specification indicator ($\eta_{\text{Specification}}$) and time indicator (η_{Time}) as follows. This definition implies that the higher the factor is, the better the situation.

$$\eta_{\text{Specification}} = \frac{\text{Specification}}{\text{Cost}} \quad (4-11)$$

$$\eta_{\text{Time}} = \frac{\text{Cost}}{\text{Time}} \quad (4-12)$$

Figure 101 represents a radar chart which illustrates the evolution of the project characteristics from the initial status to the final status. The chart demonstrates an increase (approximately 28 %) in the budget from the initial to the final status. The intended budget comparison represents the cost difference between the primary designs and the applied solutions therefore the rest of the cost is excluded. The 28 % increase in the budget was the consequence of an increase (six times more) in specifications (better design, better equipment...) and a decrease in delay (2.6 times less).

Such compromise was found necessary in order to guaranty a good quality machine as well as respecting the deadline scheduled for project completion.

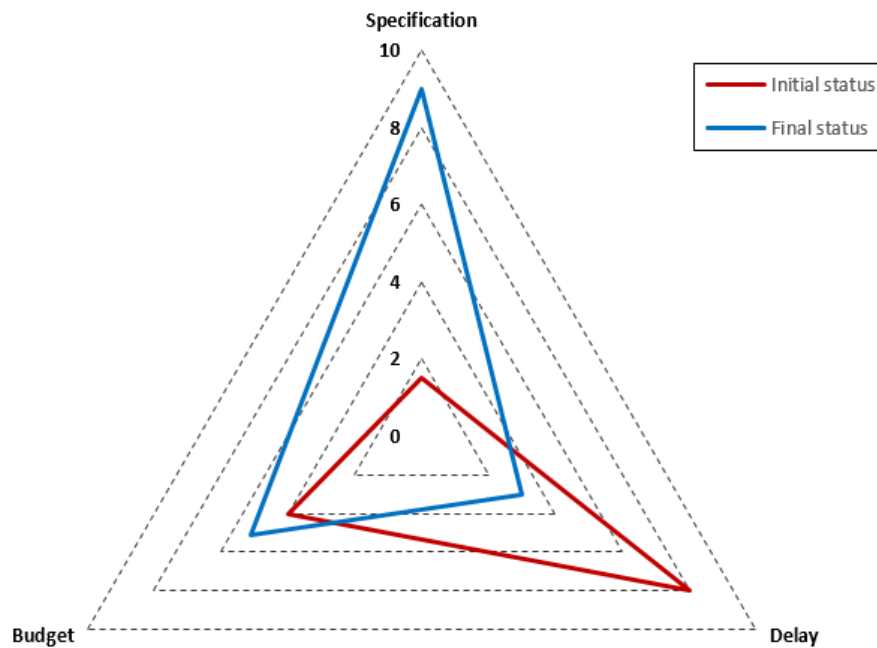


Figure 101: Project management’s radar chart for initial and final status.

Table 15 exposes the values for the specification ($\eta_{\text{Specification}}$) and time (η_{Time}) indicators at the initial and final status of the project. Both indicators have higher values at the final status which justifies the increase in budget. Such compromise was necessary to insure the completion and success of the project.

	Initial status	Final Status
$\eta_{\text{Specification}}$	0.4	1.8
η_{Time}	0.5	1.7

Table 15: Project management indicators

Table 16 gives a detailed idea of the machine’s cost while Appendix F encloses the necessary documents of the several purchases. The list shows only the purchased materials and/or the machined pieces at private firms. The rest of the pieces was machined at our laboratory, with zero cost, therefore it was excluded from the table.

Equipments	Supplier	Price in euro (IVA included)
Roll and Slip arm	OMERO	2684.00
Pneumatic pistons and tanks	Fratelli BONO	828.00
Pneumatic system and valves	PANAR	672.00
Tubes for the columns	SPIROL	598.00
Horizontal plates	G&B s.r.l	512.00
Speed reducer Bonfiglioli	MATRA	702.00
Vertical plates	Dipartimento di Fisica	512.40
Bushings for horizontal plates	Dipartimento di Fisica	512.40
Forks for Cardan Joints	CARDAN TEC	338.00
Spider for cardan joints	CATI	150.00
Splined shaft with sleeves	CATI	278.00
Sleeve's housing	Toma s.a.s. di Brilli Massimiliano	239.00
Bearing plate	Toma s.a.s. di Brilli Massimiliano	220.00
Planetary gear unit – Bonfiglioli	CATI	916.00
Steering wheel & screws	CATI	20.00
Various bearings	CATI	335.50
Load cell	SMART Mechanical	6000.00
Step motors & drivers	R.T.A	1018.46
Linear actuator	CATI	284.00
Speed reducer oil (SHEEL 4 Kg)	CATI	77.00
TOTAL in euro (IVA included)		16896.76

Table 16: List of prices

4.11 Conclusion

As mentioned previously, tire testing is a fundamental and necessary step to create a realistic tire model in order to have a better understanding of vehicle handling and stability. The extremely high price of a tire testing machine makes it impossible for our laboratory to purchase one. On the other hand, tire testing in private facilities is also expensive which will limit the amount of required tests and therefore limits our research.

This major concern pushed our group (Motorcycle Dynamics research Group) to take the initiative of designing and building a tire testing machine that shares the accuracy of the available machine in the market but at a reduced cost. The first machine was the Mototiremeter which was built a long time ago. As described in Chapter 2, such machine was old and out of date therefore a complete update of the hardware and software was performed and the machine was used to test several tires for different manufacturer and also write some articles (Chapter 3).

After gaining a good experience on the Mototiremeter, the research group decided to launch a new prototype (Chapter 4) that offers major advantages over the Mototiremeter. Table 16 summarizes the total cost of the machine which comes approximately to 17000 euro with taxes included. Such price is relatively negligible compared to the tire machines in the market therefore the primary objective was achieved. Such prototype breaks the barrier by offering a cheap and permanent alternative for tire testing. This helps our group to expand researches in the area of vehicle dynamics (specifically handling and stability for motorcycles) without major concerns about tire testing cost. This prototype offers the possibility of measuring the longitudinal forces (acceleration and braking) as well as performing transient test which will allow us to exploit such area in research and publish some articles.

Acquiring experience on the new tire machine will allow us to improve it more in the future and hopefully build a more advanced prototype using a continuous running flat belt instead of the rotating disk (Figure 5). The running flat belt system is much more expensive than the rotating disk but it offers many advantages such the compact size, the straight running therefore the absence of the turn force (Figure 41) and the possibility of testing at higher speeds without excessive vibrations.

Another interesting point, for the next prototype, will be to design it with one column for height control instead of two. Such design idea have the advantage of saving space since the machine will be half the size, but the real advantage will be in the time saved to setup the machine accurately. Having two columns requires having them perfectly parallel in order to insure a smooth vertical motion which is really hard to obtain due the floor inclination and welding distortion... In addition having one column will avoid the problem of moving both sides together accurately which saves time and increase the testing precision.

The use of the pneumatic system was justified by using the air's compression as a spring-damper system for the wheel due the surface imperfection and the disk vibrations. It will be better to design the next prototype with a hydraulic system which offers more thrust force and precision than the air system. Such precision is needed in order to adjust the height depending on the toroid radius of the tire. A spring-damper can be incorporated on the slip arm to substitute the air spring damper system. Having a real spring- damper system will allow the possibility of tuning to have a better control of the motion damping in function of the disk speed and other factors as well.

It would be interesting to design a smarter solution for mounting the wheel on the hub of the machine in order to save time. Each rim has different dimension so it is important to design a solution that takes into account the majority of the standard rims. Implementing a dynamic system for tire pressure control is not necessary but can be advantageous.

The two tire machines are controlled by mean of an old motion controller implemented in the computer. Such motion control is old and out of date. It will be important in the future to update the whole motion control system by using a more advanced motion controller like the PXI motion controller from National Instruments. Such motion controller can be directly plugged on a Compact-Rio chassis, also from National Instruments, which allow an easier and better motion control. This system substitutes the need of desktop computer, it can be directly connected to a laptop by mean of a USB cable.

The data acquisition represents the most important part since it provides us with all the necessary measurements to analyze and better understand tire's behavior. In order to make such process more beneficial, it can be interesting to add pressure sensor to have readings of the dynamic tire pressure variation, as well as infrared temperature sensor to have data of the tire temperature at the center of carcass and also on the sidewalls. As mentioned at the beginning, pressure and temperature are two important factors that influence the behavior of a tire.

Bibliography

- [1] G. Cocco, *Motorcycle Design and Tecnology: How and Why*, 1999.
- [2] T. Takahashi, T. Yamada and T. Nakamura, "Experimental and theoretical study of the influence of tyres on straight running motorcycle weave response. SAE Paper 840248," 1984.
- [3] V. Cossalter, A. Doria, M. Formentini and M. Peretto, "Experimental and numerical analysis of the influence of tyres' properties on the straight running stability of a sport-touring motorcycle," *Veh Syst Dyn.* 2012;50(3):357-375..
- [4] V. Cossalter, R. Lot and F. Maggio , "The Inflence of Tyre Properties on the Stability of a Motorcycle in Straight Running and Curves," *Proceedings of the 2002 SAE Automotive Dynamics and Stability Conference*.
- [5] R. Lot, "A Motorcycle Tire Model for Dynamic Simulations: Theoretical and Experimental Aspects," 2002-2003.
- [6] v. Cossalter, R. Lot and M. Massaro, "The chatter of racing motorcycles," 2008.
- [7] J. Neubauer and D. Freitag, "Tire Development in the Spirit of Sustainable Mobility," vol. 63, no. 5, pp. 182-186, 2010.
- [8] Mihon and Liviu, "Tyre Quality Influence on Fuel Consumption for Motor Vehicles," vol. 20, pp. 751-752, 2009.
- [9] P. Pillai, "Effect of tyre overload and inflation pressure on rolling loss (resistance) and fuel consumption of automobile and truck/bus tyres," vol. 11, no. 5, pp. 406-412, 2004.
- [10] S. Thiele, D. Bellgardt and M. Holzleg, "Polymer functionalization - Novel rubber for tire tread application," vol. 61, no. 5, pp. 244-245, 2008.
- [11] R. Lot and N. Dal Bianco, "Lap time optimisation of a racing go-kart," 2015.
- [12] T. D. Gillespie, *Fundamentals of Vehicle Dynamics*, Warrendale, PA: SAE International, 1992.
- [13] J. Y. Wong, *Theory of Ground Vehicles*, New York: John Wiley and Sons, 2001.
- [14] H. Taghavifar and A. Mardani, "Investigating the effect of velocity, inflation pressure, and vertical load on rolling resistance of a radial ply tire," 2013.
- [15] V. Cossalter, V. Favaron and T. Jomaa, "The effect of tire inflation pressure on weave stability," *Vehicle System Dynamics*, 2016.
- [16] F. Farroni, D. Giordano, M. Russo and F. Timpone, "TRT: thermo racing tyre a physical model to predict the tyre temperature distribution," vol. 49, no. 3, pp. 707-723, 2014.
- [17] C. Angrick, "Influence of Tire Core and Surface Temperature on Lateral Tire Characteristics," 2014.
- [18] G. Leister, "New Procedures For Tyre Characteristic Measurement," *Vehicle System Dynamics*, 2007.
- [19] H. Pacejka, *Tyre and vehicles dynamics*, second ed., SAE International and Elsevier, 2005.
- [20] N. Ruffo, "Relazione riassuntiva macchina per la misura dei pneumatici di tipo motociclistico," 2000-2001.
- [21] N. Ertugrul, *LabVIEW for Electric Circuits, Machines, Drives, and Laboratories*, Prentice Hall, 2002.

- [22] B. Mihura, LabVIEW for Data Acquisition, Prentice Hall PTR, 2001.
- [23] . B. Heiing and M. Ersoy, Chassis Handbook: Fundamentals, Driving Dynamics, Components, Mechatronics, Perspectives, Vieweg+Teubner Verlag, 2011.
- [24] A. Doria, I. Taraborelli and T. Jomaa, "Identification of the mechanical properties of tires for wheelchair simulation," *The Open Mechanical Engineering Journal*, 2016.
- [25] E. Magrab, S. Azarm, B. Balachandran and J. Duncan, An engineer's guide to MATLAB: with applications from mechanical, aerospace, electrical, civil, and biological systems engineering, Prentice Hall, 2011.
- [26] V. Cossalter, Motorcycle dynamics. 2nd ed., 2007.
- [27] E. De Vries and H. Pacejka, "Motorcycle tyre measurements and models," 1998.
- [28] D. Lu, K. Guo, H. Wu and N. Moshchuk , "Modelling of tire overturning moment and loaded radius," 2007.
- [29] T. Takahashi, M. Hada and K. Oyama, "New Model of Tire Overturning Moment Characteristics and Analysis of Their Influence on Vehicle Rollover Behavior," 2010.
- [30] V. Cossalter, A. Doria, E. Giolo, L. Taraborelli and M. Massaro, "Identification of the characteristics of motorcycle and scooter tyres in presence of large variations in inflation pressure," *Veh Syst Dyn.* 2014;52(10):1334-1354.
- [31] V. Cossalter, M. Massaro and G. Cusimano, "The effect of the inflation pressure on the tyre properties and the motorcycle stability," *Proceedings of the Institution of Mechanical Engineers, Part D: Journal of Automobile Engineering* 2013; 227(1480):1480-1488.
- [32] A. Doria, M. Tognazzo, G. Cusimano, V. Bultink, A. Cooke and B. Koopman, "Identification of the mechanical properties of bicycle tyres for modelling of bicycle dynamics," *Vehicle System Dynamics: International Journal of Vehicle Mechanics and Mobility*, 51:405–420, 2012.
- [33] R. Lot and E. Cappelletti, "Progettazione di un braccio strumentato per la macchina di misura degli pneumatici.," Padova, 2013-2014.

Nomenclature

P	Perimeter expressed in millimeters
F	Force applied expressed in Newton
F_x	Longitudinal force expressed in Newton
F_y	Lateral force expressed in Newton
F_z	Vertical force expressed in Newton
M_x	Overtuning moment expressed in Newton meter
M_y	Rolling resistance moment expressed in Newton meter
M_{y_0}	Rolling resistance moment expressed in Newton meter at zero slip and roll
M_z	Self-aligning or twisting moment expressed in Newton meter
rr	Rolling radius expressed in millimeter
tr	Toroid radius expressed in millimeter
α	Slip angle expressed in degree
γ	Roll (camber) angle expressed in degree
β	angle expressed in radians (it can be the slip or roll angle)
S_r	Slip ratio (without unit)
V_l	Longitudinal speed expressed in meter per second
Ω_w	Rotational speed of the wheel expressed in radians per second
K_R	Radial stiffness expressed in Newton per millimeter
K_L	Lateral stiffness expressed in Newton per millimeter
Δ	Displacement expressed in millimeter
π	≈ 3.14
B	Stiffness factor
C	Shape factor
D	Peak factor
E	Curvature factor
m_r	Twisting torque (or rolling resistance) coefficient
t_w	Twisting torque (or rolling resistance) coefficient
μ_x	Longitudinal coefficient of friction
$P_{C_{x_1}}$	Shape factor for C_x (=1.5 by default)
λ_{C_x}	Scale factor for F_x (=1 by default)
$P_{K_{x_1}}$	Longitudinal slip stiffness (=50 by default)
$\lambda_{K_{x_k}}$	Scale factor for slip stiffness (=1 by default)
CH0	first channel on the national instrument module
CH1	Second channel on the national instrument module
CH2	Third channel on the national instrument module
CH3	Fourth channel on the national instrument module
txt	extension for text files type
DAQ	Acronym for Data acquisition
CAD	Acronym for computer-aided design
SKF	Acronym for Svenska Kullagerfabriken, a bearing manufacturer company
RTA	Acronym for a company in the emotion control industry
r_w	Rim width expressed in millimeters
T_{roll}	Required torque at the roll shaft
T_{input}	Output torque of the speed reducer
T_{output}	Input torque of the speed reducer

List of figures

Figure 1: Grant chart illustrating the carried activities during the three doctoral years.	7
Figure 2: The FlatTrac III Classic from MTS.....	10
Figure 3: Calspan tire test machine.....	11
Figure 4: Delft-tire test trailer.....	12
Figure 5: Mototiremeter testing machine.....	14
Figure 6: The coordinate system for the definition of tire forces and torques.....	14
Figure 7: Old Control Unit of the Mototiremeter.....	15
Figure 8: Bad wiring.....	16
Figure 9: Roll switch (left side) and Slip switch (right side).....	16
Figure 10: Useless hardware.....	16
Figure 11: Removal of useless hardware.....	16
Figure 12: Proper wiring.....	17
Figure 13: New workstation – Front view.....	17
Figure 14: New workstation – Rear view.....	17
Figure 15: New switchbox.....	18
Figure 16: Front panel of the old software.....	18
Figure 17: New control block diagram.....	19
Figure 18: New DAQ block diagram.....	19
Figure 19: New front panel – First stage.....	20
Figure 20: New front panel – Final stage.....	20
Figure 21: Switch to power the hardware.....	21
Figure 22: Ethernet cable for NI-DAQ chassis.....	21
Figure 23: Cable connections to the NI-9237 for “Mototiremeter”.....	21
Figure 24: Path of the software for current machine.....	22
Figure 25: Rolling Radius measurement.....	24
Figure 26: Toroid radius measurement.....	24
Figure 27: Toroid radius calculation software.....	25
Figure 28: Radial stiffness test.....	25
Figure 29: Lateral stiffness test.....	26
Figure 30: Lateral displacement measurement.....	26
Figure 31: Side slip test.....	27
Figure 32: Camber test.....	27
Figure 33: Combined test.....	28
Figure 34: Radial stiffness results for front tires.....	29
Figure 35: Radial stiffness results for rear tires.....	29
Figure 36: Lateral stiffness results for front tires.....	30
Figure 37: Lateral stiffness results for rear tires.....	30
Figure 38: Side slip force for front tires at vertical load 1000N.....	31
Figure 39: Side slip force for rear tires at vertical load 1000N.....	31
Figure 40: Camber force for rear tires at vertical load 1000N.....	32
Figure 41: Curvature effect in case of positive and negative side slip angle (α).....	34
Figure 42: Corrected curvature data (dots) with Pacejka fitting curves.....	34
Figure 43: Exported data in Excel.....	35
Figure 44: Exported Pacejka coefficients in Excel.....	35
Figure 45: Overturning moment.....	38
Figure 46: Tire fitting software - Browse folder.....	39
Figure 47: TIRE_FITTING_V6 – Step one.....	40
Figure 48: TIRE_FITTING_V6 – Step two.....	41
Figure 49: TIRE_FITTING_V6 – Step three.....	41
Figure 50: Structural stiffness versus inflation pressure for front (90/90-21) and rear (130/80-17) tires.....	42
Figure 51: Side slip and camber stiffness in function of the inflation pressure for front (90/90-21) and rear (130/80-17) tires.....	42
Figure 52: Twisting and self-aligning torque stiffness in function of the inflation pressure for both tires.....	43
Figure 53: Forces and torques of wheelchair and bicycle tires in reference conditions (vertical load 400 N, inflation pressure 4 bar and disc speed 4 km/h).....	44

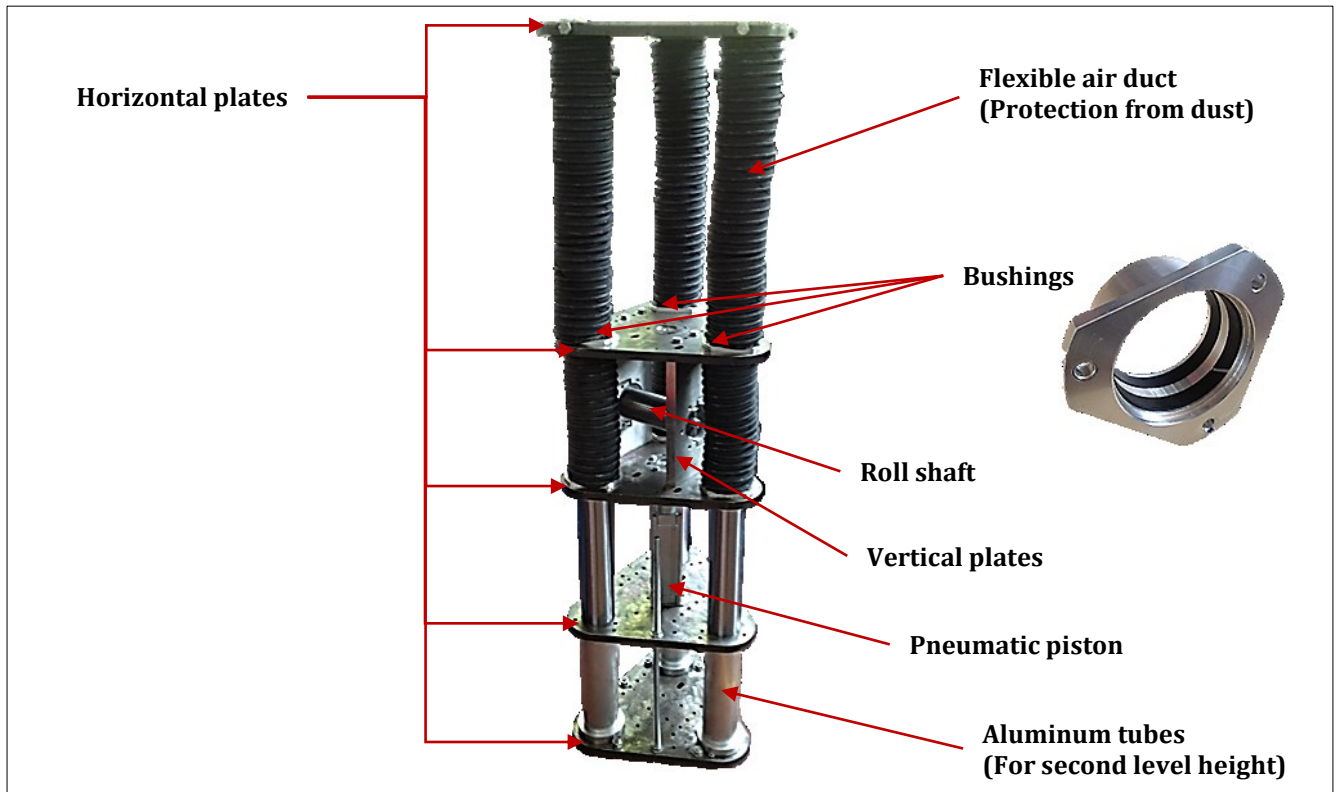
Figure 54: Effect of forward speed on side slip force	45
Figure 55: Effect of inflation pressure on tire forces and torques	45
Figure 56: Effect of vertical load on tire forces and torques	46
Figure 57 : New tire testing machine (CAD design and real picture)	48
Figure 58: Column assembly	49
Figure 59: Horizontal Plate designs	50
Figure 60: Holes adjustments	50
Figure 61: Base plate fixed on the ground	50
Figure 62: Welding	51
Figure 63: Welding cover	51
Figure 64: Column welding on bench	52
Figure 65: Welding on the bottom of the base	52
Figure 66: Vertical Plate designs	52
Figure 67: Bushing	53
Figure 68: Bushing modification	53
Figure 69: Speed reducer from Bonfiglioli for roll motion	54
Figure 70: Piston's mounting plate	55
Figure 71: Toroid center migration in function of the roll axis height	55
Figure 72: Pneumatic circuit	57
Figure 73: Portion of the pneumatic system	58
Figure 74: Electric box to operate the pneumatic system	58
Figure 75: Electric circuit	59
Figure 76: Roll arm assembly	60
Figure 77: Cross section of the roll arm.	60
Figure 78: Cross section of bearing assembly	61
Figure 79: Joint design solutions	61
Figure 80: Slip arm assembly	62
Figure 81: Shaft assembly	62
Figure 82: Planetary gear unit from "Bonfiglioli" for slip motion.	63
Figure 83: Cross section of sleeve assembly	64
Figure 84: Handle bar for height adjustment	65
Figure 85: Slip motion solutions	65
Figure 86: Wheel assembly	66
Figure 87: Toroid center migration in function of roll axis lateral position	66
Figure 88: Lateral adjustment mechanism (Cross section of wheel assembly)	67
Figure 89: Wheel hub	67
Figure 90: Control section of the new software	69
Figure 91: DAQ section – Similar part	69
Figure 92: DAQ section – Additional part.	70
Figure 93: Portion of the motion control system (Drivers)	72
Figure 94: Electric connections between the step motor, the drive and the UMI-7764	73
Figure 95: Global motion control system	74
Figure 96: Portion of the data acquisition system (NI cDAQ-9178 and NI 9237)	75
Figure 97: Load cell axes	76
Figure 98: Global DAQ system	77
Figure 99: Path of the software for the new machine	78
Figure 100: Project management diagram	79
Figure 101: Project management's radar chart for initial and final status.	81

List of tables

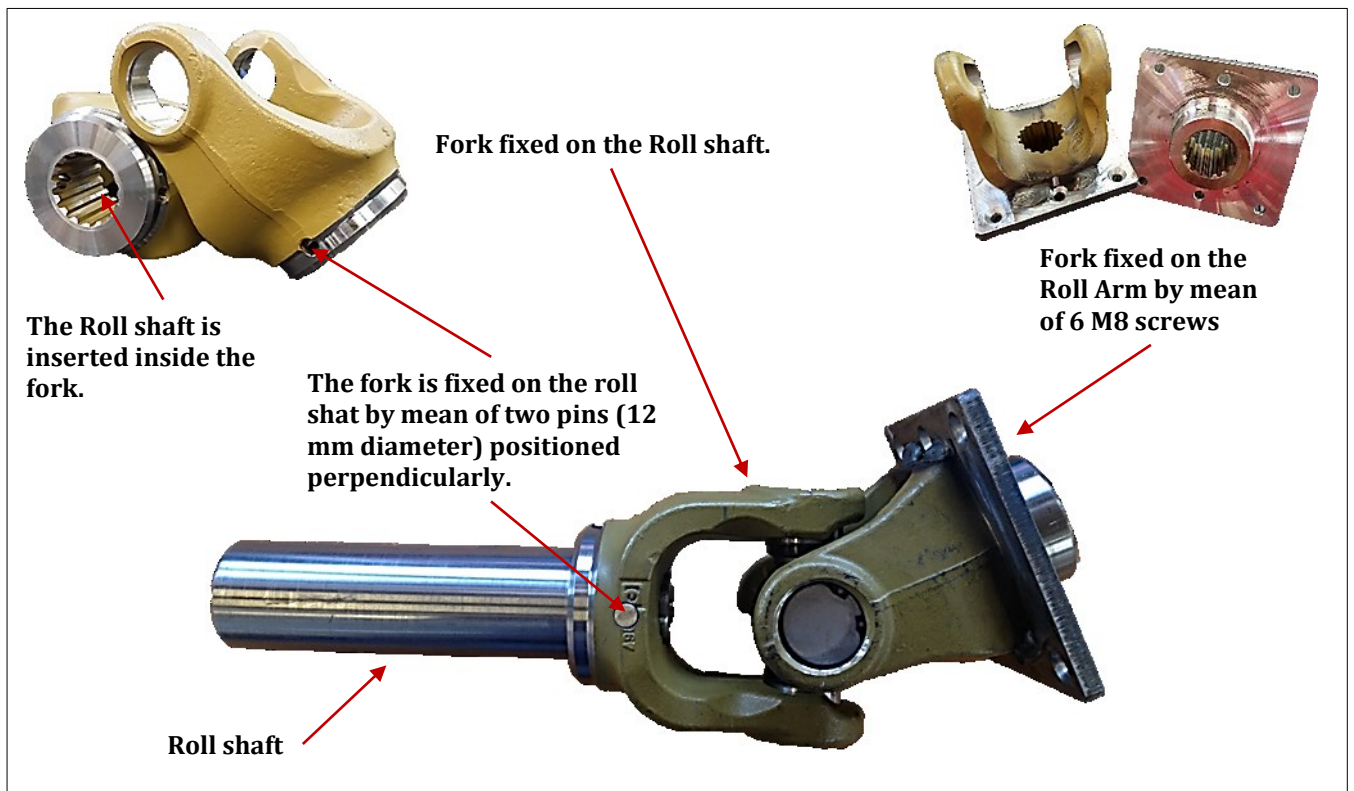
<i>Table 1: Measurement file from test session</i>	32
<i>Table 2: Magic formula coefficients</i>	35
<i>Table 3: Twisting torque coefficients</i>	36
<i>Table 4: Rolling resistance torque coefficients</i>	36
<i>Table 5: ALL_SLIP</i>	36
<i>Table 6: PACEJKA & PACEJKA_MYMZ</i>	37
<i>Table 7: Modified SLIP_DATA and ROLL_DATA</i>	39
<i>Table 8: Speed reducer characteristics for roll motion</i>	54
<i>Table 9: Pneumatic symbols</i>	56
<i>Table 10: Electrical symbols</i>	59
<i>Table 11: Characteristics of the planetary gear unit for slip motion</i>	63
<i>Table 12: Load cell's cable connections</i>	78
<i>Table 13: Cost comparison between the design solutions for the machine joints</i>	80
<i>Table 14: Cost comparison between design solutions for the vertical adjustment mechanism of the slip arm</i> ...	80
<i>Table 15: Project management indicators</i>	81
<i>Table 16: List of prices</i>	82

Appendix A

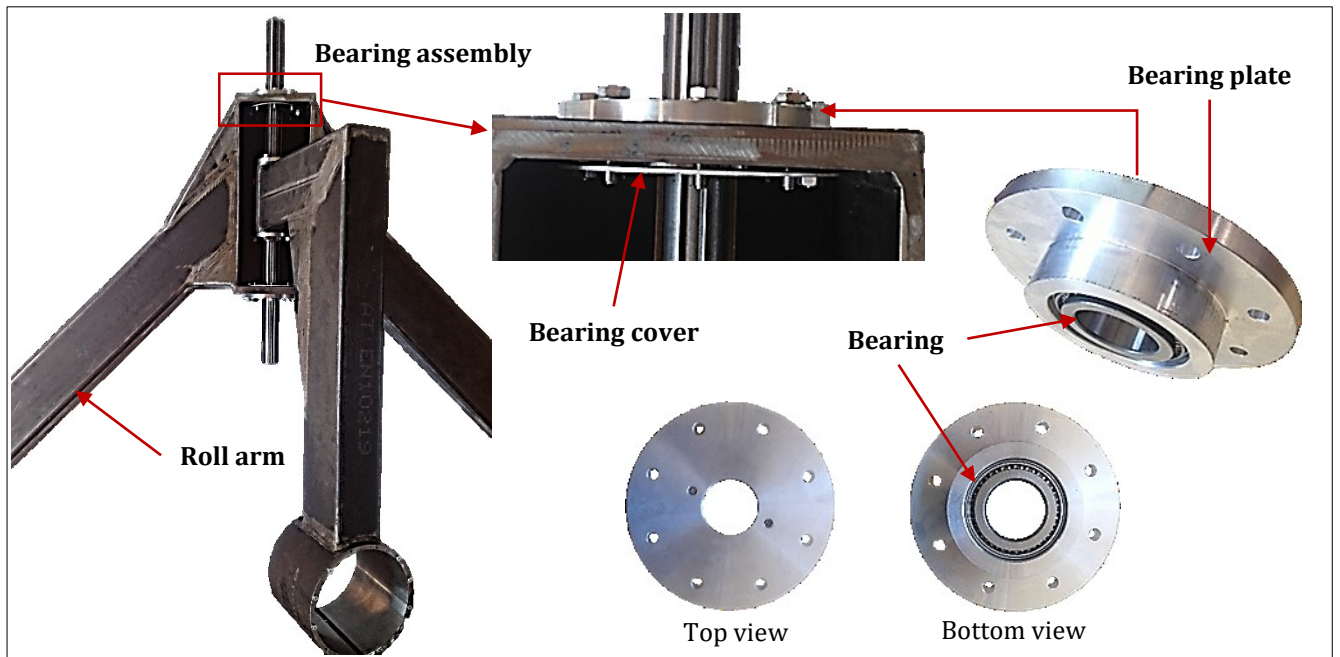
Column assembly



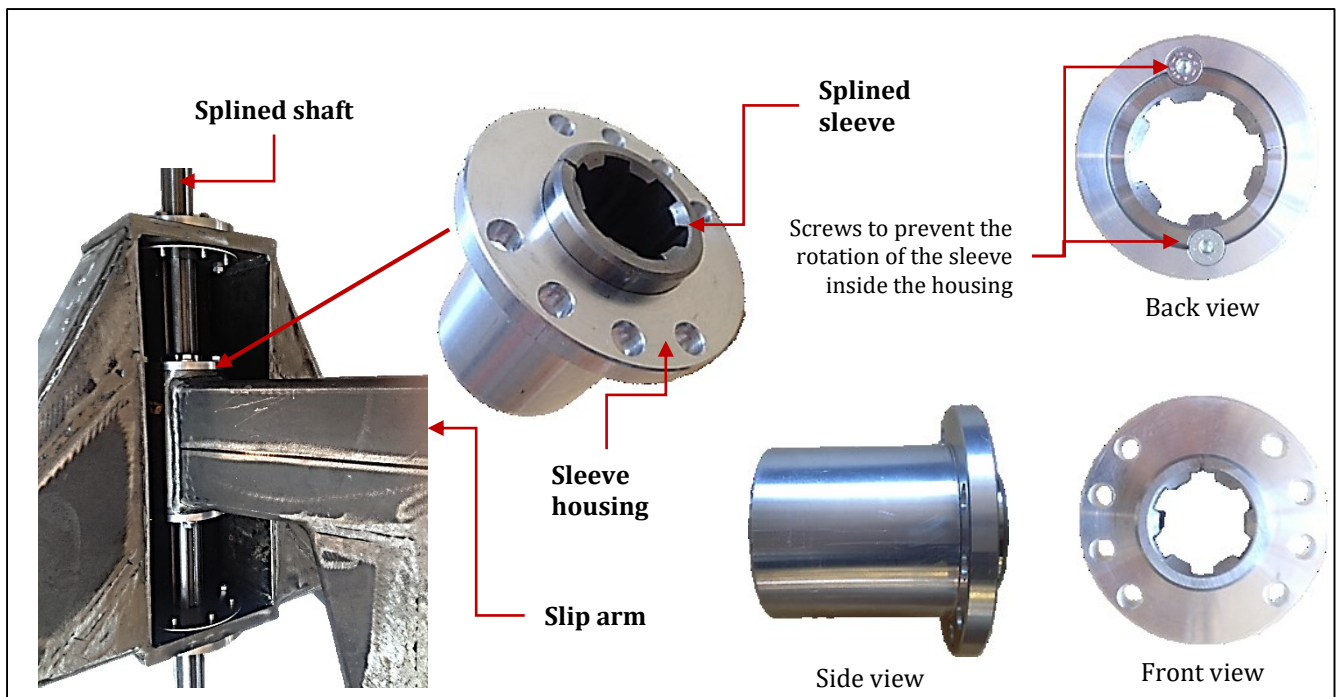
Roll shaft & Cardan joint



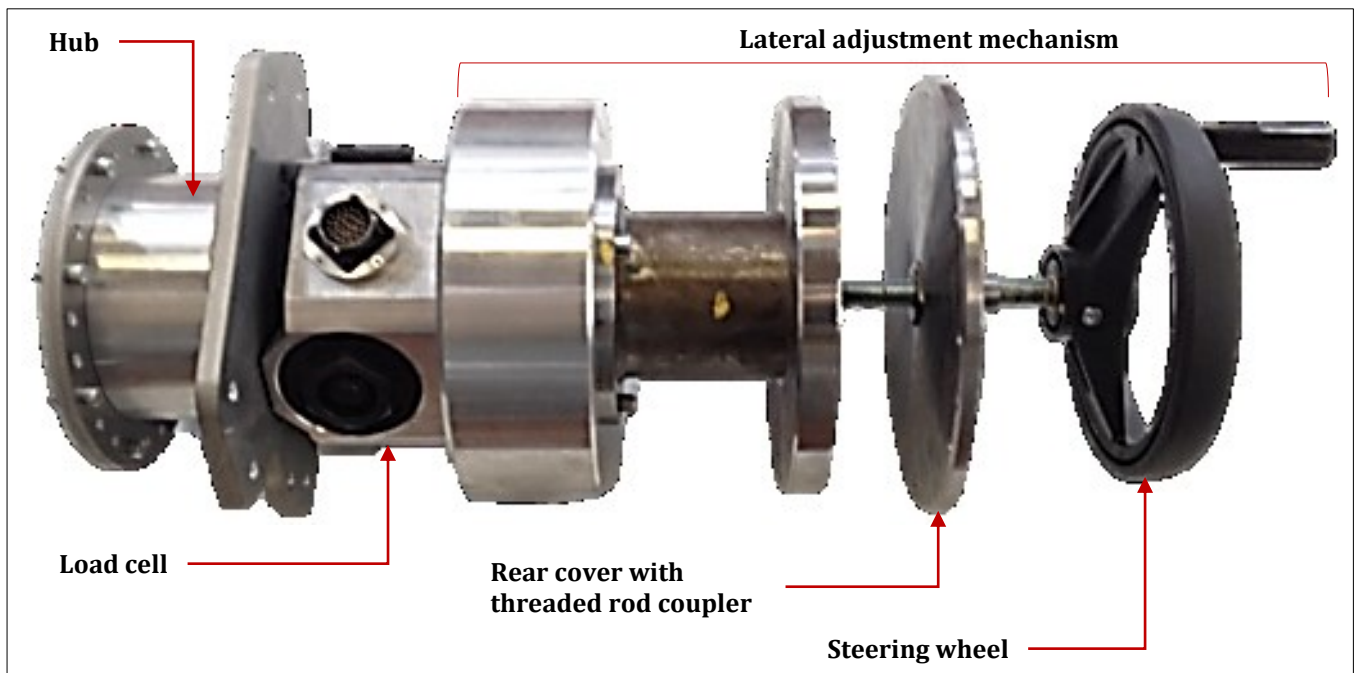
Roll arm assembly



Slip arm assembly

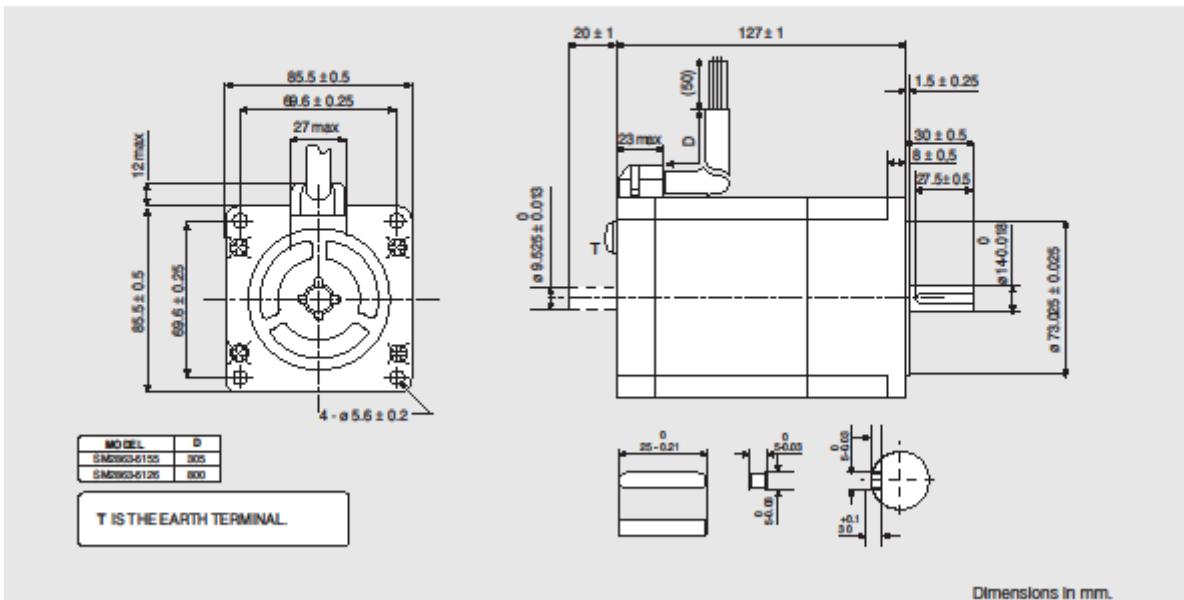


Wheel assembly



Appendix B

SANYO DENKI SANMOTION SM 2863-5155



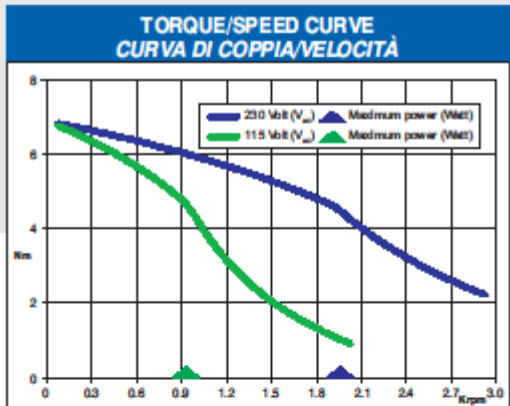
MODEL	D
SM2863-6155	305
SM2863-6126	800

T IS THE EARTH TERMINAL.

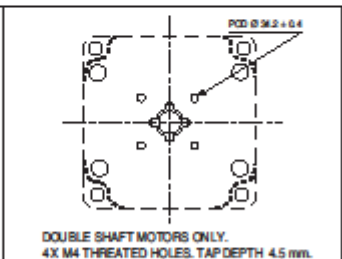
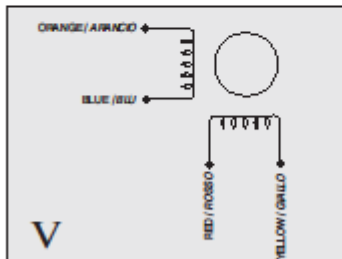
Dimensions in mm.

FEATURES CARATTERISTICHE	
MODEL MODELLO	SM2863 - 6155 (SM2863 - 5126)
BASIC STEP ANGLE	1.8° ± 0.09°
BIPOLAR PARALLEL CURRENT (Amp)	4
RESISTANCE (Ohm)	1
INDUCTANCE (mH)	7.9
BIPOLAR HOLDING TORQUE (Ncm)	920
ROTOR INERTIA (Kgm ² x 10 ⁻⁷)	4500
THEORETICAL ACCELERATION (rad x sec ⁻²)	20500
BACK E.M.F. (V/Krpm)	241
MASS (Kg)	4
INTERNATIONAL STANDARDS	UL, CSA, CE, RoHS
INSULATION VOLTAGE (V)	250 Vac (350 Vdc)
PROTECTION DEGREE - INSULATION CLASS	IP43 - F
LEADS CODE	V


Codes between brackets refer to double shaft models.
Le sigle tra parentesi si riferiscono ai modelli biassiale.

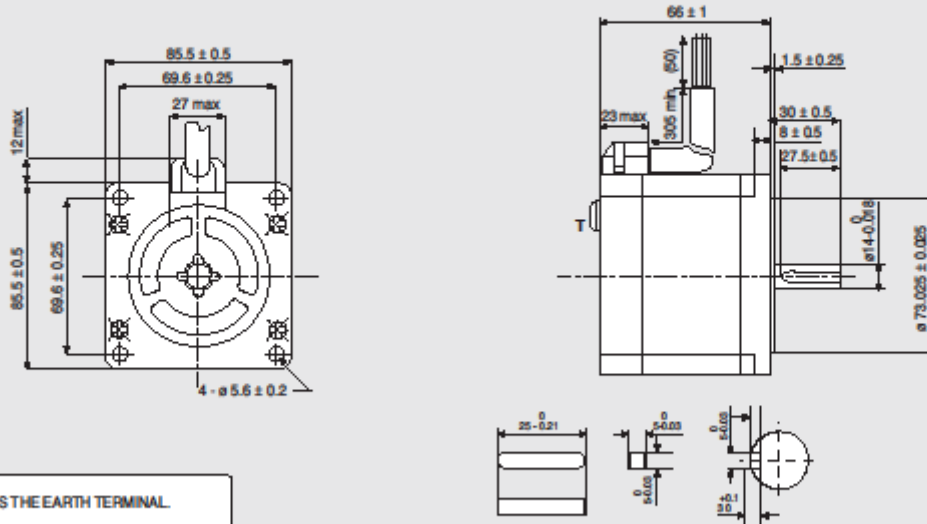


R.T.A. s.r.l. PAVIA (ITALY) SANYO DENKI CO., LTD (JAPAN)



Suggested R.T.A. driver: X-PLUS B Series, X-MIND Series.

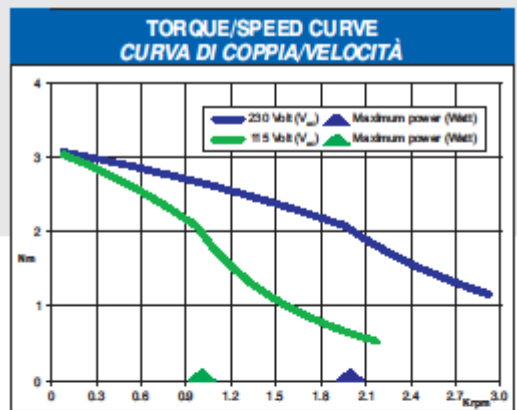
 <p>R.T.A. s.r.l. Via E. Mattei - Fraz. Divisa 27020 MARCIGNAGO (PV) ITALY Tel. +39.0382.929.855 - Fax +39.0382.929.150 www.rta.it</p>	<p>R.T.A. Deutschland GmbH Bublitzer Straße 34 40599 DÜSSELDORF (Germany) Tel. +49.211.749.668.60 - Fax +49.211.749.668.66 www.rta-deutschland.de</p>	<p>R.T.A. IBERICA-Motion Control Systems S.L. C/Generalitat 22, 1° 3° 08850 GAVA - BARCELONA (Spain) Tel. +34.936.388.805 - Fax +34.936.334.595 www.rta-iberica.es</p>
--------------------------------------------------------------------------------------------------------------------------------------------------------------------------------------------------------------------------------------------------	------------------------------------------------------------------------------------------------------------------------------------------------------------------------------	-----------------------------------------------------------------------------------------------------------------------------------------------------------------------------------------------



T IS THE EARTH TERMINAL.

Dimensions in mm.

FEATURES CARATTERISTICHE	
MODEL MODELLO	SM2861 - 5055
BASIC STEP ANGLE	1.8° ± 0.09°
BIPOLAR PARALLEL CURRENT (Amp)	2
RESISTANCE (Ohm)	2.2
INDUCTANCE (mH)	15
BIPOLAR HOLDING TORQUE (Nm)	350
ROTOR INERTIA (Kg·m ² × 10 ⁻⁷)	1480
THEORETICAL ACCELERATION (rad × sec ⁻²)	24300
BACK E.M.F. (V/Krpm)	180
MASS (Kg)	1.7
INTERNATIONAL STANDARDS	UL, CSA, CE, RoHS
INSULATION VOLTAGE (V)	250 Vac (350 Vdc)
PROTECTION DEGREE - INSULATION CLASS	IP43 - F
LEADS CODE	V



R.T.A. s.r.l. PAVIA (ITALY) SANYO DENKI CO., LTD (JAPAN)



Suggested R.T.A. driver: X-PLUS B Series, X-MIND Series.



R.T.A. s.r.l.
Via E. Mattei - Frax. Divisa
27020 MARCIGNAGO (PV) ITALY
Tel. +39.0382.929.855 - Fax +39.0382.929.150
www.rta.it

R.T.A. Deutschland GmbH
Bublitzler Straße 34
40599 DÜSSELDORF (Germany)
Tel. +49.211.749.668.60 - Fax +49.211.749.668.66
www.rta-deutschland.de

R.T.A. IBERICA-Motion Control Systems S.L.
C/Generalitat 22, 1° 3°
08850 GAVA - BARCELONA (Spain)
Tel. +34.936.388.805 - Fax +34.936.334.595
www.rta-iberica.es

INTRODUZIONE

STEP E DIREZIONE

ADVANCED

ANALOG INPUT

PROGRAMMABILI

EtherCAT

CANopen

Azionamenti Serie **X-PLUS B4.1**

INTRODUZIONE

- Nuovo azionamento per motori passo-passo prodotto da R.T.A. con alimentazione diretta da rete (da 110 V_{ac} a 230 V_{ac}) specificamente sviluppato per applicazioni ove occorre configurare alte performance applicative con ridotta rumorosità acustica e ridotte vibrazioni.
- Target: applicazioni evolute ove occorrono alta precisione, bassa rumorosità acustica e morbidezza di movimento.
- La perfetta sintesi tra alta potenza e bassa rumorosità acustica.

HIGHLIGHTS

- Full digital microstepping drive.
- Adaptive microstepping fino a 3.200 passi/giro.
- Gestione intelligente del profilo di corrente che consente di ottenere ottimi risultati in termini di morbidezza di movimento, bassa rumorosità e vibrazioni.
- Sistema di controllo alimentato evoluto, capace tuttavia di preservare la tradizionale semplicità d'uso degli azionamenti R.T.A.



UNO DEI PIÙ COMPATTI DRIVER AL MONDO CON ALIMENTAZIONE DIRETTA DA RETE (110 - 230 VAC)

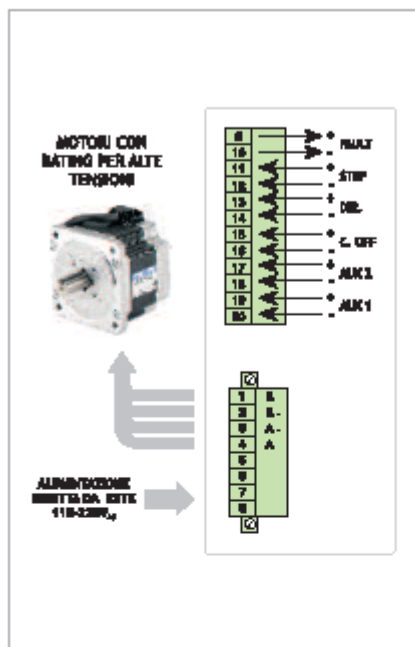
Serie	Modello	V _{ac} range (Volt)	I _r min. (Val. di picco) (Amp)	I _r max. (Val. di picco) (Amp)	Dimensioni (mm)
X-PLUS	B4.1	da 110 a 230 +/- 15%	2,4	4,0	152x129x46

CARATTERISTICHE TECNICHE

- Range tensione di alimentazione: 110-230 V_{AC}.
- Range di corrente: 2,4-4 Amp. Impostazione di 4 valori intermedi mediante dip-switch.
- Microstepping: 400, 800, 1.600 e 3.200. Impostazione mediante dip-switch.
- Riduzione automatica di corrente a motore fermo.
- Gestione del profilo di corrente impostabile mediante dip-switch.
- Protezioni:
 - Protezione di minima e massima tensione.
 - Protezione contro il corto circuito alla uscita motore.
 - Protezione termica.
- Evoluta sistema di smorzamento per il massimo controllo di rumorosità e vibrazioni.
- Versione in scatola metallica con connettori a vite estraibili. Massima compattezza.
- Ingressi opto-isolati per garantire la massima immunità al rumore.
- Non necessita di ventilazione forzata.
- Necessita accoppiamento con motori passo-passo dotati di rating per alta tensione e con flange non inferiori ad 86 mm.
- Garanzia: 24 mesi.



SCHEMA DI PRINCIPIO POTENZA E LOGICA



INTRODUZIONE

STEP E DIREZIONE

ADVANCED

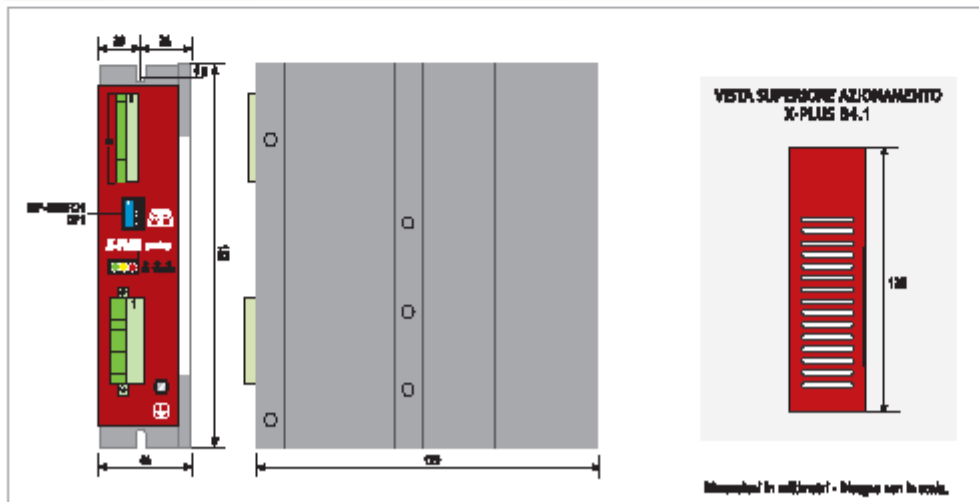
ANALOG INPUT

PROGRAMMABILI

ETHERCAT

CanOpen

INGOMBRI MECCANICI



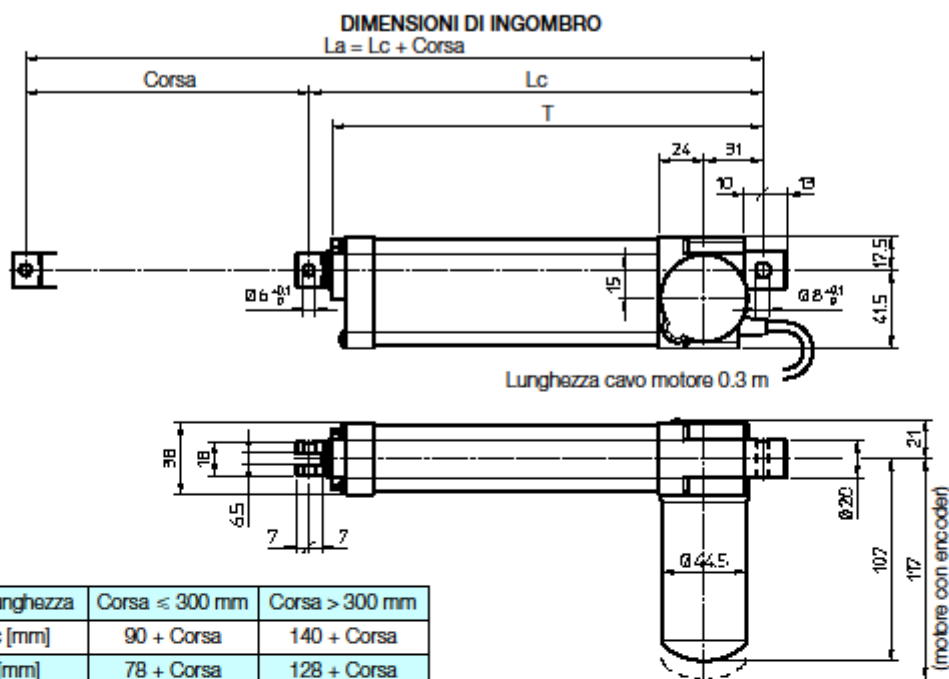
© R.T.A. s.r.l. ROMA (Italy) CAI - 02 - 14



RTA s.r.l.
Via E. Mattei - P.zza. Miriam
00192 ROMA (Italy) ITALY
Tel. +39.062.328.000 - Fax +39.062.328.000
www.rta.it

RTA Distribution GmbH
Bühlerstr. 34
40499 Düsseldorf (Germany)
Tel. +49.211.748.098.00 - Fax +49.211.748.098.00
www.rta-distribution.de

RTA. SERVO-Motion Control Systems S.L.
C/Barceloneta 23, 1º 2º
08004 GIRONA - BARCELONA (Spain)
Tel. +34.936.209.000 - Fax +34.936.204.000
www.rta-servo.com



Lunghezza	Corsa ≤ 300 mm	Corsa > 300 mm
Lc [mm]	90 + Corsa	140 + Corsa
T [mm]	78 + Corsa	128 + Corsa

CODICE CORSA	CORSA [mm]	LUNGHEZZA		MASSA [kg]
		Lc [mm]	La [mm]	
C50	50	140	190	0.85
C100	100	190	290	1.10
C150	150	240	390	1.25
C200	200	290	490	1.40
C250	250	340	590	1.55
C300	300	390	690	1.70

PRESTAZIONI E CARATTERISTICHE

- Carico in tiro - spinta fino a 1 300 N
- Velocità lineare fino a 52 mm/s
- Corsa standard: 50, 100, 150, 200, 250, 300 mm (corsa min. limitata da interruttori FC: 50 mm) (per corse diverse o maggiori contattare Ufficio Tecnico)
- Carcassa e attacco posteriore in alluminio
- Tubo di spinta in alluminio anodizzato - tolleranza f8
- Attacco anteriore in alluminio
- Motori CC 12, 24 o 36V con filtro anti-disturbo elettromagnetico (caratteristiche motori a pagina 69)
- Fattore di utilizzo a carico max.: 15% su 10 min a (-10...+40)°C
- Posizione motore standard come sul disegno dimensionale (destra, cod. RH)
- Grado di protezione: IP65
 - test IP6X secondo EN 60529 §12 §13.4-13.6
 - test IPX5 secondo EN 60529 §14.2.5 (test effettuati con attuatore fermo, non in movimento)
- Lubrificato a vita, esente da manutenzione

ACCESSORI

- Tubo di spinta in acciaio inossidabile (cod. SS)
- Due interruttori di fine corsa, interni all'attuatore, registrabili (cod. FC2)
- Due interruttori di fine corsa, interni all'attuatore, registrabili con arresto del motore (cod. FC2X)
- Un interruttore per posizione intermedia (cod. FC)
- Encoder incrementale a due canali su albero motore:
 - 1 imp/giro (cod. GI 21)
 - 4 imp/giro (cod. GI 24)
 (schemi di collegamento vedi pagina 75)

Numero impulsi per 100 mm di corsa	Rapporto			
	RN2	RN1	RL2	RL1
GI 21	192	383	483	967
GI 24	767	1 533	1 933	3 867

OPZIONI

- Motore montato sul lato opposto (sinistro, cod. LH)
- Attacchi ruotati di 90° (cod. RPT 90)

Appendix C

CILINDRI DIN ISO 15552 – PROFILATI Ø32-125 DIN ISO 15552 CYLINDERS – PROFILED Ø32-125



TESTATE COVERS	ALLUMINIO PRESSOFUSO DIE-CASTED ALUMINUM
TUBO TUBE	ALLUMINIO ANODIZZATO ANODIZED ALUMINUM
GUARNIZIONI SEALS	POLIURETANO + NBR POLYURETHANE + NBR
BRONZINA BUSH	BRONZO SINTERIZZATO SINTERED BRONZE
ASTA* PISTON ROD	ACCIAIO CROMATO CHROMIUM COATED STEEL

*Tutti i cilindri sono disponibili, su richiesta, anche con asta INOX AISI 304.
Par ordinare, aggiungere "I" al codice standard.
*All cylinders are available also with AISI 304 stainless steel piston rod.
To order add "I" to the standard code number.

PRESSIONE DI FUNZIONAMENTO WORKING PRESSURE	TEMPERATURA DI IMPIEGO TEMPERATURE	FLUIDO WORKING FLUID
MAX 10 BAR	-20°C +80°C CON ARIA SECCA -20°C +80°C WITH DRY AIR	ARIA COMPRESSA FILTRATA E LUBRIFICATA E NON FILTERED AND LUBRICATED OR NOT COMPRESSED AIR

VERSIONI DISPONIBILI AVAILABLE VERSIONS

CDE_X-CDEM_X-CDEP_X-CDEMP_X-CDEA_X-CDEMA_X-CDEAP_X-CDEMAP_X

CORSE STANDARD STANDARD STROKES

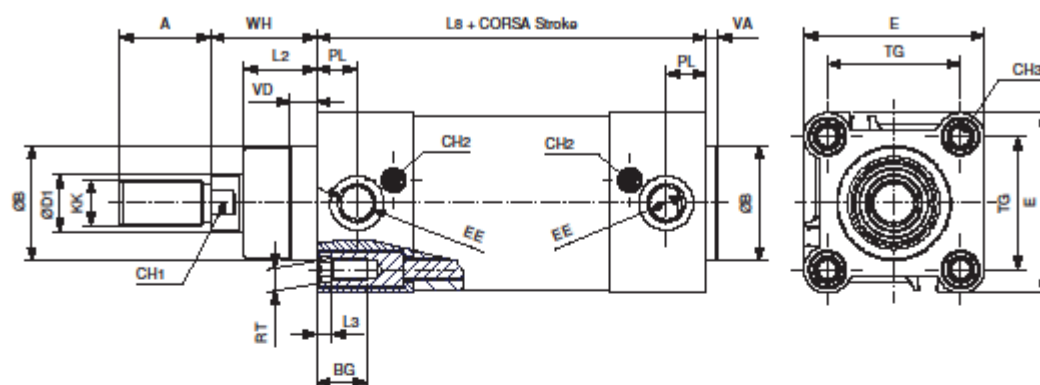
Ø mm	10	25	40	50	80	100	125	160	200	250	300	320	400	500
32	☐	☐	☐	☐	☐	☐	☐	☐	☐	☐	☐	☐	☐	☐
40	☐	☐	☐	☐	☐	☐	☐	☐	☐	☐	☐	☐	☐	☐
50	☐	☐	☐	☐	☐	☐	☐	☐	☐	☐	☐	☐	☐	☐
63	☐	☐	☐	☐	☐	☐	☐	☐	☐	☐	☐	☐	☐	☐
80	☐	☐	☐	☐	☐	☐	☐	☐	☐	☐	☐	☐	☐	☐
100	☐	☐	☐	☐	☐	☐	☐	☐	☐	☐	☐	☐	☐	☐
125	☐	☐	☐	☐	☐	☐	☐	☐	☐	☐	☐	☐	☐	☐

DOPPIO EFFETTO
DOUBLE ACTING

DOPPIO EFFETTO AMMORTIZZATO DOUBLE ACTING CUSHIONED

CDEAØ/...X

CDEMAØ/...X



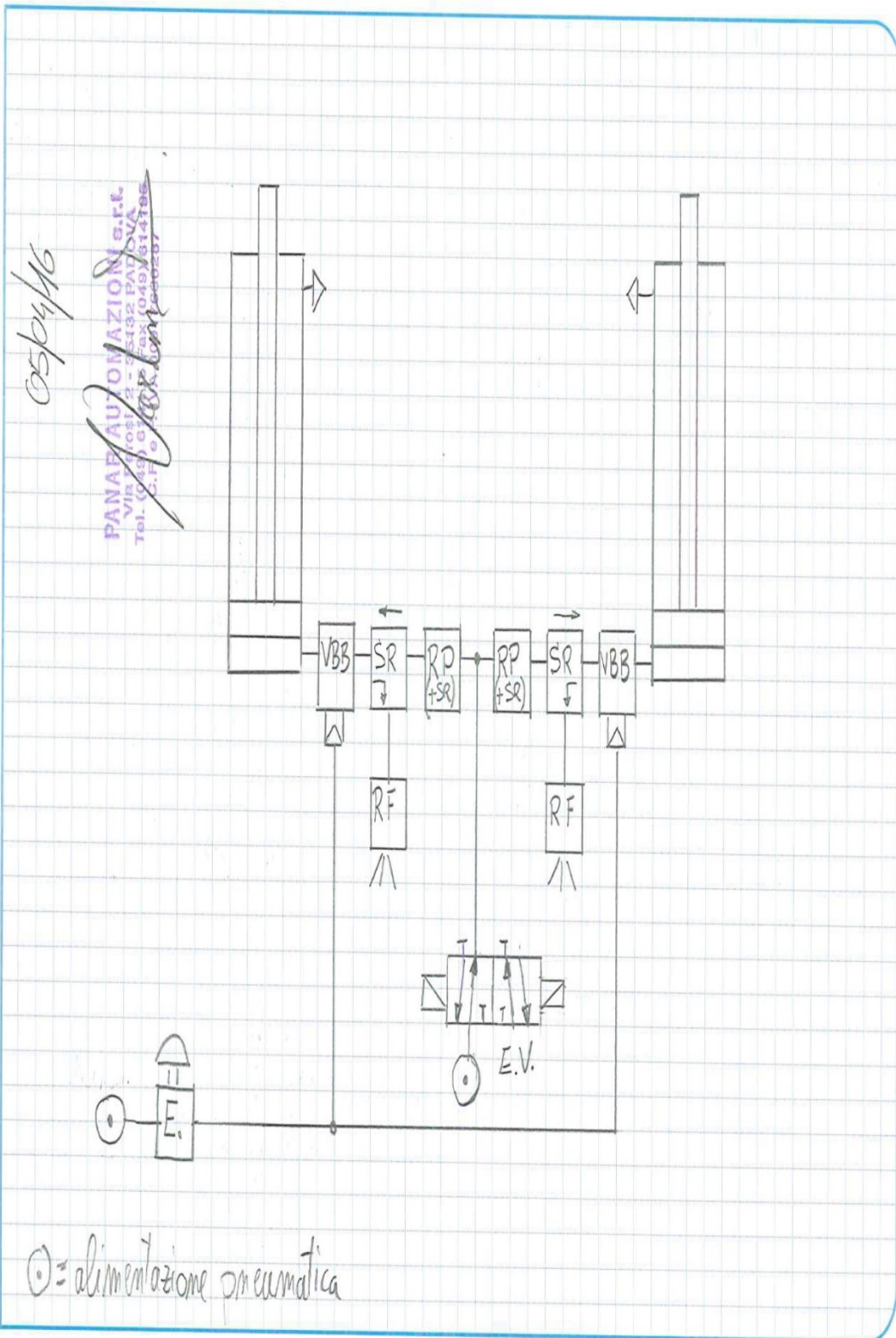
DIMENSIONI DIMENSIONS

Ømm	ØD1	KK	A	ØB	VD	VA	L2	RT	BG	L3	TG	EE	PL	WH	LB	E	CH1	CH2	CH3
32	12	M10x1.25	22	30	9.5	4	18	M6	16.5	5	32.5	1/8"G	12.5	26	94	47	10	2.5	6
40	16	M12x1.25	24	35	9.5	4	22	M6	16.5	5	38	1/4"G	14	30	105	54	13	2.5	6
50	20	M16x1.5	32	40	9.5	4	25.5	M8	17.5	5	46.5	1/4"G	14	37	106	63	17	2.5	8
63	20	M16x1.5	32	45	9.5	4	25	M8	17.5	5	56.5	3/8"G	16.5	37	121	74	17	2.5	8
80	25	M20x1.5	40	45	10	4	35	M10	17.5	//	72	3/8"G	17	46	128	93.5	22	4	6
100	25	M20x1.5	40	55	10	4	38	M10	17.5	//	89	1/2"G	18	51	138	110	22	4	6
125	32	M27x2	54	60	11	6	46	M12	20.5	//	110	1/2"G	18	65	160	137.5	27	4	8

FORZE DI TRAZIONE E SPINTA (6 BAR) TRACTION AND THRUST FORCES (6 BAR)

Ø mm	FORZA DI SPINTA (N) THRUST FORCE (N)	FORZA DI TRAZIONE (N) TRACTION FORCE (N)
32	458	394
40	716	601
50	1180	939
63	1775	1596
80	2863	2583
100	4474	4194
125	6991	6532

Appendix D



SCHEMA A BLOCCHI → LEGENDA

E. = azionamento (indipendente, separato) per lo sblocco del moto dei cilindri. Fin tanto che non viene attivato i 2 cilindri non possono essere azionati. Segnale pneumatico di pilotaggio

VBB = Valvola di blocco bidirezionale ad azionamento pneumatico. Costituisce di fatto un blocco all'ingresso/uscita di aria da e per il cilindro. Filetto 1/4"

SR = Scarico Rapido. Via "di fuga" per l'aria che fuoriesce dalla camera di spinta del cilindro. Filetto 1/4"

RF = Regolatore di Flusso. Installato a valle dell'elemento SR ne regola il flusso di uscita costituendo un freno pneumatico alla discesa del cilindro e permettendone quindi il controllo di velocità.

RP = Regolatore di Pressione. Permette di regolare la pressione a valle in valore inferiore rispetto alla pressione di alimentazione variando così la forza di spinta del cilindro. La funzione (+SR) incorpora nel regolatore uno scarico rapido che consente una migliore risposta alla regolazione della pressione in uscita

E.V = Elettovalvola (tensione da definire) per l'azionamento dei cilindri. Ha 2 segnali, uno per la salita ed uno per la

NUOVA DELGRAF S.p.A. - Tel. Fax 049 80207

PANAR Da 30 anni SPECIALISTI in automazioni
Idee - Realizzazioni - Componentistica per
oleopneumatica - vuoto - lubrificazione - apparecchiature automatiche di lavoro - strumentazione

Sede: 35132 PADOVA - Via Avanzo, 67 - Tel. 049 614334 (10 linee)
Fax 049 614195 - e-mail: panar@panar.com - web: www.panar.com
Filiali a VI: Tel. 0444 923607 - Fax 0444 923473 - TV: Tel. 0422 305680



Di qualsiasi marca o costruite apposta anche
1 solo pezzo con garanzia certificata
ANCHE IN POCHI MINUTI

discesa dei cilindri. Azionabile tramite 2 interruttori/
pulsanti elettrici non inclusi nella fornitura.

⊙ = alimentazione pneumatica (2 ÷ 10 bar)

▷ = Silenziatore (bronzo o plastica) per la compensazio-
ne dell'aria nella camera superiore del cilindro

Nota: la simultaneità del movimento dei cilindri può
essere realizzata in maniera "approssimativa" mediante
la regolazione combinata di RF + RF per ogni
linea di alimentazione.

L'impiego di boccole di scaricamento adeguate al
carico e la massima riduzione del gioco di oscillazione
del carico sono le migliori opzioni per una
buona simultaneità.

(Schema pneumatico con simbologia "ufficiale" al
momento della consegna della merce)

PANAR AUTOMAZIONI s.r.l.
Via Perosi, 2 - 35132 PADOVA
Tel. (049) 041359 Fax (049) 814195
C.F. 017892207

PANAR Da 30 anni SPECIALISTI in
automazioni

Idee - Realizzazioni - Componentistica per
oleopneumatica - vuoto - lubrificazione - apparecchiature automatiche di lavoro - strumentazione

Sede: 35132 PADOVA - Via Avanzo, 67 - Tel. 049 614334 (10 linee)
Fax 049 614195 - e-mail: panar@panar.com - web: www.panar.com
Filiali a VI: Tel. 0444 923607 - Fax 0444 923473 - TV: Tel. 0422 305680

Filiali a VI: Tel. 0444 923607 - Fax 0444 923473 - TV: Tel. 0422 305680



**GUARNIZIONI
EXPRESS**

Di qualsiasi marca o costruite apposta anche
1 solo pezzo con garanzia certificata
ANCHE IN POCHI MINUTI

ANCHE IN POCHI MINUTI

Appendix E



SMARTMechanical_CompanyS.r.l.
P.IVA 03834010161
Cap.Soc. € 10.000,00 I.v.
N° REA BG-412189

Headquarters
Via Tonale, 9
24061 Albano S. Alessandro
(BG) ITALY

SM_LC Six axes load cell

User's manual
Version 1.5, 12-06-2013

+39 035 4521485
+39 035 4521082

info@smartmechanical-company.it

www.smartmechanical-company.it

1

Foreword and contacts

This manual has been written to allow an easy use of the SM_LC sensor, a six-axes load cell manufactured by SMARTMechanical_Company a spin-off of the Politecnico di Milano.

For any further clarification on the SM_LC sensor, please contact:
info@smartmechanical-company.it

Index

1. Technical specifications	4
2. Connection scheme	6
3. Loads definition	7
4. Load cell structure	8
5. Error analysis	10
6. Maintenance	12
7. Disclaimer	12

1. Technical specifications

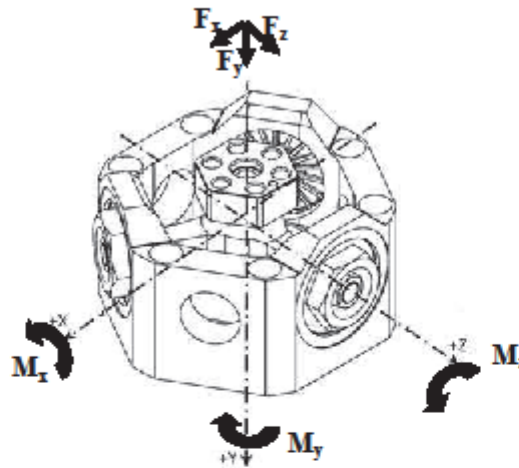


Fig.1 - SM_LC sensor

Maximum loads

F_x 5000 N
 F_y 10000 N
 F_z 5000 N
 M_x 500 Nm
 M_y 250 Nm
 M_z 500 Nm

Stiffness

K_x $28 \cdot 10^6$ N/m
 K_y $80 \cdot 10^6$ N/m
 K_z $28 \cdot 10^6$ N/m

Accuracy

F_x : $\pm 0.60\%$ (maximum error $\pm 2 \sigma$)
 F_y : $\pm 0.14\%$ (maximum error $\pm 2 \sigma$)
 F_z : $\pm 0.64\%$ (maximum error $\pm 2 \sigma$)
 M_x : $\pm 0.40\%$ (maximum error $\pm 2 \sigma$)
 M_y : $\pm 0.41\%$ (maximum error $\pm 2 \sigma$)
 M_z : $\pm 0.74\%$ (maximum error $\pm 2 \sigma$)

Crosstalk

< 0.8%

Linearity error (according to ISO 376)

< 0.2%

Resolution

< 0.5 N (0.05Nm)

Calibration matrix M_{0p}

11288.68937	438256.8895	-5888.388903	-222890.7623	-833.1416596	-221521.3852
400002.2148	-4568.453644	396556.5147	-6461.005225	400756.0604	983.5761287
1514.907169	9753.886975	13432.07048	376061.4749	-6122.874401	-382429.2446
-24889.55682	198.538957	12384.77859	-383.3546536	12067.04138	546.6181548
293.8666553	24310.79621	361.8764227	23917.2678	204.8056923	24650.36148
143.5151482	-239.2502396	-21557.14676	574.0772986	22137.54295	-178.2116348

$$F = M_{0p} \cdot \Delta V$$

2. Connection scheme

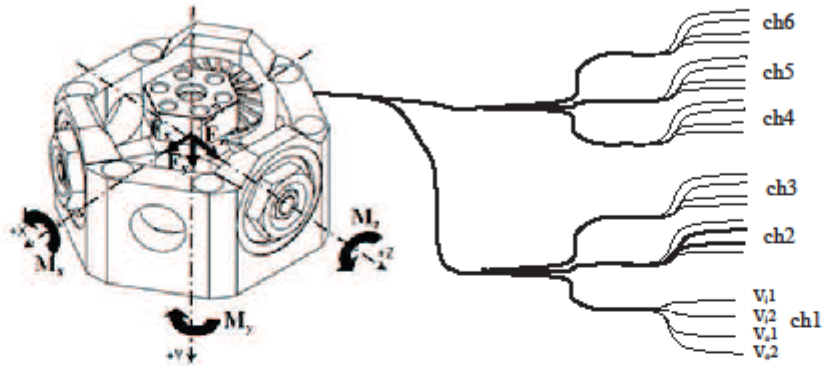


Fig.2 – Schematical Connection scheme of the SM_LC sensor

3. Loads definition

The loads and moments direction, their versor and the moment reference point P are defined in Fig.3.

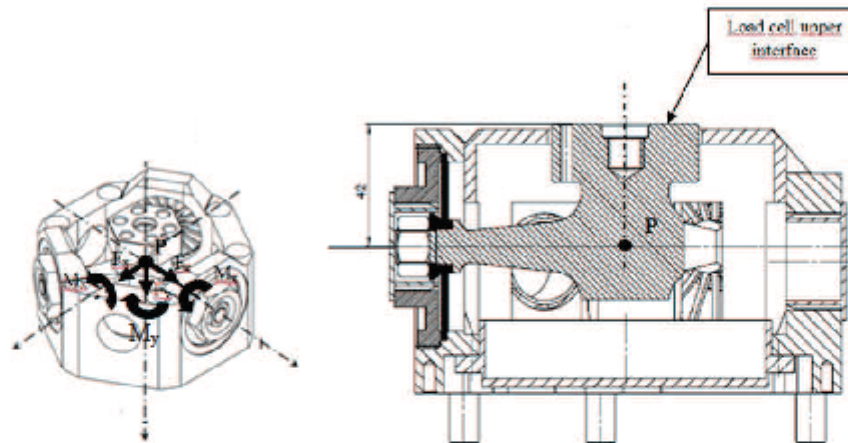


Fig. 3 - SM_LC sensor - Loads definition

4. Load cell structure

Lower mechanical interface

N. 6 holes for M10 10.9 screws.

N. 6 threaded holes M14 x 1.5 (this is a secondary option for fastening the load cell lower interface).

The recommended tightening torque for both fixations is 50 Nm.

Two reference holes for steel pins define the z axis orientation on the lower interface plane.

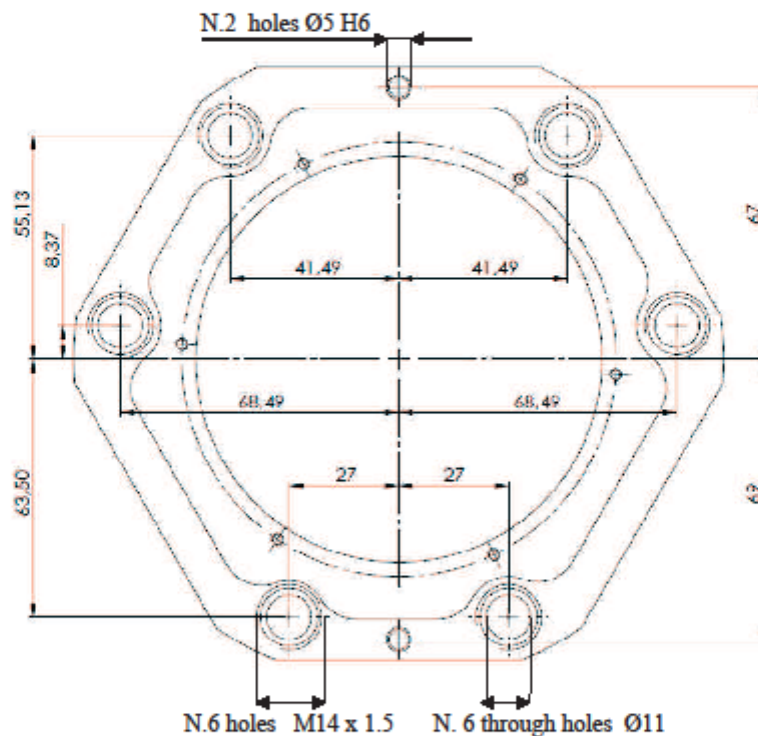


Fig. 4 – Lower mechanical interface

Upper mechanical interface

N. 6 threaded holes for M10x1.25 12.9 screws.

Recommended tightening torque: 85 Nm.

The center hole and a steel pin hole define the z axis orientation on the upper interface plane.

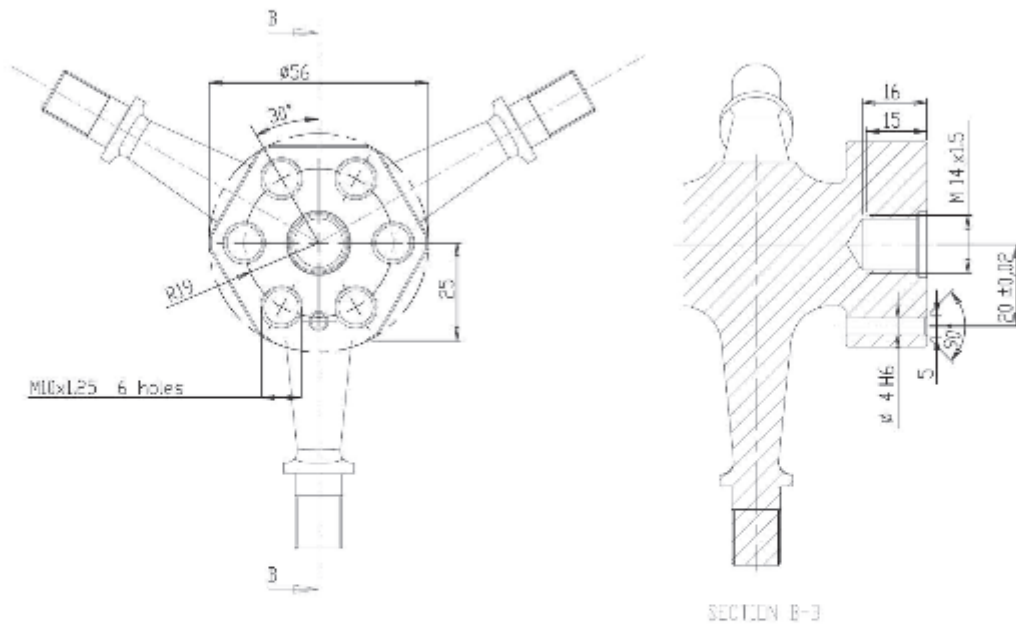


Fig. 5 – Upper mechanical interface

5. Error analysis

5.1 Measurement errors

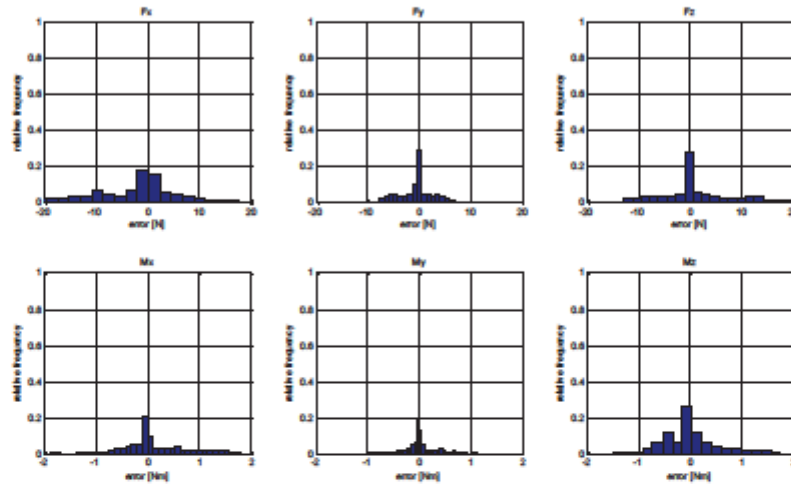


Fig.6 - Errors of load cell output channels - Histograms

	Fx [N]	Fy [N]	Fz [N]	Mx [Nm]	My [Nm]	Mz [Nm]
Std. deviation absolute	11.9	5.8	12.8	0.8	0.4	1.4
Std. deviation in % of max. load	0.3002	0.0733	0.3213	0.2039	0.2057	0.3721

Table 1 – Errors of load cell output channels - Results

5.2 Linearity errors

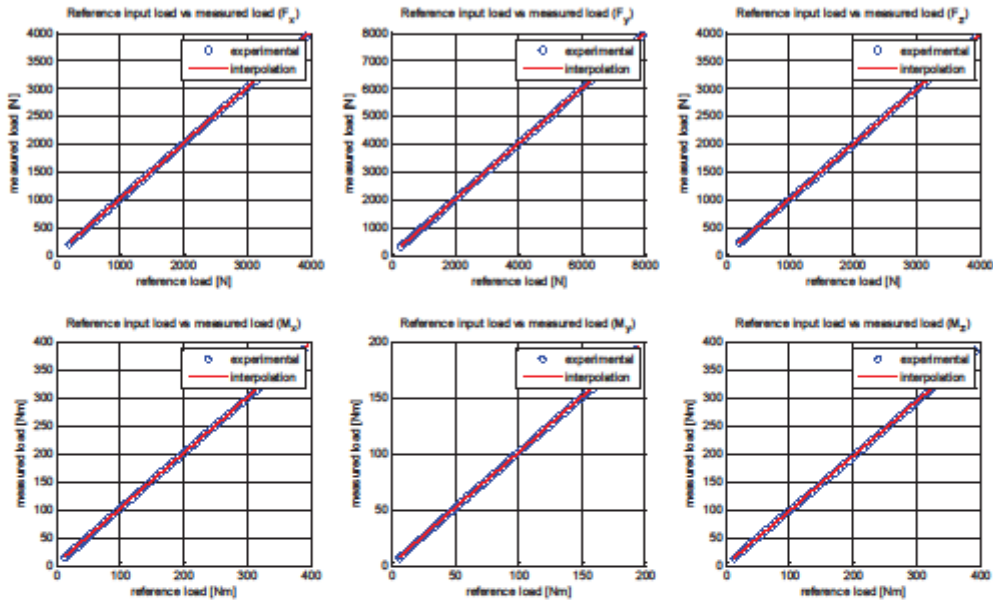


Fig. 7 - Linear interpolation diagrams

	F_x [N]	F_y [N]	F_z [N]	M_x [Nm]	M_y [Nm]	M_z [Nm]
Interpolation uncertainty in % according to ISO 376	0.5701	0.3594	0.7495	0.9525	1.0570	2.0687
R^2	1	1	1	1	1	1

Table 2 - Linear interpolation results

6. Maintenance

Periodic calibration of the sensor is required to maintain traceability to national standards. Biannual recalibration is recommended. For harsh applications or durability testing the sensor could require more frequent recalibration.

7. Disclaimer

The information in this document is subject to change without notice. The manual is periodically revised to reflect and incorporate changes made to the system.

SmartMechanical_Company assumes no responsibility for any errors or omissions in the document.

SmartMechanical_Company does not recommend the use of the load cell for applications wherein failure or malfunction threatens life or makes injury probable. Anyone who uses the load cell within any potentially life-threatening system must obtain prior consent based upon assurance that a malfunction of the load cell does not pose direct or indirect threat of injury or death, and (even if such consent is given) shall indemnify SmartMechanical_Company from any claim, loss, liability, and related expenses arising from any injury or death resulting from use of the load cell.

Appendix F



UNIVERSITA' DEGLI STUDI DI PADOVA
Dipartimento di Ingegneria Industriale DII

VIA GRADENIGO, 6/A 35131 PADOVA PD

Codice Fiscale 80066480281 - Partita Iva 00742430283

Ordine N. : DII0000424

ISTITUZIONALE

Data Emissione: 13/05/2014
Previsioni N. 2014/NOR/9 del 28.04.2014.

CUP: C91H1064220005

CIG: Z610F2C07A

Codice Funz.105892

Codice Fiscale 05911860242 - Partita IVA 03041860242

FORNITORE: FAX N. 0415514978

Spett.le

O.Me.Re. Srl

VIA VIAGRI 20

36010 ZANE' VI ITALIA

Modalità di pagamento: CB Bonifico bancario - Termini Pagamento: 30 gg. ricevimento fattura

Dipendenza: CASSA RURALE ED ARTIGIANA DI ROANA - CASSA RURALE ED ART. DI ROANA CRED.COOP

Cir: D ABI: 08772 CAB: 60890 Num.Conto: 006000356250 IBAN: IT4210877260890006000356250

Vi preghiamo di fornirci le merci/servizi sottoindicati:

VO CF	OTA	DESCRIZIONE	VALU TA	% IVA	IMPORTO NETT. IN VALUTA	SCONTO in VALUTA	TOTALE IN VALUTA
1	1.00	REALIZZAZIONE SU MISURA SECONDO NOSTRE SPECIFICHE E DISSEGNI DI BRACCIO A V (componente aggiuntivo macchina misura pneumatici) COME DA VS. OFFERTA 2014/NOR/9 DEL 28.04.2014 ALLEGATA ALLA PRESENTE	EUR	22,00	2.200,00000	0,00	2.200,00
Totale Ordine in Valuta					2.200,00		
Totale Sconto					0,00		
Totale Imponibile in Euro					2.200,00		
Totale Iva in euro (su euro 2.200,00)					484,00		
Totale Ordine in Euro					2.684,00		

Modalità di consegna: PORTO FRANCO NE SEDE

Indirizzo di consegna: LABORATORIO DI MECCANICA APPLICATA - VIA VENEZIA, 1 35131 PADOVA (CA. PROF. ROBERTO DI TEL. 049/8276806)

Data Prevista:

Note: Inerte/Prezzo.

- L'aggiudicatario assume gli obblighi di tracciabilità dei flussi finanziari di cui alla legge 13 agosto 2010, n. 136 e s.m.i., a pena di nullità assoluta del contratto.
- L'esecuzione di transazioni avvenute senza avvalersi di bonifici bancari o postali ovvero degli altri strumenti idonei a consentire la piena tracciabilità delle operazioni ai sensi della legge 13 agosto 2010, n. 136 e s.m.i determina la risoluzione di diritto del contratto. Resta salvo il diritto al risarcimento di eventuali danni o ulteriori oneri sostenuti dall'Ente.
- L'aggiudicatario si impegna a dare immediata comunicazione alla Stazione Appaltante ed alla Prefettura-Ufficio Territoriale del Governo della Provincia di competenza della notizia dell'inadempimento delle proprie controparte (subappaltatore/subcontratto) agli obblighi di tracciabilità finanziaria.

Il Responsabile dei fondi

D.S. CO. L. 2014/56482 € 2.003,00
D.S. CO. L. 2014/56490 € 1.000,63

COPIA PER IL FORNITORE

Il Responsabile della Struttura

[Signature]

D.S. CO. L. 2014/48486 per € 680,37 QUOTA PARTE.



F.LLI BONO S.p.A.
 Cap. Soc. € 850.000 i.v.
 P.IVA e C.F. 01265870244
 Reg. Imp. Vicenza n° REA 156571
 E-mail: bono@bonofili.it
 Web: www.bonofili.it

Sede Legale e Amministrativa
 VIA DELL'ECONOMIA, 131
 36100 VICENZA (VI) IT
 Tel. 0444.990990
 Fax 0444.990900

Filiale
 VIA LAGO DI LUGANO, 28
 36015 SCHIO (VI) IT
 Tel. 0445.575333
 Fax 0445.575375

OFFERTA OFV14-004519 del 11/06/2014

Pagina 1

LUOGO DI CONSEGNA					SPETTABILE				
UNIVERSITA'DEGLI STUDI PADOVA VIA OTTO FEBBRAIO 1848, 2 35122 PADOVA (PD) Italia					UNIVERSITA'DEGLI STUDI PADOVA VIA OTTO FEBBRAIO 1848, 2 35122 PADOVA (PD) Italia				
CLIENTE	P.I	CODICE FISCALE	VS. RIF. COMMESSA	DATA	VALIDITA' OFF.	VALUTA	ZONA		
C57724	IT00742430283	80005480281	E-MAIL ING.GIOLO	11/06/14		EUR	1051		
CONDIZIONI DI PAGAMENTO			NS. BANCA	VS. CONTATTO		SCONTO			
BONIFICO BANCARIO 30 GG. FM			IT04Y0200860350000003749689 UNICREDIT	ING.GIOLO					
TERMINI DI RESA			TRASPORTO A CURA		VETTORE		CONV. VETTORE		
DAP FRANCO VS. STABIL - PORTO FRANCO			Vettore						
ID	Articolo	Descrizione	U.M.	Qtà	Prezzo Listino	80%	Netto Unitario	Importo riga	Consegna da ordine
		Alla c.a. Ing. Enrico Gioio Cordiali saluti Roberto Giacomazzi							
1	0703001698	CILINDRO CDEMA-063-0125-X	PZ	2	81,38	30	56,966	113,93	15gg
2	0702009107	SERBATOIO 200L 11B ORIZZONTALE VERNICIATO SER00030	PZ	2	203,00		203,00	406,00	15gg
3	0709000202	MANOMETRO 111.10.063 12 BAR 1/4R 8593310	PZ	2	10,46	20	8,368	16,74	DISP.
4	0706004273	RUBINETTO SFERA 0448-09-17 G3/8	PZ	2	47,27	25	35,4525	70,90	15gg
5	0702007192	RACCORDO T PARI 3104-10-00	PZ	1	6,19	25	4,6425	4,64	DISP.
6	0706004263	RACCORDO TERMINALE DIRITTO 3101-10-17 G3/8	PZ	8	3,32	25	2,49	19,92	DISP.
7	0701006950	SILENZIATORE BRONZO 80538 G3/8"	PZ	2	1,61	25	1,2075	2,41	DISP.
8	1110000248	RUBINETTO DI SPURGO 025 3/8"	PZ	2	1,349	25	1,01175	2,02	DISP.
9	1110000200	TAPPO TCEI CILINDRICO 0919-00-27 G3/4	PZ	2	1,68	25	1,26	2,52	DISP.
10	1110000195	TAPPO TCEI CILINDRICO 0919-00-21 G1/2	PZ	2	1,50	25	1,125	2,25	DISP.
11	0702008072	RACCORDO TERMINALE DIRITTO 3175-10-21 R1/2	PZ	4	3,64	25	2,73	10,92	DISP.
12	0706004233	RACCORDO TERMINALE DIRITTO 3101-06-13 G1/4	PZ	2	1,71	25	1,2825	2,56	DISP.
13	1110000174	RIDUZIONE CONICA 0904-13-17 R3/8xG1/4	PZ	2	0,65	25	0,4875	0,97	DISP.
14	0706004385	RACCORDO TERMINALE DIRITTO 3114-06-13 G1/4	PZ	2	3,31	25	2,4825	4,96	DISP.
15	1105001261	TUBO ELASTOLLAN PUR C98 8x10 NERO 25m 98C8X10-N-25	PZ	1	23,95	25	17,9625	17,96	DISP.
ANNOTAZIONI			CONTATTO ROBERTO.GIACOMAZZI		TOTALE MERCE 678,70				
DESCRIZIONE IVA 22% IVA		% IVA 22,00	IMPONIBILE 678,70	IMPORTO IVA 149,31	IVA 149,31		TOTALE OFFERTA 828,01 EUR		

In caso di ritardo pagamento verranno conteggiati gli interessi legali di mora al tasso ufficiale BCE maggiorato di 8 punti e un importo forfettario di euro 40,00 a titolo di risarcimento del danno, ai sensi del D.Lgs 09/11/2012 n.192 art.5 e art.6



FORNITURE
TECNICO INDUSTRIALI

F.LLI BONO S.p.A.
 Cap. Soc. € 890.000,00
 P.IVA e C.F. 01205870244
 Reg. Imp. Venezia n° REA 155571
 E-mail: bono@bono.it
 Web: www.bono.it

Sede Legale e Amministrativa
 VIA DELL'ECONOMIA, 181
 36100 VICENZA (VI) IT
 Tel. 0444 306880
 Fax 0444 306600

Filiale
 VIA LAGO DI LUGANO, 28
 36015 SCHIO (VI) IT
 Tel. 0445 676300
 Fax 0445 675275








DOCUMENTO DI TRASPORTO (D.P.R. 14/08/1996 n°72) DDT14-015774 del 31/07/14 Pagina 1

DESTINAZIONE MERCE		SPETTABILE				
LABORATORIO DI MECCANICA APPLICATA VIA VENEZIA, 1 36101 PADOVA (PD) Italia		UNIVERSITA' DEGLI STUDI PADOVA V.A OTTO FEBBRAIO 1848, 2 35122 PADOVA (PD) Italia				
INTESTATARIO 057724	P.I. IT00742450290	C.F. 0000600291				
TERMINI DI RECA DAF - FRANCO VS. STADIL - PORTO FRAN		TRASPORTO A CURA Vettore	VEETTORE M/FNATO			
		NR. CONVENZIONE				
Pos	Codice Articolo	Descrizione	UM	Quantità		
-		As. Circo vendita n. 0214-01-844 del 11/06/14 Vs. Ordine N. 010000593 del 11/06/14 Al. c.a. Ing Enrico Glajo Al. c.a. P. di Roberto Lal				
		Filialmenti Vs. Circo 010000308 C.U. P. 08101100422000 CIG Z356FDD070				
1	0709000602	MANOMETRO 111170.030 120MM 14-8 5085510	pz	2		
2	0709007189	RACCORDO T PARI 3104-10-03	pz	1		
3	0709004283	RACCORDO TERMINALE D RITTO 3104-10-17 G35	pz	0		
4	0701000850	SILENZIATORE BRONZO 50538 G38*	pz	2		
5	1110000248	RUBINETTO DI SFUGGIO G25 3-0	pz	2		
6	1110000280	TAPPO TOP CILINDRICO 08-940-27 G34	pz	2		
7	1110000195	TAPPO TOP CILINDRICO 08-940-21 G12	pz	2		
8	0703008672	RACCORDO TERMINALE D RITTO 3104-10-21 G12	pz	4		
9	0709004233	RACCORDO TERMINALE D RITTO 3104-10-13 G14	pz	2		
10	1110000176	INDUGO L CONICA 092-12-17 H284G14	pz	2		
11	0709004305	RACCORDO TERMINALE D RITTO 3104-10-13 G14	pz	2		
12	1106001281	TUBO ELASTICLAN PUR 028 8x10 NERO 25M 2808210-028	pz	1		
13	0700004270	RUBINETTO SPERA 044-03-17 G38	pz	2		
14	0702009107	SERBATOIO 603L 118 0722.VERNICIATO SERD03000	pz	2		
15	0708001826	CILINDRO CRENA 060-0125-X	pz	2		
CAUSALI DI TRASPORTO Vendita		ASPETTO DEI BENI A VISTA	NR. COLL 2	VOLUME cm³	PESO NETTO Kg	PESO LORDO Kg 130,00
VEETTORE M/FNATO		ANNOTAZIONI				
P.IVA 00386650302 Reg. Imp. PD24576724 VIA V.M. CORICELLI 23 PADOVA Tel. 049 7734727 Fax 049 5004833		DATA E ORA INIZIO TRASPORTO 31/07/14 14.00		FIRMA DEL DESTINATARIO <i>Enrico Glajo</i>		
		FIRMA DEL VETTORE <i>[Firma]</i>		FIRMA DEL CONDUCENTE		

ORIGINALE per DESTINATARIO

50 anni di esperienza : a vostra disposizione

I nostri settori di specializzazione : Pneumatica – Oleodinamica – Vuoto – Strumentazione – Lubrificazione – Robotica – Bloccaggi manuali e automatici – Tavole rotanti – Presse pneumatiche – Alimentatori lineari e circolari – Unità a forare – Unità a macchiare – Cilindri elettrici lineari – Tubi aria ed olio – Pompe pneumatiche – Raccordi per aria, vuoto, oleodinamica – Raccordi speciali per impieghi non convenzionali – Vibratori pneumatici , elettrici , idraulici – Realizzazione Impianti pneumatici "chiavi in mano"

<p>GUARNIZIONI SPECIALI A PROGETTO</p>  <p>Produzione su misura per quanto richiesto fino a 1000000mm</p> <p><i>"Se non la trovate, ve la costruiamo noi"</i></p>	 <p>Consegna in tempi brevi</p>	 <p>Soluzioni ai vostri problemi</p>	 <p>Progettazione Impianti olio - aria</p>	 <p>Assistenza tecnica</p>	 <p>Documentazione e cataloghi</p>	 <p>Consulenza presso vs. sede</p>
<p>Offerta/Conferma d'Ordine n° :051/16ND.2</p> <p><small>Come da Vostra richiesta, di pregio sottoporvi la nostra migliore OFFERTA per quanto riportato, alle nostre «CONDIZIONI GENERALI DI VENDITA» che alleghiamo alla presente e che devono essere risultate debitamente firmate in caso di Vostra conferma. La Vostra accettazione sarà quindi "CONFERMA D'ORDINE"</small></p>		<p>PD : 11/04/2016 Ns.Rif: NARDIN D. FAX: Tel:</p>		<p>Spett. Ditta : UNIVERSITA' di PADOVA Dip. Ing. Ind. Padova</p>		
<p>Alla cortese attenzione Prof. MASSARO MATTEO</p>						

Q.tà	DESCRIZIONE	Prezzo unitario €.
*** MODIFICA ALLA PRECEDENTE OFFERTA ***		
01	<p>Fornitura componentistica sfusa, non assemblata, per vostro impianto pneumatico comprendente:</p> <ul style="list-style-type: none"> - 1 elettrovalvola a passaggio maggiorato 1/4" comprensiva di bobine 24VCC. Pulsante di azionamento NON incluso - 2 regolatore di pressione con scarico rapido incorporato e manometro - 2 scarico rapido con regolatore di flusso unidirezionale - 4 silenziatore a largo flusso - 10 mt tubo extraflex Ø6x4 colore azzurro - 1 elettrovalvola con bobina per azionamento (separato) valvole di blocco. Tensione da definire. Pulsante di azionamento NON incluso - raccorderia varia per collegamento di quanto sopra esposto ai vostri cilindri <p>Per quanto sopra esposto, prezzo a voi riservato netto €.</p> <p>Consegna: tutto il materiale è attualmente disponibile</p>	185,00
xx	Frenafiletto medio (confezione singola da 10ml) cad. netto €.	7,80
25	Disponibilità : 4 pezzi pronti / altro : 3-4 giorni	
25	Anello di guida tipo I/DRW 80/3 (<u>equivalente</u>) in resina acetilica cad. netto €.	2,75
25	Consegna: 3-4 gg d.r.o.	
	Wiper tipo WRM 314 348/C (<u>equivalente</u>) in NBR cad. netto €.	5,20
	Consegna: 3-4 gg d.r.o.	
*** AGGIUNTA DEL 11/04/2016 ***		
01	Elemento filtrante aria (ingresso) 1/4" cad. netto €.	25,00
02	Valvole di blocco (bidirezionale) fil. 1/4" ad azionamento pneumatico cad. netto €.	35,00
01	Schema a blocchi + legenda per impianto (già fornito) €.	60,00
10	Tubo Ø4x2,5 poliuretano per collegamenti mt./netto €.	0,40

Altre condizioni di fornitura:

CONCILIAZIONE: Nell'eventualità di contestazioni o controversie, le parti concordano preliminarmente per un tentativo di conciliazione presso la Camera di Commercio di Padova. In ogni possibile altro caso, le parti concordano che il **FORO COMPETENTE** sia esclusivamente quello di Padova.

CONSEGNA (in giorni lavorativi, salvo imprevisti) da ricevimento copia della presente controfirmata : **vedi corpo offerta**

PAGAMENTO: solito in uso con noi Vostra Partita IVA: **Cod. CAB: Cod. ABI:**

BANCA D'APPOCCIO: **SPEDIZIONE:** vostro ritiro presso nostra sede di Padova

IMBALLI al costo se non altrimenti definito - RESA: franco nostra sede PD con spedizione a vostro carico se non diversamente concordato - RISCHIO TRASPORTO: a carico vostro - VALIDITA' QUOTAZIONI: 15 gg. lavorativi dalla data odierna - ESCLUSIONI: Interventi esterni alla ns. Sede non sono mai compresi, tranne il caso in cui ciò non abbiano una specifica quotazione e modalità espone in offerta. In generale, ogni altra voce o servizio non specificatamente inclusi nella presente offerta - **CONFERMA:** renderci controfirmata la presente offerta e gli eventuali allegati, secondo quanto previsto dalla normativa ISO9002 per la certificazione di qualità.

AVVERTENZE: in caso di Vostra conferma, il prezzo ricevuto dalla presente offerta è da intendersi "chiavi in mano" e da Voi controfirmata per accettazione, di immediati di dare corso all'ordine.

DA COMPLETARE PER L'ACCETTAZIONE DELL'ORDINE (a cura del cliente)

Data: **Firma LEGGIBILE:** **Timbro:**

Sede Legale : Via Lorenzo Perosi , 2 – 35132 – Padova Tel: 049/614155 (10 linee r.a.) - Fax: 049/614195 - CF/PI:00917630287 - R.E.A.:158880

Internet: www.panar.com E-mail: direzione@panar.com



SIDERURGICA PRODOTTI OLEODINAMICI

SIPROL s.r.l.

Via De Nicola, 7 - 36075 Montecchio Maggiore (VI)

Tel / Fax 0444.695703

www.siprol.it - info@siprol.it

P.IVA / C.F. 03242200248

Spett.: UNIVERSITA' DI PADOVA

c. Att.: Ing. Enrico Giolo

Oggetto: Offerta

Facciamo seguito alla richiesta dell'Ing. Giolo e formuliamo la seguente offerta

Tubo St 52/E355 senza saldatura, cromato esternamente 25 +/- 5 micron, tol. f7, cert. 3.1

d. 80 f7 x 10 (interno 60) 2 barre lungh. 6 - 7 metri (fatturate per intero)

le 2 barre saranno tagliate in 6 pz x 1300 0/+ 5 mm + consegna degli spezzoni rimanenti
eur/m 70 + iva

Consegna: settimana 31 - 32

Imballo: su nr. 1 bancale al costo eur 8 + iva

Resa: con nostro vettore con addebito in fattura eur 80 + iva

Pagamento: ri.ba 30 gg fm data fattura

In attesa di vostro riscontro inviamo

Distinti saluti
Ing. E. Rodeghiero
Siprol srl

09/07/16



CARPENTERIA - REALIZZAZIONE - PROGETTAZIONE
TAGLIO A GETTO D'ACQUA - PLASMA - OXY
PIEGA LAMIERA 12 X 7 MT - 20 X 5 MT

Spett.le

Università degli Studi di Padova
Motorcycle Dynamics Research Group
Office +39.049.827.6715

Alla cortese attenzione di : Ing. Enrico Giolo

Oggetto : OFFERTA

In riferimento a vs. gentile richiesta, comunichiamo ns. quotazione per eventuale fornitura di :

Q.TA'	DESCRIZIONE	COSTO UNIT.
10 PZ	PARTICOLARI DIS. 01.004.13.01_BRACCIO TRASLATE_HORIZONTAL PLATE_01 REV01_CUT_PROFILE MATERIALE S 275 JR SP. 20 MM GREZZO NOTE : <ul style="list-style-type: none">- PER FORI DI DIMENSIONE INFERIORE A DIAMETRO 20 MM ; SI ESEGUIRANNO PICCOLI SEGNI DI CENTRAGGIO O PICCOLI FORI- PREVEDERE SOVRAMETALLO PER SUCCESSIVE LAVORAZIONI ESCLUSIONI : <ul style="list-style-type: none">- LAVORAZIONI MECCANICHE E TRATTAMENTI SUPERFICIALI	€/CAD 42,00 + IVA

Consegna : 4 / 5 gg lavorativi circa

Reso : f.co G&B srl - Este (PD)

Trasporto : da concordare all'ordine

Pagamento : al ritiro

Rimaniamo a disposizione per qualsiasi evenienza e cogliamo l'occasione per porgere
distinti saluti.

Este, 09/07/14

G. & B. S.R.L.

G. & B. S.R.L. - Via G. Begaro, 6 - 35042 ESTE (PD) tel. 0429/603463 fax 0429/602266
P.I./C.FISC. 02114680289 - C.C.I.A.A. PD 208777 - Cap. sociale : € 100.000,00 i.v.
www.gebsrl.it - info@gebsrl.it



UNIVERSITA' DEGLI STUDI DI PADOVA
Dipartimento di Ingegneria Industriale DII

VIA GRADENIGO, 6/A 35131 PADOVA PD
Codice Fiscale 80306480281 - Partita Iva 00747430283

Ordine N. : DH10000590

ISTITUZIONALE

Data Emissione: 26/06/2014
Provvedimento N. 206 del 26/06/2014.

CUP: C91J11004220005

CIG: Z7F0FDE234

Codice Prov: 04339

Codice Fiscale: 00818320288 - Partita IVA: 00818320288

Spett.le

MA.TRA. S.R.L.

Via Jacopo da Montegrana n.27/A

35132 PADOVA PD ITALIA

Modalità di pagamento: CB - Bonifico bancario - Termini Pagamento: 30 gg. ricevimento fattura

Dipendenza: CASSA DI RISPARMIO DI PADOVA E ROVIGO - PADOVA - VIA VALERI 1

Cin: N. ABI: 66225 CAB: 12163 Num.Conto: 015925110197 IBAN: IT5430622512163015925110197

Vi preghiamo di fornirci le merci/servizi sottoindicati:

VO CF	QTA	DESCRIZIONE	VALU TA	% IVA	IMPORTO UNIT. IN VALUTA	SCONTO IN VALUTA	TOTALE IN VALUTA
1	1,00	RIDUTTORI MVI/W 49/116/U RAPP 1-397 PAM 71 135 (C00613 7X56)	EUR	22,00	575,00000	0,00	575,00
Totale Ordine in Valuta					575,00		
Totale Sconto					0,00		
Totale Imponibile in Euro					575,00		
Totale Iva in euro (su euro 575,00)					126,50		
Totale Ordine in Euro					701,50		

Modalità di consegna: PORTO FRANCONI, SEDE

Incarico di consegna: Laboratorio di Meccanica Applicata - Via Venezia 1, Padova - tel. Prof. Roberto Lovig, E-mail: Gioia tel. 049-8276713

Data Prevista:

Note: DirectPrice

Obbligo di trasmissione di fattura elettronica all'Università degli Studi di Padova esonerata dal 31 Marzo 2015.

- L'aggiudicatario assume gli obblighi di tracciabilità dei flussi finanziari di cui alla legge 13 agosto 2010, n. 136 e s.m.i. a pena di nullità assoluta del contratto.

- L'esecuzione di transazioni avvenute senza avvalersi di bonifici bancari o postali ovvero degli altri strumenti idonei a consentire la piena tracciabilità delle operazioni ai sensi della legge 13 agosto 2010, n. 136 e s.m.i determina la risoluzione di diritto del contratto. Resta salvo il diritto al risarcimento di eventuali danni o ulteriori oneri sostenuti dall'Ente.

- L'aggiudicatario si impegna a dare immediata comunicazione alla Stazione Appaltante ed alla Prefettura-Ufficio Territoriale del Governo della Provincia di competenza della notizia dell'inadempimento della propria controparte (subappaltatore/subcontrattante) agli obblighi di tracciabilità finanziaria.

Il Responsabile dei fondi:

Il Responsabile della Struttura:

COPIA PER IL FORNITORE

Cardan -Tec s.a.s. di Scarpelli S. & C.

Via Leonardo Da Vinci, 43
 41030 Bastiglia **MO**
 Tel. 059 904707 Fax 059 904707
 Part. IVA 02626890368
 Codice fiscale 02626890368
 REA 317722
 Reg. Soc. Trib.
 Iscritto nelle Imprese di **MO** al Num.Reg.Imp.026268903

Spett.le
 Università degli Studi di Padova
 Via Gradenigo 6/A
 35131 PADOVA

Destinatario
 Idem

Offerta n° 2.454 del 25/02/2016
 Oggetto Cortese attenzione:
 Gloria Maragno
 Servizio gestione contabile
 Dipartimento di Ingegneria Industriale

CODICE	DISEGNO	DESCRIZIONE	UM	QTA	PREZZO	SCONTI	IMPORTO
		FORCELLA 41x118 PER TUBO	NR	4,00	80,000		320,00
		IMBALLO	NR	1,00	3,000		3,00
Totale							323,00
Sconti							
Spese varie							15,00
Totale offerta							338,00

Pagamento BONIFICO BANCARIO ANTICIPATO
Banca di appoggio
Spedizione MEZZO CORRIERE
Validita' offerta 25/02/2016
Agente di riferimento

IL CLIENTE PER ACCETTAZIONE

D.Lgs. n. 196/03 (Codice in Materia di Protezione dei Dati Personali).
 La ns Società tratta i Vostri dati di cui è in possesso al solo fine dello svolgimento dei rapporti con Voi Intercomenti.
 Relativamente ai dati medesimi potrete esercitare i diritti previsti dall'art. 7 del D.Lgs. n. 196/2003 nei limiti ed alle condizioni previste dagli articolo 8, 9 e 10 del citato decreto .

Via Giovanni Battista Ricci, 6 / int. 8 - 35131 PADOVA (PD) Italy
 Tel. (+39) 049-651859 - Tel. (+39) 049-666014 - Fax (+39) 049-8756004
 P.E.C.: cati@catitecnici.com - Mail: info@catitalia.com - www.cati-italia.com
 Codice fiscale e Partita IVA 03037000281

COMMERCIO ARTICOLI TECNICI INDUSTRIALI



C.A.T.I. S.R.L.

God. Altorice: 03.00036

Spett.le Ditta

INTERSTRA TECNICI STRUTTI DI ED
 D.L. DI INGEGNERIA INDUSTRIALE RTI
 S.P.A. STRADINICOLA S/P
 35131 PADOVA
 Tel: 049-827.7599 Fax: 049-827.7599

Padova: 09.03.2016

G. P. R. T. S.

141 del 08.03.2016

Via: 03037000281 U. PAVI, tel. 0370370016

ATA S.p.A. Ed. V2. 03037000281@unipav.it

Pag. 1

INT. N. VOCE	DESCRIZIONE	Q.TA.	UNITA'	PREZ. UNITARIO	TOTALE	IMP. NETTO	IVA	CONSEGNA
1 1074	NUMERO SCANDALO 1074 RVA143 - N. 1 X 1000 SR	SR	1,00	102,0000	102,00	102,00	0,00	0,00
2 3137/0100	BOSSA SCANDALO 3137 RVA143 - N. 1 X 1000 SR	SR	2,00	20,5000	41,00	41,00	0,00	0,00
4 10082	BOSSA SCANDALO CON ULIZIONE DE PROTEZIONE 10082 RVA143 - N. 1 X 1000 SR	SR	2,00	34,5000	69,00	69,00	0,00	0,00
5	Spese amministrative				11,00	11,00	0,00	0,00

TOTALE 227,00

Spedizione: A 1/2 VI.
 Pagamento: D/B, D/C, C/C, C/P, C/S, C/T, C/U, C/V, C/W, C/X, C/Y, C/Z, C/AA, C/AB, C/AC, C/AD, C/AE, C/AF, C/AG, C/AH, C/AI, C/AJ, C/AK, C/AL, C/AM, C/AN, C/AO, C/AP, C/AQ, C/AR, C/AS, C/AT, C/AU, C/AV, C/AX, C/AY, C/AZ, C/BA, C/BB, C/BC, C/BD, C/BE, C/BF, C/BG, C/BI, C/BJ, C/BK, C/BL, C/BM, C/BN, C/BO, C/BP, C/BQ, C/BR, C/BS, C/BU, C/BV, C/BX, C/BS, C/BU, C/BV, C/BX, C/CA, C/CB, C/CC, C/CD, C/CE, C/CF, C/CG, C/CH, C/CI, C/CJ, C/CK, C/CL, C/CM, C/CN, C/CO, C/CP, C/CQ, C/CR, C/CS, C/CT, C/CU, C/CA, C/CB, C/CC, C/CD, C/CE, C/CF, C/CG, C/CH, C/CI, C/CJ, C/CK, C/CL, C/CM, C/CN, C/CO, C/CP, C/CQ, C/CR, C/CS, C/CT, C/CU, C/CA, C/CB, C/CC, C/CD, C/CE, C/CF, C/CG, C/CH, C/CI, C/CJ, C/CK, C/CL, C/CM, C/CN, C/CO, C/CP, C/CQ, C/CR, C/CS, C/CT, C/CU, C/CA, C/CB, C/CC, C/CD, C/CE, C/CF, C/CG, C/CH, C/CI, C/CJ, C/CK, C/CL, C/CM, C/CN, C/CO, C/CP, C/CQ, C/CR, C/CS, C/CT, C/CU, C/CA, C/CB, C/CC, C/CD, C/CE, C/CF, C/CG, C/CH, C/CI, C/CJ, C/CK, C/CL, C/CM, C/CN, C/CO, C/CP, C/CQ, C/CR, C/CS, C/CT, C/CU, C/CA, C/CB, C/CC, C/CD, C/CE, C/CF, C/CG, C/CH, C/CI, C/CJ, C/CK, C/CL, C/CM, C/CN, C/CO, C/CP, C/CQ, C/CR, C/CS, C/CT, C/CU, C/CA, C/CB, C/CC, C/CD, C/CE, C/CF, C/CG, C/CH, C/CI, C/CJ, C/CK, C/CL, C/CM, C/CN, C/CO, C/CP, C/CQ, C/CR, C/CS, C/CT, C/CU, C/CA, C/CB, C/CC, C/CD, C/CE, C/CF, C/CG, C/CH, C/CI, C/CJ, C/CK, C/CL, C/CM, C/CN, C/CO, C/CP, C/CQ, C/CR, C/CS, C/CT, C/CU, C/CA, C/CB, C/CC, C/CD, C/CE, C/CF, C/CG, C/CH, C/CI, C/CJ, C/CK, C/CL, C/CM, C/CN, C/CO, C/CP, C/CQ, C/CR, C/CS, C/CT, C/CU, C/CA, C/CB, C/CC, C/CD, C/CE, C/CF, C/CG, C/CH, C/CI, C/CJ, C/CK, C/CL, C/CM, C/CN, C/CO, C/CP, C/CQ, C/CR, C/CS, C/CT, C/CU, C/CA, C/CB, C/CC, C/CD, C/CE, C/CF, C/CG, C/CH, C/CI, C/CJ, C/CK, C/CL, C/CM, C/CN, C/CO, C/CP, C/CQ, C/CR, C/CS, C/CT, C/CU, C/CA, C/CB, C/CC, C/CD, C/CE, C/CF, C/CG, C/CH, C/CI, C/CJ, C/CK, C/CL, C/CM, C/CN, C/CO, C/CP, C/CQ, C/CR, C/CS, C/CT, C/CU, C/CA, C/CB, C/CC, C/CD, C/CE, C/CF, C/CG, C/CH, C/CI, C/CJ, C/CK, C/CL, C/CM, C/CN, C/CO, C/CP, C/CQ, C/CR, C/CS, C/CT, C/CU, C/CA, C/CB, C/CC, C/CD, C/CE, C/CF, C/CG, C/CH, C/CI, C/CJ, C/CK, C/CL, C/CM, C/CN, C/CO, C/CP, C/CQ, C/CR, C/CS, C/CT, C/CU, C/CA, C/CB, C/CC, C/CD, C/CE, C/CF, C/CG, C/CH, C/CI, C/CJ, C/CK, C/CL, C/CM, C/CN, C/CO, C/CP, C/CQ, C/CR, C/CS, C/CT, C/CU, C/CA, C/CB, C/CC, C/CD, C/CE, C/CF, C/CG, C/CH, C/CI, C/CJ, C/CK, C/CL, C/CM, C/CN, C/CO, C/CP, C/CQ, C/CR, C/CS, C/CT, C/CU, C/CA, C/CB, C/CC, C/CD, C/CE, C/CF, C/CG, C/CH, C/CI, C/CJ, C/CK, C/CL, C/CM, C/CN, C/CO, C/CP, C/CQ, C/CR, C/CS, C/CT, C/CU, C/CA, C/CB, C/CC, C/CD, C/CE, C/CF, C/CG, C/CH, C/CI, C/CJ, C/CK, C/CL, C/CM, C/CN, C/CO, C/CP, C/CQ, C/CR, C/CS, C/CT, C/CU, C/CA, C/CB, C/CC, C/CD, C/CE, C/CF, C/CG, C/CH, C/CI, C/CJ, C/CK, C/CL, C/CM, C/CN, C/CO, C/CP, C/CQ, C/CR, C/CS, C/CT, C/CU, C/CA, C/CB, C/CC, C/CD, C/CE, C/CF, C/CG, C/CH, C/CI, C/CJ, C/CK, C/CL, C/CM, C/CN, C/CO, C/CP, C/CQ, C/CR, C/CS, C/CT, C/CU, C/CA, C/CB, C/CC, C/CD, C/CE, C/CF, C/CG, C/CH, C/CI, C/CJ, C/CK, C/CL, C/CM, C/CN, C/CO, C/CP, C/CQ, C/CR, C/CS, C/CT, C/CU, C/CA, C/CB, C/CC, C/CD, C/CE, C/CF, C/CG, C/CH, C/CI, C/CJ, C/CK, C/CL, C/CM, C/CN, C/CO, C/CP, C/CQ, C/CR, C/CS, C/CT, C/CU, C/CA, C/CB, C/CC, C/CD, C/CE, C/CF, C/CG, C/CH, C/CI, C/CJ, C/CK, C/CL, C/CM, C/CN, C/CO, C/CP, C/CQ, C/CR, C/CS, C/CT, C/CU, C/CA, C/CB, C/CC, C/CD, C/CE, C/CF, C/CG, C/CH, C/CI, C/CJ, C/CK, C/CL, C/CM, C/CN, C/CO, C/CP, C/CQ, C/CR, C/CS, C/CT, C/CU, C/CA, C/CB, C/CC, C/CD, C/CE, C/CF, C/CG, C/CH, C/CI, C/CJ, C/CK, C/CL, C/CM, C/CN, C/CO, C/CP, C/CQ, C/CR, C/CS, C/CT, C/CU, C/CA, C/CB, C/CC, C/CD, C/CE, C/CF, C/CG, C/CH, C/CI, C/CJ, C/CK, C/CL, C/CM, C/CN, C/CO, C/CP, C/CQ, C/CR, C/CS, C/CT, C/CU, C/CA, C/CB, C/CC, C/CD, C/CE, C/CF, C/CG, C/CH, C/CI, C/CJ, C/CK, C/CL, C/CM, C/CN, C/CO, C/CP, C/CQ, C/CR, C/CS, C/CT, C/CU, C/CA, C/CB, C/CC, C/CD, C/CE, C/CF, C/CG, C/CH, C/CI, C/CJ, C/CK, C/CL, C/CM, C/CN, C/CO, C/CP, C/CQ, C/CR, C/CS, C/CT, C/CU, C/CA, C/CB, C/CC, C/CD, C/CE, C/CF, C/CG, C/CH, C/CI, C/CJ, C/CK, C/CL, C/CM, C/CN, C/CO, C/CP, C/CQ, C/CR, C/CS, C/CT, C/CU, C/CA, C/CB, C/CC, C/CD, C/CE, C/CF, C/CG, C/CH, C/CI, C/CJ, C/CK, C/CL, C/CM, C/CN, C/CO, C/CP, C/CQ, C/CR, C/CS, C/CT, C/CU, C/CA, C/CB, C/CC, C/CD, C/CE, C/CF, C/CG, C/CH, C/CI, C/CJ, C/CK, C/CL, C/CM, C/CN, C/CO, C/CP, C/CQ, C/CR, C/CS, C/CT, C/CU, C/CA, C/CB, C/CC, C/CD, C/CE, C/CF, C/CG, C/CH, C/CI, C/CJ, C/CK, C/CL, C/CM, C/CN, C/CO, C/CP, C/CQ, C/CR, C/CS, C/CT, C/CU, C/CA, C/CB, C/CC, C/CD, C/CE, C/CF, C/CG, C/CH, C/CI, C/CJ, C/CK, C/CL, C/CM, C/CN, C/CO, C/CP, C/CQ, C/CR, C/CS, C/CT, C/CU, C/CA, C/CB, C/CC, C/CD, C/CE, C/CF, C/CG, C/CH, C/CI, C/CJ, C/CK, C/CL, C/CM, C/CN, C/CO, C/CP, C/CQ, C/CR, C/CS, C/CT, C/CU, C/CA, C/CB, C/CC, C/CD, C/CE, C/CF, C/CG, C/CH, C/CI, C/CJ, C/CK, C/CL, C/CM, C/CN, C/CO, C/CP, C/CQ, C/CR, C/CS, C/CT, C/CU, C/CA, C/CB, C/CC, C/CD, C/CE, C/CF, C/CG, C/CH, C/CI, C/CJ, C/CK, C/CL, C/CM, C/CN, C/CO, C/CP, C/CQ, C/CR, RINGRAZIANDO PER AVERE STATO INTERPELLATO, SINCERAMENTE SALUTANDO.

[Signature]
 G. P. R. T. S.



Toma s.a.s. di Brilli Massimiliano

Via A. Doria 32 - 35010 Gazzo (PD) - Italia
Tel. 049/5995044 Fax 049/5995093
e-mail: info@tomatome.it Internet: www.tomatome.it
C.F./P.Iva 03660950282 Reg. Imprese 03660950282

Preventivo nr. **12/2016 PD** del **07/04/2016**

Destinatario

UNIVERSITA'DEGLI STUDI DI PADOVA D.I.I.
Via Venezia, 1
35131 Padova (PD)

C.F. 80006480281 P.Iva 00742430283

Destinazione

UNIVERSITA'DEGLI STUDI DI PADOVA D.I.I.
Via Venezia, 1
35131 Padova (PD)

Codice	Descrizione	Quantità	Prezzo	Sconto	Importo	Iva
	STAFFA DISCO ANT	1 pz	€ 120,0000		€ 120,00	22
	PIASTRA STERZO SUPERIORE	1 pz	€ 320,0000		€ 320,00	22
	PIASTRA STERZO INFERIORE	1 pz	€ 350,0000		€ 350,00	22
	PIASTRA FRENO POST	1 pz	€ 130,0000		€ 130,00	22
	BOCCOLA PIASTRA INF	1 pz	€ 25,0000		€ 25,00	22
	BOCCOLA SUPERIORE	1 pz	€ 25,0000		€ 25,00	22
	PORTA CUSCINETTO	2 pz	€ 20,0000		€ 40,00	22
	SUPPORTO CUSCINETTI FORCELLONE	2 pz	€ 10,0000		€ 20,00	22
	CENTRAGGIO PERNO FORCELLONE	2 pz	€ 12,0000		€ 24,00	22
	INSERTO DX CERCHIO	1 pz	€ 15,0000		€ 15,00	22
	BEARING PLATE	2 pz	€ 90,0000		€ 180,00	22
	BOCCOLA TELAIO	2 pz	€ 10,0000		€ 20,00	22
	ASSE STERZO	1 pz	€ 80,0000		€ 80,00	22
	INSERTI FRONTALI	2 pz	€ 45,0000		€ 90,00	22
	CANOTTO:INS PORTA GHIERA	2 pz	€ 30,0000		€ 60,00	22
	CENTRAGGIO RUOTA	2 pz	€ 10,0000		€ 20,00	22
	BUSHING PLATE	2 pz	€ 98,0000		€ 196,00	22

Pagamento: Da concordare

Tot. imponibile € 1.715,00
Tot. Iva € 377,30

Consegna: Da concordare

Spedizione: Franco ns officina

Tot. documento € 2.092,30

Capitale Sociale € 80.000,00 i.v.
 R.F.A.: PD-104475
 Reg. Imprese Padova 00207760281
 Reg. Esportati Commercio PD- 532
 Codice ATECO 06.89.95
 Vat Code IT 00207760281
 Partita IVA 00207760281
 Codice Fiscale 00207760281



COMMERCIO ARTICOLI TECNICI INDUSTRIALI

Via Giovanni Dattista Ricci, 6 / int. 0 - 35131 PADOVA (PD) Italy
 Tel. (+39) 049-651855 - Tel. (+39) 049-666014 - Fax (+39) 049-8756084
 P.E.C.: cati-italia@arubapec.it - Mail: info@cati-italia.com - www.cati-italia.com

Spett.le Ditta

UNIVERSITA' DEGLI STUDI DI PD
 DIP. DI INGEGNERIA INDUSTRIALE DII
 VIA GRADENIGO, 6/A
 35131 PADOVA PD
 Tel: 049-827.7500 Fax: 049-827.7599

Padova: 11.07.2016

O F F E R T A

Num.: 445 Del 11.07.2016

Vs. Riferimento: VERBALE 05/07/15 SIG.TARIFF COMAA Cod.cliente: 06.05056 Pag. 1
 Alla c.a. Eqr.Vs. PROF.VITTORIO COSEALTER

NR	Articolo	Descrizione	U.M.	Qta'	Prezzo Unitario	Scento	Consegna	Iva
1	8222	RIDUTTORE EPICICLOIDALE IC 120.2.50.LGN.FN.CD.14.KF	%	1,00	708,9900	NETTO	20 GGI. D.R.O.	220
2	80K95032063	CALIBRATORE ROK 55 32X63	%	1,00	31,6600	NETTO	FRONDA S.V.	220
3		GRISTOSH SPARK PLEGGIA AMMORTIZZAZIONE	%	1,00	10,0000	NETTO		220
VALIDITA' OFFERTA: 30 GG								
TOTALE							750,650	

Rea: FRANCO NS.MAG.
 Spedizione: A 1/2 VS.
 Pagamento: BON.BANCARIO 30 GG.DF.
 Banca: IT-93-0-36225-63120-07400713003K
 ABI: 06225 CAB: 63120
 Imballo: GRATIS
 Emesso da: MONICA

VEITORE:

Destinazione merce:
 DIP. DI INGEGNERIA IND. DE DII
 VIA VENEXIA, 1
 35131 PADOVA PD
 049-3276793

Ringraziando per essere stati interpellati, distintamente saluti.

C.A.T.I. S.R.L.

Capitale Sociale € 99.000.000 i.v.
 R.F.A.: PD-104479
 Reg. Imprese Padova: 00207760291
 Reg. Esenti al Commercio: PD-1532
 Codice AICUX: 48.89.99
 Vor. Code: IT 00207760291
 Partita IVA: 00207760291
 Codice Fiscale: 00207760291



Via Giovanni Dattista Ricci, 6 / int. 6 - 35131 PADOVA (PD) Italy
 Tel. (+39) 049-851855 - Tel. (+39) 049-666014 - Fax (+39) 049-8756084
 P.E.C.: cati-italia@arubapec.it - Mail: info@cati-italia.com - www.cati-italia.com

Spett.le Ditta

UNIVERSITA' DEGLI STUDI DI PD
 DIP. DI INGEGNERIA INDUSTRIALE III
 VIA GRADENIGO, 6/A
 35131 PADOVA PD
 Tel: 049-827.7500 Fax: 049-827.7599

Padova: 22.05.2014

C O F F E R T A

Num.: 295 Del 22.05.2014

Vs. Riferimento: E-MAIL DEL 13/05/2014
 Alla c.a. Dg2.Vs. ING. ENRICO GIOLIO

Doc. cliente: 00.36056

Pag. 1

NR	Articolo	Descrizione	U.n.	Qta'	Prezzo Unitario	Scotto	Consegna	Iva
1		VITE R.D.S. R 50-5-600 CT	ES	1,00	158,7000	NETTO	5/6 GG. D.R.C.	22
2		CHIODICOLA R.D.S. FSI 50-5-4	ES	2,00	258,5700	NETTO	5/6 GG. D.R.C.	22
3	16012	16012 CUSCINETTO NTN	ES	3,00	31,6000	NETTO	FRONTA S.V.	22
4	32005	32005X CUSCINETTO NTN	ES	8,00	16,2300	NETTO	FRONTA S.V.	22
5	32008	4P-32008X - 32008X CUSCINETTO NTN	ES	2,00	23,0300	NETTO	FRONTA S.V.	22
6	61905	61905 CUSCINETTO SKF	ES	1,00	16,0500	NETTO	FRONTA S.V.	22
7	32014	32014X CUSCINETTO NTN	ES	2,00	60,7500	NETTO	FRONTA S.V.	22
8								
9		VALIDITA' OFFERTA: 10 GG.						

TOTALE 1.004,090

Resa: FRANCO NS. MAG.

Spedizione: A 1/2 VS.

VEITORE:

Destinazione merce:

Pagamento: BON. SANCARIS 30 GG. DP.

ITEM

Banca: IP-93-0-36225-63120-07400713693X

ABI: 36225 CAB: 83120

Inballo: GRATIS

Emesso da: MONICA

Ringraziando per essere stati interpellati, distintamente salutiamo: C.A.T.I. S.R.L.



UNIVERSITA' DEGLI STUDI DI PADOVA
Dipartimento di Ingegneria Industriale DII

VIA GRADENIGO, 6/A 35131 PADOVA PD

Codice Fiscale 80006480281 - Partita Iva 00742430283

Ordine N. : DII0000588

ISTITUZIONALE

Data Emissione: 26/06/2014
Preventivo N. 295 del 22/05/2014.

CUP: C91J11004220005

CIG: ZD16FDD8EF

Codice Forn.: 1158

Codice Fiscale: 80067760281 - Partita IVA: 00207760281

FORNITORE FAX N. 0498756084

Spett. le

C.A.T.I. srl

VIA G.B. RICCI 6/INTERNO 8
35131 PADOVA PD ITALIA

Modalità di pagamento: CB Bonifico bancario - Termini Pagamento: 30 gg. ricevimento fattura

Dipendenza: MONTE DEI PASCHI DI SIENA - PADOVA - VIA VERDI

Cin: C ABE 01030 CAB: 12190 Num.Conto: 000002204590 IBAN: IT8703103012190000002204590

Vi preghiamo di fornirci le merci/servizi sottoindicati:

VO CR	QTA	DESCRIZIONE	VALUTA	% IVA	IMPORTO UNIT. IN VALUTA	SCONTO in VALUTA	TOTALE IN VALUTA
1	1,00	VITE R.JAN. R 50-5-600 L70	EUR	22,00	158,70000	0,00	158,70
2	2,00	CITROCCIOIA R.D S. PSI 50-5-4	EUR	22,00	255,57000	0,00	517,14
3	3,00	16012 CUSCINETTO NTN (ART. 16012)	EUR	22,00	21,50000	0,00	94,80
4	8,00	3205XU CUSCINETTO NTN (ART. 3205)	EUR	22,00	16,23000	0,00	129,84
5	2,00	4T- 3208X - 3208X CUSCINETTO NTN (ART. 3208)	EUR	22,00	25,83000	0,00	96,00
6	1,00	61905 CUSCINETTO SKF (ART. 61905)	EUR	22,00	15,95000	0,00	16,05
7	3,00	32014XU CUSCINETTO NTN (ART. 32014)	EUR	22,00	60,75000	0,00	121,50
Totale Ordine in Valuta			EUR		1.084,09		
Totale Sconto			EUR		0,00		
Totale Imponibile in Euro			EUR		1.084,09		
Totale Iva in euro (su euro 1.084,09)			EUR		238,50		
Totale Ordine in Euro			EUR		1.322,59		

Modalità di consegna: PORTOFRANCO ES. SUE

Indirizzo di consegna: Laboratorio di Meccanica Applicata - via Venezia 1 - Padova - Prof. Roberto Leoni - Enrico Gilio - tel. 049/8275715

Data Prevista:

Note: Dueno/Forze

L'obbligo di trasmissione di fattura elettronica all'Università degli Studi di Padova decorre dal 31 Marzo 2015

- L'aggiudicatario assume gli obblighi di tracciabilità dei flussi finanziari di cui alla legge 15 agosto 2010, n. 136 e s.m.i., a pena di nullità assoluta del contratto.



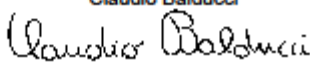
- L'esecuzione di transazioni avvenute senza avvalersi di benefici bancari o postali ovvero degli altri strumenti idonei a consentire la piena tracciabilità delle operazioni ai sensi della legge 15 agosto 2010, n. 136 e s.m.i determina la risoluzione di diritto del contratto. Resta salvo il diritto al risarcimento di eventuali danni o ulteriori oneri sostenuti dall'Ente.

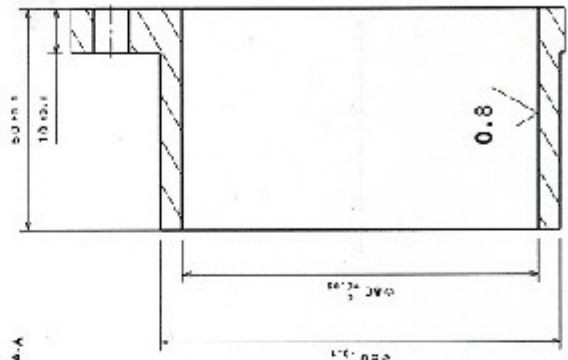
- L'aggiudicatario si impegna a dare immediata comunicazione alla Stazione Appaltante ed alla Prefettura-Ufficio Territoriale del Governo della Provincia di competenza della notizia dell'insediamento della propria controparte (subappaltatore/subcontraente) agli obblighi di tracciabilità finanziaria.

D.S.O. L. 20/06/14/18792

DIPARTIMENTO
DI INGEGNERIA INDUSTRIALE
Il Direttore

DIPARTIMENTO
DI INGEGNERIA INDUSTRIALE
Il Direttore

 		<h1>OFFERTA</h1>		
<input type="checkbox"/> R.T.A. S.r.l. Via E. Mattei - Frazione Divisa 27020 MARCIGNAGO (PV) Tel. 0382.929.855 (r.a.) - Fax 0382.929.150 http://www.rta.it - e-mail: info@rta.it		<input checked="" type="checkbox"/> FILIALE NORD-EST Via D. Alighieri, 4/a 30034 MIRA (VE) Tel. 041.56.00.332 - Fax 041.56.00.165 e-mail: rtane@rta.it	<input type="checkbox"/> FILIALE CENTRO-SUD Via D. Alighieri, 41 60025 LORETO (AN) Tel. 071.75.00.433 - Fax 071.97.77.64 e-mail: rtacs@rta.it	
Cliente: Università degli studi di Padova - Dipartimento Ingegneria Industriale		Riferimento: Ing. Tarek JOMAA Telefono: 339/8481634 Fax: trk.jomaa@gmail.com		
Offerta N°: NE-200/2016	Redatto da: Claudio Balducci	Data: 27/09/2016	Pag.: 1 / 1	
Oggetto: Come da Vs. Richiesta , Vi inviamo la ns. offerta riferita al seguente materiale.				
Pos.	Q.tà	Codice	Descrizione	Prezzo cad. IVA esclusa
1	01 pz	SM 2863 5155	Motore passo-passo SANYO serie SM. Coppia di tenuta bipolare 920 Ncm.	€ 150,89
2	01 pz	SM 2861 5055	Motore passo-passo SANYO serie SM. Coppia di tenuta bipolare 360 Ncm.	€ 100,71
3	02 pz	X-PLUS B4.1	X-PLUS B è il nome di una serie di azionamenti chopper di tipo bipolare ministepp adatta al pilotaggio di motori passo passo a due fasi con quattro, sei o otto fili uscenti. Gli azionamenti X-PLUS B sono alloggiati all'interno di un contenitore metallico atto al fissaggio a parete, di dimensioni 152 x 129 x 46 mm. Possono essere alimentati direttamente da rete (110 o 230 V) rendendo inutile, nella maggioranza dei casi, il trasformatore di alimentazione. L'ampio range della tensione facilita l'uso degli azionamenti della serie X-PLUS B in una grande varietà di applicazioni e nella maggior parte dei paesi del mondo.	€ 291,60
Condizioni fornitura				
Legame valutario	Pos. 1, 2: Prezzo fisso			
Consegna	7 ÷ 10 gg lavorativi data ordine			
Pagamento	Bonifico Bancario Anticipato			
Trasporto	A mezzo vs. corriere porto assegnato o nostro (GLS o BRT) con porto franco e spese in fattura.			
Validità offerta	3 mesi	Imballo	Gratuito	
Note:				
A Vs. disposizione per eventuali chiarimenti, cogliamo l'occasione per presentare distinti saluti. <div style="text-align: right;"> R.T.A. S.r.l. Ufficio Commerciale Claudio Balducci  </div>				



Section view A-A
SCALE: 1:1

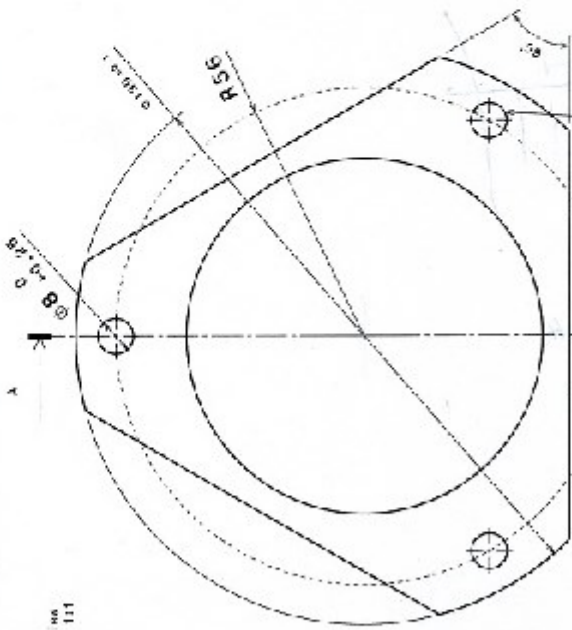
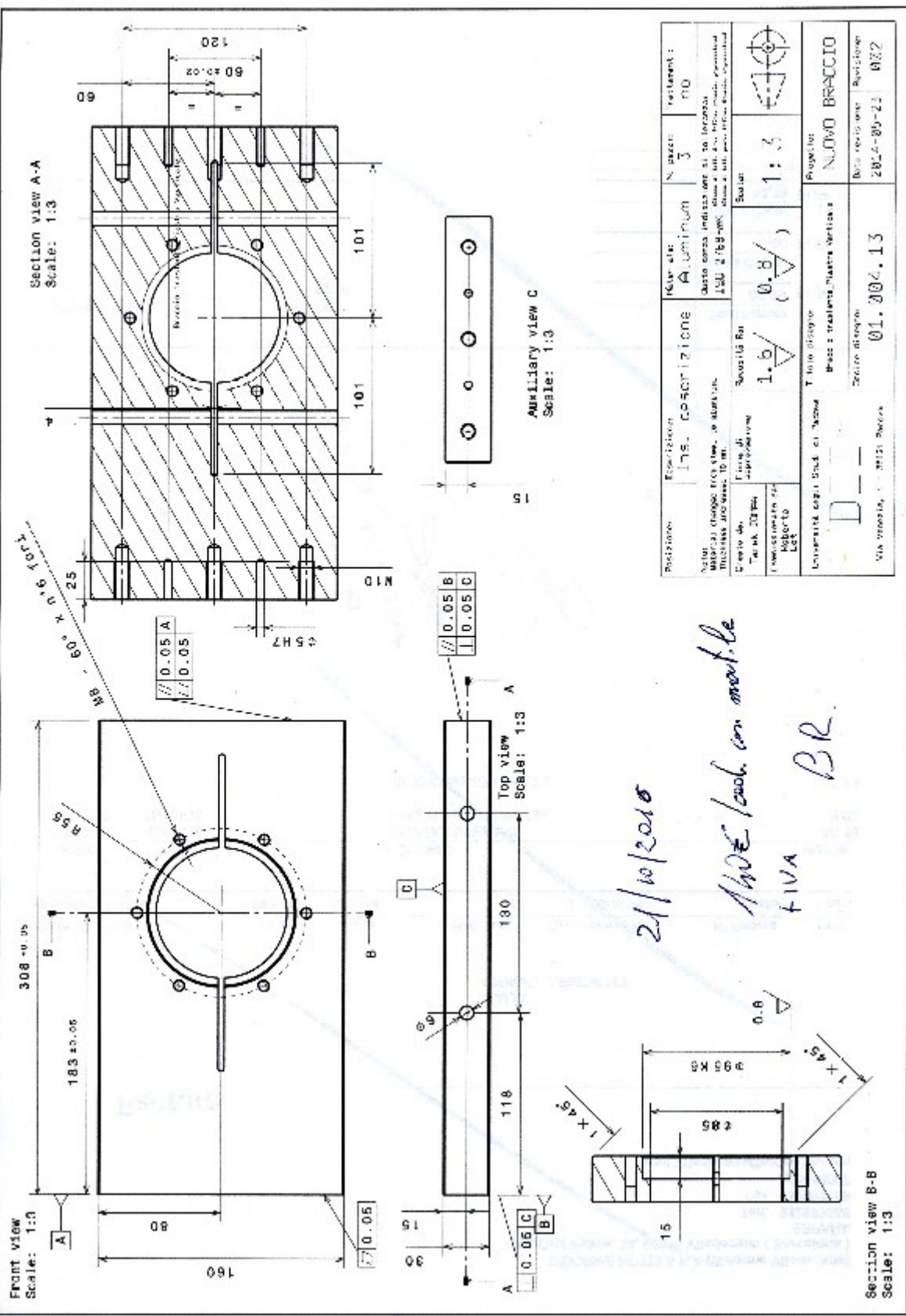


Fig. 111
Scale: 1:1

Part Name	Description	Material	Quantity	Unit	Part Number
	205 - DESCRIZIONE	81 - 011-10		24	
Note: <small>Se la parte non è specificata, si intende che la parte è in acciaio.</small>					
Material	Part Name	Material	Quantity	Unit	Part Number
205 - DESCRIZIONE	81 - 011-10	81 - 011-10	24		
Note: <small>Se la parte non è specificata, si intende che la parte è in acciaio.</small>					
Material	Part Name	Material	Quantity	Unit	Part Number
205 - DESCRIZIONE	81 - 011-10	81 - 011-10	24		
Note: <small>Se la parte non è specificata, si intende che la parte è in acciaio.</small>					
Material	Part Name	Material	Quantity	Unit	Part Number
205 - DESCRIZIONE	81 - 011-10	81 - 011-10	24		
Note: <small>Se la parte non è specificata, si intende che la parte è in acciaio.</small>					
Material	Part Name	Material	Quantity	Unit	Part Number
205 - DESCRIZIONE	81 - 011-10	81 - 011-10	24		
Note: <small>Se la parte non è specificata, si intende che la parte è in acciaio.</small>					



24/10/2010
35 ref. cad. con sm. la
1111 BR



Capitale Sociale € 96.000,00 i.v.
 R.E.A.: PD-104479
 Reg. Imprese Padova 00207790281
 Reg. Escenti e Commercio PD-1532
 Codice ATECO 48.89.09
 Vat Code IT 00207790281
 Partita IVA 00207790281
 Codice Fiscale 00207790281



COMMERCIO ARTICOLI TECNICI INDUSTRIALI

Via Giovanni Battista Ricci, 6 / Int. 8 - 35131 PADOVA (PD) Italy
 Tel. (+39) 049-651855 - Tel. (+39) 049-666014 - Fax (+39) 049-8758084
 P.E.C.: cati-italia@arubapec.it - Mail: info@cati-italia.com - www.cati-italia.com

Spett.LE Ditta

UNIVERSITA' DEGLI STUDI DI PD
 DIP. DI INGEGNERIA INDUSTRIALE D11
 VIA GRADENIGO, 6/A
 35131 PADOVA PD
 Tel: 049-827.7500 Fax: 049-827.7599

Padova: 21.11.2016

O F F E R T A

Num.: 729 Del 21.11.2016

Vs. Riferimento: E-MAIL DEL 25/10/16 SIG.TAREK JOMAA Cod.ciente: 00.06056 Pag. 1
 Alla c.a. Egr.Vs. trk.jomaa@gmail.com

NR	Articolo	Descrizione	J.n.	Qta'	P.zzo Unitario	Sconto	Consegna	Iva
1	2222	ATTUATORE LINEARE ELETTROMECC LMR01 RLI C103 RF DC24V FC2X CON VITE TRAPEZOIDALE LMR01 FINECORSA ELETTRICI INTEGRATI	PZ	1,00	233,4500	NETTO	6 SETT.NE D.D.	220
2		AZIONATI A CANNE, DI FACILE						
3		TARATURA, CABLAGI DIRETTAMENTE						
4		SUL MOTORE PER L'ARRESTO AUTO-						
5		MATICO DELL'APPIATORE SENZA						
6		RELE' ESTERNI - MOTORE IN						
7		CORRENTE CONTINUA 24V						
8		CARATTERISTICHE DIMENSIONALI E						
9		PRESTAZIONI COME DA CATALOGO						
10		ALLEGATO (NR 5 PAGINE)						
11	188150350	PUNTO DI OLIO SHELL DA KG.4 OMALA S4 W320 EX TIVELA 8320	PZ	1,00	50,3500	NETTO	PRONTA	220
12		SPESE GESTIONE PUBBLICA AMM.NR	PZ	1,00	10,0000	NETTO		220

TOTALE 303,800

Rosa: FRANCO NS.MAG.
Spedizione: A 1/2 VS.
Pagamento: BON.BANCARIO 30 GG.DF.
Banca: IT-93-0-36225-63120-07400713683X
ABI: 06225 **CAB:** 63120
Inballo: GRATIS
Emesso da: MONICA

VEITORE:
Destinazione merce:
 DIP. DI INGEGNERIA IND.LE D11
 VIA VENEZIA, 1
 35131 PADOVA PD
 049-8276793

Ringraziando per essere stati interpellati, distintamente salutiamo.

C.A.T.I. S.R.L.

Table of Contents

DEDICATION.....	2
ACKNOWLEDGEMENTS.....	3
ABSTRACT.....	4
SOMMARIO.....	5
INTRODUCTION	6
CHAPTER 1 – STATE OF THE ART	8
1.1 THE FLATTRAC III CLASSIC FROM MTS	10
1.2 CALSPAN TIRE TEST MACHINE	11
1.3 DELFT-TIRE TEST FROM TASS INTERNATIONAL	12
1.4 OUR TIRE TESTING MACHINES	12
CHAPTER 2 - MOTOTIREMETER.....	13
2.1 HARDWARE PROBLEMS	15
2.2 HARDWARE UPDATE	16
2.3 SOFTWARE PROBLEMS	18
2.4 SOFTWARE UPDATE	19
2.4.1 First stage	19
2.4.2 Final stage.....	20
2.5 INSTRUCTIONS	21
2.5.1 Hardware	21
2.5.2 Software.....	22
CHAPTER 3 - TIRE TESTS & DATA ELABORATION	23
3.1 TEST DESCRIPTION	24
3.1.1 Rolling radius	24
3.1.2 Toroid Radius	24
3.1.3 Radial stiffness.....	25
3.1.4 Lateral Stiffness	26
3.1.5 Side Slip.....	27
3.1.6 Camber.....	27
3.1.7 Combined Test	28
3.2 TEST RESULTS	29
3.2.1 Radial stiffness.....	29
3.2.2 Lateral stiffness.....	30
3.2.3 Side Slip.....	31
3.2.4 Camber.....	32
3.3 TIRE_FITTING_V1	32
3.3.1 Purpose	32
3.3.2 Inputs	32
3.3.3 Outputs	33
3.3.4 Fitting formulas.....	35
3.3.5 Fundamental elements	36

3.3.6 Advantages	37
3.4 TIRE_FITTING_V3	37
3.4.1 Purpose	37
3.4.2 Inputs	37
3.4.3 Outputs	37
3.4.4 Fitting formulas.....	37
3.4.5 Additional elements.....	39
3.4.6 Advantages	39
3.4.7 Instructions	39
3.5 TIRE_FITTING_V6.....	40
3.5.1 Purpose	40
3.5.2 Inputs	40
3.5.3 Advantages	40
3.5.4 Instructions	40
3.6 ISSUED PAPERS AND ARTICLES.....	42
3.6.1 <i>The effect of the inflation pressure of tires on motorcycle weave stability.....</i>	42
3.6.2 <i>Identification of the mechanical properties of tires for wheelchair simulation.....</i>	43
CHAPTER 4 - NEW TIRE TESTING MACHINE.....	47
4.1 COLUMN ASSEMBLY.....	49
4.1.1 <i>Horizontal plate</i>	49
4.1.2 <i>Vertical Plate.....</i>	52
4.1.3 <i>Bushing</i>	53
4.1.4 <i>Speed reducer</i>	53
4.1.5 <i>Piston's Mounting Plate.....</i>	55
4.1.6 <i>Pneumatic system.....</i>	55
4.1.7 <i>Electric system</i>	58
4.2 ROLL ARM ASSEMBLY	60
4.2.1 <i>Bearing plate and cover.....</i>	61
4.2.2 <i>Universal Joint.....</i>	61
4.3 SLIP ARM ASSEMBLY	62
4.3.1 <i>Shaft.....</i>	62
4.3.2 <i>Speed reducer</i>	63
4.3.3 <i>Sleeve's housing.....</i>	64
4.3.4 <i>Vertical motion</i>	64
4.3.5 <i>Slip motion</i>	65
4.4 WHEEL ASSEMBLY	66
4.4.1 <i>Lateral adjustment.....</i>	66
4.4.2 <i>Wheel hub.....</i>	67
4.5 SOFTWARE DEVELOPMENT	68
4.5.1 <i>Motion control.....</i>	68
4.5.2 <i>DAQ (data acquisition).....</i>	69
4.6 THE CONTROL SYSTEM.....	70
4.6.1 <i>Workstation</i>	70
4.6.2 <i>NI-PCI 7334 (Motion Controller)</i>	70

4.6.3 NI-UMI 7764 (<i>Universal Motion Interface</i>).....	71
4.6.4 <i>Step motor driver</i>	71
4.6.5 <i>Step motor</i>	72
4.7 DAQ (DATA ACQUISITION) SYSTEM	75
4.7.1 <i>Load Cell</i>	75
4.7.2 <i>NI-9237 module</i>	76
4.7.3 <i>NI cDAQ-9178</i>	76
4.7.4 <i>Workstation</i>	76
4.8 INSTRUCTIONS.....	78
4.8.1 <i>Hardware</i>	78
4.8.2 <i>Software</i>	78
4.9 MACHINE SETUP	78
4.10 PROJECT MANAGEMENT	79
4.11 CONCLUSION.....	83
BIBLIOGRAPHY.....	85
NOMENCLATURE.....	87
LIST OF FIGURES.....	88
LIST OF TABLES	90
APPENDIX A.....	91
APPENDIX B.....	94
APPENDIX C.....	99
APPENDIX D.....	101
APPENDIX E.....	104
APPENDIX F.....	117